

Investigation and Characterization of Flavor to Food Matrix Interactions using Solid  
State Nuclear Magnetic Resonance

A Dissertation  
SUBMITTED TO THE FACULTY OF  
UNIVERSITY OF MINNESOTA  
BY

Margaret Louise Jilek

IN PARTIAL FULFILLMENT OF THE REQUIREMENTS  
FOR THE DEGREE OF  
DOCTOR OF PHILOSOPHY

Devin G. Peterson PhD.

September 2016

© Margaret Louise Jilek 2016

## **Acknowledgements**

Though the pursuit of a doctorate is a wholly self-fulfilling pursuit it cannot be successfully achieved without the guidance, support and inspiration of members from several community groups in the candidate's life. This small space of type must summarize those crucial contributions.

Thank you to Dr. Devin G. Peterson, for the greatest contributions to my success in this endeavor; faith in my abilities and the freedom to execute my ideas.

Thank you to truly great collaborators, we indulged our curiosity and achieved some fascinating results; Dr. Tata Gopinath, Dr. Michelle Miller, Mr. Geoff Harms, Dr. Leslie Morgret and Dr. Tim Cooper.

Thank you to my committee members; Dr. Gary A. Reineccius, Dr. Ted P. Labuza, Dr. Gianluigi Veglia and Dr. David Zyzak who are an endless source of valuable input and thoughtful questions. I hope I remain as engaged and passionate about my work as they are about theirs.

Thank you to my coworkers and bunker buddies; Dr. Smaro Kokkinidou, soon-to-be Dr. David Potts, Dr. Ian Ronningen and soon-to-be Dr. Kenny Smith for the good times, lots of laughter and sometimes tears. I couldn't have remained sane without you.

Thank you to family and friends. Most of you may not have been familiar with the process of obtaining a doctorate or the complexities of academic research but it never impacted your ability to love and support me. Thank you, Mr. Scott Jilek.

## **Dedication**

This thesis is dedicated to the pursuit of truth through scientific study may it quench the thirst for knowledge and prove useful to the World.

## **Abstract**

The intermolecular interactions between flavor molecules and the matrix of foods are known to influence flavor release during consumption and consequently product acceptability. The forces thought to govern flavor-food interactions have been modeled and the phenomena observed studies to build useful conventions regarding flavor release kinetics. However, the mechanistic interactions themselves remain largely uncharacterized and the dynamics of the interactions unstudied. The overall goal of this research project is to develop a research platform which can characterize and observe the dynamics of flavor to matrix interactions, typical in a gum base formulation.

In the initial phase of the research project, solid state nuclear magnetic resonance (ssNMR) was applied to characterize molecular interactions and interaction dynamics at the atomic scale in flavored gum base model systems (chapter 4). Preferential interactions between flavor compounds (Melonal and ethyl propionate) and components of conventional chewing gums bases were detected and quantified. Melonal was shown to preferentially bind with polyisobutylene (PIB) over polyvinyl acetate (PVAc) whereas ethyl propionate was shown to preferentially bind with polyvinyl acetate. Chemical shift perturbances were calculated for Melonal in mixtures of PIB and PVAc providing site-specific information regarding how Melonal interacts with conventional gum matrices. The carbonyl carbon of Melonal was shown to be most responsive to changes in the

composition of the polymer matrix suggesting that this functional group was a key interaction site with conventional gum polymeric materials. This methodology provided a means to study flavor to matrix interactions in situ, determine if preferential binding behavior exists and determine which functional groups on the flavor compounds were involved in the intermolecular interactions with conventional chewing gum matrix materials.

Next, in chapter 5, isotopically enriched model polymer matrices were utilized to assess differences in flavor to matrix interactions as the physical properties but not the chemical properties of the matrix changed. Specialized polymers were synthesized in varying molecular weights (MW) to produce a short MW matrix with a soft texture and a long MW matrix with a firm texture. The short MW, long MW and mixtures of the short and long MW matrices were mixed with a carbon-13 labeled flavor compound, acetophenone. The interaction of acetophenone with these matrices and the mobility of acetophenone in these matrices were studied using ssNMR techniques. Acetophenone was shown to be more mobile, and therefore more available to release, in mixtures of short and long MW matrices than in either the short or long alone. The ssNMR data also suggested that the methyl carbon of acetophenone participates in weaker intermolecular interactions with the matrices than the aromatic carbons. These observations were compared to traditional kinetic flavor release and partitioning measurement techniques. Partition coefficients for acetophenone in these matrices were measured but did not suggest differences in flavor release behavior. Acetophenone release profiles were

generated using an artificial chewing device and atmospheric chemical ionization mass spectrometry (APCI-MS). The release profiles also showed greater release from mixed short and long MW matrices than either the short or long MW matrices alone. The release of acetophenone from the matrices was also quantified using solvent extraction and gas chromatography mass spectrometry (GC/MS). Quantification confirmed that more acetophenone released from blended short and long MW materials. Solid state NMR techniques were able to predict that blends of short and long MW matrix polymers have a synergistic effect regarding flavor release phenomena. These effects were overlooked by a traditional thermodynamic based prediction method, the measurement of water to gum matrix partition coefficients, termed log cP.

Finally, in chapter 6, ssNMR techniques were used to further characterize the interaction of the flavor compound, acetophenone, with custom designed polymer materials. The impact of polymer type and MW on the strength of interactions of a flavor compound was examined. Homopolymers of poly-epsilon decalactone (D) and polylactide (L) as well as differentially isotopically labeled DL diblocks of these materials were combined with carbon-13 labeled acetophenone. Cross polarization magic angle spinning (CP-MAS) and insensitive nuclei enhanced by proton transfer (INEPT) confirmed the D block and acetophenone as the mobile components of this system and L as the more rigid component. CP-MAS analysis observed that L block interacts very closely with acetophenone but does not have an effect on the mobility of D blocks when combined with L as a DL diblock. INEPT analysis observed that

acetophenone was more mobile from longer MW DL diblock material and therefore would be predicted to be more available for release during consumption. Two dimensional INEPT analyses confirmed that molecular mobility and therefore potential for release of acetophenone is indeed greater for the D over the L block as well as for longer MW DL over shorter MW DL diblocks. The intermolecular interactions between acetophenone and the D block were further evidenced by two-dimensional nuclear Overhauser effect spectroscopy (NOESY) combined with INEPT. These interactions were reported to occur between the aromatic carbons of acetophenone and the hydrocarbon backbone and side chains of D block. The strength of these interactions was affected by changes to the MW of the polymer matrix and suggested decreased interaction strength between shorter MW polymers and acetophenone. Conversely, this suggests greater flavor release potential from shorter MW DL diblock copolymers.

In summary, the implementation and refinement of ssNMR techniques was able to provide deep insight into the flavor to matrix interactions which govern flavor release. This technology and approach has the ability to make significant gains in the understanding of the mechanisms involved in flavor release from food matrices.

## Table of Contents

Acknowledgements.....	i
Dedication.....	ii
Abstract.....	iii
Table of Contents.....	vii
List of Tables.....	ix
List of Figures.....	x
Chapter 1 Introduction.....	1
Chapter 2 Literature Review .....	4
2.1 Flavor Perception .....	4
2.3 Chewing Gum .....	7
2.3.1 Composition and Production of Chewing Gum.....	7
2.3.2 Use of chewing gum .....	11
2.4 Flavor Release from Chewing Gum .....	13
2.4.1 Flavor Release Models .....	13
2.4.2 Flavor Release Techniques.....	16
2.4.2.1 In vitro Techniques.....	16
2.4.2.2 In vivo Techniques.....	20
2.4.3 Flavor Release Conventions .....	24
2.4.3.1 Gumbase Composition.....	24
2.4.3.2 Chewing Efficiency.....	25
2.4.3.3 Aroma and Taste Interactions.....	26
2.4.3.4 Matrix Design for Optimal Performance.....	28
2.5 The Work Presented.....	29
Chapter 3 Solid State Nuclear Magnetic Resonance as a Tool to Understand Flavor Release .....	31
3.1 Background.....	31
3.2 Principles of Solid State NMR.....	33
3.3 High Resolution-ssNMR Techniques .....	33
3.3.1 Application of One-Dimensional ssNMR Techniques.....	36
3.3.2 Application of Two-Dimensional ssNMR Techniques.....	39

3.4 Interpretation of INEPT signals.....	41
3.4.1 Interpretation of INEPT cross peak intensity .....	42
3.4.2 Interpretation of INEPT cross peak shifts .....	43
3.4.4 Interpretation of degree and direction of cross peak shift.....	47
3.4.5 Quantification of Two –Dimensional INEPT Cross Peak Shifts .....	51
3.5 Interpretation of two-dimensional NOESY-INEPT cross peaks .....	54
3.5.1 Identification of NOESY-INEPT generated cross peaks .....	54
3.5.2 Interpretation of changes to NOESY-INEPT cross peaks.....	55
Chapter 4 Investigation of intermolecular interactions between flavor and conventional gum matrix materials using solid state nuclear magnetic resonance.....	57
4.1 Abstract .....	57
4.2 Introduction.....	58
4.3 Materials and methods.....	62
4.4 Results and Discussion.....	66
Chapter 5 Influence of texture on flavor release dynamics.....	87
5.1 Abstract .....	87
5.2 Introduction.....	88
5.3 Materials and Methods.....	92
5.4 Results and Discussion.....	103
Chapter 6 Investigation of intermolecular interactions between flavor molecules and model matrix polymers using solid state nuclear magnetic resonance .....	120
6.1 Abstract .....	120
6.2 Introduction.....	121
6.3 Materials and Methods.....	123
6.4 Results and Discussion.....	129
Chapter 7 References .....	160
Appendices .....	165
Appendix A: Design and fabrication of an artificial chewing device.....	165

## List of Tables

Table 2-1 Basic Formulation for Standard Stick Chewing Gum (adapted from Fritz) .	8
Table 2-2 Example bubble gum base formulation (adapted from Fritz).....	9
Table 2-3 Basic sweetener system for a sugar-free chewing gum (adapted from Fritz) .	10
Table 3-1 Acronyms for solid state nuclear magnetic resonance (ssNMR) techniques.	35
Table 3-2 Solid state nuclear magnetic resonance (ssNMR) techniques and applicability .....	36
Table 4-1 Matrix to water partition coefficients for flavor compounds in model polymer matrices.* .....	67
Table 4-2 Linear trend lines for <sup>13</sup> C shifts for Melonal versus PIB content.....	80
Table 4-3 Linear trend lines for <sup>13</sup> C shifts for ethyl propionate versus PVAc content .....	81
Table 5-1 Physical properties for model polymer matrices. ....	94
Table 5-2 Sample weights for samples analyzed by ssNMR. ....	102
Table 5-3 Matrix to water partition coefficients for acetophenone in model matrix mixtures*.....	104
Table 5-4 Maximum peak intensities and acetophenone concentration for flavor release profiles generated by APcI-MS. <sup>a</sup> .....	107
Table 5-5 Flavor content in model matrix mixtures before and after artificial chewing. ....	108
Table 6-1 Physical properties for model matrix materials.....	125
Table 6-2 Sample weights for samples analyzed by ssNMR. ....	128
Table 6-3 Gumbase/matrix to water partition coefficients for acetophenone in model matrix materials.....	130
Table 6-4 Carbon and proton resonances for model matrix components and acetophenone.....	146
Table 6-5 Poly-epsilon-decalactone (D) to acetophenone (Aceto) NOESY-INEPT cross peak intensities.....	153
Table 6-6 Acetophenone (Aceto) to poly-epsilon-decalactone (D) NOESY-INEPT cross peak intensities.....	156

## List of Figures

Figure 2-1 The chewing machine coupled to an APCI-MS[16].	19
Figure 2-2 Diagram of chewing device used to evaluate volatile and non-volatile compound release from chewing gum[17].	19
Figure 3-1 Cross peak shift of flavor when free, combined with matrix A and combined with matrix B.	44
Figure 3-2 Cross peak shift of flavor when free, combined with matrix A, matrix B and a combination of A &B near the A domain.	44
Figure 3-3 Cross peak shift of flavor when free, combined with matrix A, matrix B and a combination of A &B near the B domain.	45
Figure 3-4 Cross peak shift of flavor when free, combined with matrix A, matrix B and a combination of A &B.	46
Figure 3-5 Cross peak shift of flavor when free, combined with matrix A, matrix B and a combination of A &B experiencing non-selective exchange.	47
Figure 3-6 Model of cross peak shifts experiencing non-preferential interactions with surrounding matrix.	48
Figure 3-7 Model cross peak shifts plotted against matrix composition with a linear trendline applied, non-preferential interactions.	49
Figure 3-8 Model of cross peak shifts experiencing preferential interactions with surrounding matrix component A.	49
Figure 3-9 Model cross peak shifts plotted against matrix composition with a linear trendline applied, preferential interactions.	50
Figure 3-10 Model of cross peak shifts where no cross peak shift is observed.	50
Figure 4-1 Direct polarization-magic angle spinning (DP-MAS) spectra of Melonal in model polymer matrices.	70
Figure 4-2 Cross polarization-magic angle spinning (CP-MAS) spectra of Melonal in model polymer matrices.	72
Figure 4-3 INEPT spectra (one-dimensional) for Melonal in model matrix mixtures.	74
Figure 4-4 Two-dimensional INEPT spectra for Melonal with corresponding number assignments.	76
Figure 4-5 Two-dimensional INEPT spectra for Melonal (black) overlaid with two-dimensional INEPT spectra for Melonal with PVAc (red). Resonance of the carbonyl carbon enlarged to show detail.	77
Figure 4-6 <sup>13</sup> C chemical shift for one of the methyl carbons (C9) belonging to Melonal plotted against polyisobutylene (PIB) content with linear trendline applied.	79
Figure 4-7 Chemical shift perturbances for Melonal in model polymer matrices.	82
Figure 4-8 Two-dimensional INEPT cross peak for the carbonyl carbon of Melonal in various model matrices	84
Figure 5-1 Acetophenone release profiles from model matrices	106

Figure 5-2 Overlay of one-dimensional DP-MAS spectra for mixtures of acetophenone in model matrices. Aceto=acetophenone, D=polyepsilon decalactone, L =polylactide .....	111
Figure 5-3 Overlay of two-dimensional INEPT spectra for mixtures of acetophenone in model matrices.....	113
Figure 5-4 Overlay of the two-dimensional INEPT cross peak from polylactide in mixtures of acetophenone and model matrices.....	114
Figure 5-5 Overlay of two-dimensional-INEPT acetophenone cross peaks for acetophenone in model matrices. ....	115
Figure 5-6 Acetophenone cross peak intensities in various model matrices plotted against carbon position.....	116
Figure 6-1 DP-MAS spectra for short D and L homopolymers with acetophenone 4 w/w%.....	131
Figure 6-2 DP-MAS spectra for <sup>13</sup> C-DL short MW (blue) and D <sup>13</sup> C-L Long MW (black) with acetophenone 4 w/w%. ....	132
Figure 6-3 CP-MAS spectra for short D and L homopolymers with acetophenone 4 w/w%, x=spinning side band irregularity. ....	134
Figure 6-4 CP-MAS spectra for D with acetophenone, 4 w/w% at -14 (black) and 38°C (blue). ....	135
Figure 6-5 CP-MAS spectra for <sup>13</sup> C-DL short MW (blue) and D <sup>13</sup> C-L Long MW (black) with acetophenone 4 w/w%. ....	136
Figure 6-6 CP-MAS spectra for <sup>13</sup> C-DL short MW (blue) and <sup>13</sup> C-DL Long MW (black) with acetophenone 4 w/w%. ....	137
Figure 6-7 CP-MAS spectra for D <sup>13</sup> C-L short MW (blue) and D <sup>13</sup> C-L Long MW (black) with acetophenone 4 w/w%, x=spinning side band irregularities.....	138
Figure 6-8 One-dimensional INEPT spectra for short D (blue) and L (black) homopolymers with acetophenone 4 w/w%.....	140
Figure 6-9 One-dimensional-INEPT spectra for <sup>13</sup> C-DL short MW (blue) and D <sup>13</sup> C-L Long MW (black) with acetophenone 4 w/w%. ....	141
Figure 6-10 One-dimensional-INEPT spectra for <sup>13</sup> C-DL short MW (blue) and <sup>13</sup> C-DL Long MW (black) with acetophenone 4 w/w%. ....	142
Figure 6-11 One-dimensional-INEPT spectra for D- <sup>13</sup> C L short MW (blue) and D- <sup>13</sup> C L Long MW (black) with acetophenone 4 w/w%. ....	143
Figure 6-12 Labeled structures for model matrix materials and acetophenone, ★ = position of carbon-13 enrichment. ....	145
Figure 6-13 Two-dimensional INEPT spectra for acetophenone combined with model DL matrix materials, 4 w/w%.....	147
Figure 6-14 Acetophenone cross peak intensities in various model matrices plotted against carbon position.....	148
Figure 6-15 Two-dimensional NOESY-INEPT spectra for acetophenone in model DL matrix materials. ....	150

Figure 6-16 Matrix to acetophenone interactions identified by the presence of NOESY-INEPT cross peaks. ....	151
Figure 6-17 Matrix material to acetophenone NOESY-INEPT cross peaks for acetophenone in model matrices. ....	152
Figure 6-18 Acetophenone to matrix interactions identified by the presence of NOESY-INEPT cross peaks. ....	155
Figure A-7-1. Schematic drawing of the design for an artificial chewing device. ....	166
Figure A-7-2 Fabricated artificial chewing device with temperature controller. ....	167
Figure A-7-3 Lower assembly for artificial chewing device. ....	167
Figure A-7-4 Interior of the sample chamber of the chewing device. ....	168
Figure A-7-5 Upper assembly of the artificial chewing device. ....	169
Figure A-7-6 Dimensions for the chewing device in centimeters (cm). ....	170
Figure A-7-7 Dimensions in centimeters for the interior of the sample chamber. ....	170

## **Chapter 1 Introduction**

The study of flavor release from food matrices is a complex and challenging area of flavor research. Previous research in the field has sought to develop predictive physicochemical models[1] that can be used to understand both the equilibrium and non-equilibrium forces thought to drive flavor release from food matrices. These models have focused on increasing understanding of release in a wide range of flavor and food matrices rather than increasing the fundamental understanding of these intermolecular interactions. In general, these studies have acknowledged that the predicted outcome may be modified by texture, chewing efficiency and microstructure of the matrix.

Studies which have examined the kinetic release of flavor from food matrices have relied on classic analytical techniques familiar to flavor chemistry[2]. Many of these techniques involve indirect measurement of flavor release from matrices by extracting the flavor from the matrix. As such, kinetic and static flavor release profiles can be generated and confirm or reject hypotheses from physicochemical models. However, these techniques do not provide information regarding the strength or location of the intermolecular interactions at hand. It is also difficult to account for the impact of matrix textures changes using most of these techniques. The

differences in flavor delivery between samples of different textures can be measured but the impact of the texture change of the molecular interactions themselves is not understood.

The forces which drive flavor release could be better understood by the development of a research approach and techniques which can study thermodynamic and kinetic phenomena. Solid state nuclear magnetic resonance (ssNMR) is a type of NMR which, like solution state NMR, can observe the spectra resulting from excitation of atomic nuclei. As such, NMR has long been used to characterize and elucidate the structures of compounds in many scientific fields. Unlike solution state NMR, ssNMR retains orientation dependent information allowing for the observation of molecular dynamics and the characterization of an intra and intermolecular interactions[3]. This ability to also observe molecular dynamics suggest that can provide a means of characterization and observation of the intermolecular interactions between flavor molecules and food matrices. These interactions can be observed in situ and as the matrix undergoes changes.

This thesis will examine the development and employment of ssNMR techniques as an analytical platform to characterize and observe the dynamics of flavor to matrix interactions. The study and modeling of flavor release will be reviewed in chapter 2. Chapter 3 will introduce the foundational theory supporting solid state NMR along with several

techniques and interpretation of ssNMR spectra resulting from one or two dimensional experiments. These techniques were then applied to a series of studies to assess the type of information that could be added to the field of flavor release study using these newly applied techniques. Chapter 4 details the study of flavor to matrix interactions between selected flavor compounds and conventional gum base matrix materials as the composition of the matrix is adjusted. In chapter 5, a model matrix system was used to examine the effect of matrix texture changes on the flavor to matrix interactions using ssNMR techniques and comparing the information gained to release profiles generated by atmospheric pressure chemical ionization-mass spectrometry (APCI-MS). Lastly, several ssNMR techniques were used to examine the interactions between flavor and well defined model matrices and hypothesize the type and strength of intermolecular interactions occurring between flavor and matrix materials in chapter 6.

## **Chapter 2 Literature Review**

### **2.1 Flavor Perception**

Food provides essential nutrition but the study of food focuses on many aspects of its functionality and involves in-depth research of ingredients from cultivation to consumption. Humans develop powerful sensory associations with the consumption of food, recognized as flavors, which ultimately act as drivers for food selection and can thus have an impact on health. Flavor perception is a combination of sensory inputs from tastants, aromas, textures, trigeminal effects, sounds and memories. While nutrition is an important aspect of food choice, flavor is still the most important factor in food quality and consumer acceptance. Understanding flavor perception has traditionally relied on study and characterization of aroma molecules interacting with the nasal olfactory epithelium and taste molecules interacting with taste receptors. Although elucidating the molecular drivers of sensory perception is important it is only one part of the sensory experience. In order for aromas and tastants to be perceived they ought to be released from food through diffusion, partitioning and mastication and reach aroma and taste receptors. This aspect of flavor perception has been traditionally explored; however, limited information

exists regarding the effect of food composition on flavor release and sensory perception.

## 2.2 Study of Flavor Release and Perception

Study of aroma and taste release is necessary for food researchers to understand how to promote or suppress certain flavor attributes and ultimately optimize food formulations and flavor quality. Research regarding flavor release is often divided along different platforms such as dairy, beverages or confectionary or matrices such as emulsions, foams, solids, liquids, amorphous polymers. This division somewhat reduces system complexity and allows for the study of aroma and taste molecule interactions in the various microenvironments that occur in foods. For example, foams are a discontinuous gas phase dispersed in a continuous liquid phase versus a pie crust which is an amorphous mixture of fats distributed through an amorphous mixture of carbohydrate polymers strengthened by proteins. In general, flavor release has been understood for a given platform or matrix by evaluating the phase changes that occur as the food is consumed and flavor molecules are released. Traditionally, physicochemical properties have been used to predict flavor release from food matrices as phase changes may occur often incorporating non-equilibrium models. The result of such research approaches is the establishment of conventions regarding flavor release specific to the platform or matrix. Often, the studies highlight the complex

interplay between the physicochemical properties, texture and microstructure of the matrix. Among samples of a given food matrix, several textures and microstructures are present due to both natural and artificial processing. Kinetic flavor release studies may measure differences in flavor release among these samples. However, often there is little difference in the chemical composition of the matrix among these samples. This means physicochemical models will fail to predict changes in flavor release among samples with similar matrix composition. Further techniques may be added to determine if there are differences in texture or microstructure. The observations are then combined to hypothesize how or why flavor release is impacted. There are no current approaches which attempt to study the interactions themselves as they are impacted by these changes.

The focus of this thesis is to develop a new technological approach which will have the ability to study flavor to matrix interactions in-depth and in situ. This new analytical platform will be used to characterize the interactions and observe the dynamics of the flavor to matrix interactions. These changes will be observed between matrices that do and do not differ in chemical composition as the texture and microstructure of the matrix are altered.

Many food matrices have been used to study flavor release. These include egg albumen, polysaccharide gels and apple and many others[2, 4-6]. Each has a particular use and the kinetics of the flavor release is unique to

each matrix. For example polysaccharide gels might slowly melt in the mouth releasing flavor over a few minutes whereas foam made from egg albumen may dissolve and release flavor in less than ten seconds. It is important to consider the release mechanism and integrity of the food matrix before attempting to study the kinetics and driving forces of flavor release. Some matrices are well suited for an in depth study of flavor to matrix interactions and flavor release mechanisms. An ideal matrix for flavor release study would be well characterized, able to withstand mastication and available in several textures. Chewing gum fulfills these requirements and will be the selected matrix for the study of flavor to matrix interactions and their implications for flavor release.

## 2.3 Chewing Gum

### 2.3.1 Composition and Production of Chewing Gum

Chewing gum is a confectionary product composed of flavor and sweeteners distributed through a polymeric matrix. The formulation of chewing gum is a largely trade secret process but it is known that chewing gums contain sophisticated sweetener, flavor and matrix (gum base) systems [7]. A basic formulation for chewing gum is displayed in Table 2-1 below.

**Table 2-1 Basic Formulation for Standard Stick Chewing Gum (adapted from Fritz)**

<b>Ingredients</b>	<b>%</b>
Gum base	18.00-20.00%
Glucose syrup	18.00-20.00%
Glycerine	0.50%
Flavour	0.60-1.00%
Color	0.03%
Fruit acids	0.70-2.00%
Sugar	up to 100.00%

Each sub-section of gum (sweetener, flavor and matrix) has a specialized formula. Modern chewing gum matrices contain several polymers, often of more than one molecular weight (MW), in order to optimize properties of the matrix such as extensibility, softness and bounce. For example, bubble gum formulations contain several MWs of polyvinyl acetate (PVAc) which increase the cud volume and hydration capacity of the gum, as shown in Table 2-2 below [8].

**Table 2-2 Example bubble gum base formulation (adapted from Fritz).**

<b>Ingredients</b>	<b>%</b>
Butadiene-Styrene Copolymer (SBR)	4.4
Polyisobutylene	5.6
Microcrystalline wax	11.9
Glyceral ester of partially Hydrogenated wood rosin	22.5
Polyvinyl acetate (PVAc) (12,000-16,000 MW)	6.0
PVAc (35,000-55,000 MW)	15.0
PVAc (65,000-90,000 MW)	4.0
Emulsifier (Glycerol Monostearate)	1.4
Acetylated Monoglyceride (440-455 Saponification value)	8.0
Fats	12.9
Filler	4.1
Glycerine triacetate	4.2

The gum matrices also included softeners, emulsifiers and fillers.

These matrices are composed separately from the sweetener and flavor as they require high heat to produce that would degrade the quality of the sweetener and flavor systems. The suppliers, ingredients and physical properties of matrix materials remain as specialized as they are trade secret.

The sweetener system has also become highly specialized and the sweeteners included in each formulation are carefully selected based on physical and/or sensory properties such as sweetness, crunchiness, water solubility, cooling effect, particle size and whiteness. A basic sweetener system is displayed in Table 2-3 below.[9]

**Table 2-3 Basic sweetener system for a sugar-free chewing gum (adapted from Fritz).**

<b>Ingredients</b>	<b>%</b>
Neosorb® P60W sorbitol powder	66.4
Xylisorb® 90 Xylitol powder	14.7
Mannitol 60	7.4
Lycasin® 80/55 HDS maltitol syrup	11
Aspartame	0.3
Acesulfame-K	0.2

This system includes several polyols which form the bulk sweetener component as well as sweetener syrup and high intensity sweeteners. The selection of the sweetener system is crucial as not only it provides sweetness but is the bulk of most gum formulation, carries the flavor, contributes to a pleasant texture and aids in gum production. Most modern chewing gum also contain encapsulated sweetener. The complexity of the sweetener system has increased over time as a means to extend the pleasant sensory quality of the gum for as long as possible.

As with the matrix and sweetener system the flavors added to the gum are also highly specialized and may contain flavors in several physical states and encapsulated in a variety of ways. The flavors added to the gum systems can vary greatly from a botanical oil to highly formulated mixtures

of thousands of aroma molecules and are specific to whatever sensory perception is desired.

In general, chewing gums are produced by heating the matrix in order to facilitate the incorporation of other ingredients and then mixing in the sweetener, flavor and sometimes, coloring. The ingredients are blended at various speeds and temperatures depending on the type of ingredients, mixer and ingredient metering devices used. The gum is then formed into pieces, sticks, hollow shapes etc. before cooling, conditioning and packaging. Gum is often panned to develop a smooth coating which can also contain sweeteners, colors and flavors. As each segment of production from ingredient sourcing to formulating to production is highly trade secret and patented, most research employed in the academic field references the few publicly available formulations and production schemes or obtains gum from the consumer market.

### 2.3.2 Use of chewing gum

Chewing gum is used by humans for a variety of reasons. It provides a pleasant sensory experience and may also reduce stress and prevent dental caries. It is a confectionary product that is unique in that it is only partially consumed. The remaining product is then discarded primarily due to loss of flavor and texture. Its composition (flavor and sweeteners distributed through a polymeric matrix) creates a water-soluble discontinuous phase

composed of sweeteners distributed through a water insoluble polymer continuous phase. Gum chewing is reviewed in three stages in the confectionary industry and academic research. During the initial stage of chewing (10 to 20 seconds) the gum is masticated into smaller pieces and the saliva begins to hydrate the pieces, extracting sweeteners and forming a cohesive more flexible bolus in the mouth. During the intermediate stage (1 to 8 minutes) mastication of the gum and the extractions of the sweeteners and flavors from the gum by saliva and air continues and ends when most of the sweeteners and other highly water soluble components have been extracted. Lastly, the final stage of chewing is the portion of time after the bulk sweeteners have been extracted until the gum is discarded. This stage can occur as soon as five minutes after chewing begins and last greater than sixty minutes. The total chewing time for gum depends on the gum type, formulation and consumer. It is important to note that these stages usually help dictate how to study certain facets of flavor release from chewing gum. For example, if the focus is to understand the impact of sweetener release on flavor perception, then the immediate stage of gum chewing is of interest. If however, the interaction between aroma molecules and gum matrix is of interest than the final stage of chewing would be most interesting to study for those interactions. This is because during the final stage of chewing the cud is composed largely of matrix and remaining flavor and the confounding presence of sweeteners and fillers is now gone.

Consistent release of the added flavor and sweeteners would be considered ideal product performance but the primary challenge for chewing gum manufacturers is that costly flavor compounds are retained in the matrix even after the gum has been chewed for an extended period. Elucidating flavor to matrix interactions is key to understanding why flavors are retained in the gum matrix and may provide the foundation to engineer gum matrix systems with optimized flavor release.

## 2.4 Flavor Release from Chewing Gum

### 2.4.1 Flavor Release Models

Historically, physicochemical models have been developed to predict flavor release based on the composition of the gum system[10]. These models aid in gum formulation by predicating flavor release without the need to actually measure flavor release using human subjects which is costly, time consuming and challenging due to the great variation between subject responses. Partition coefficients and solubility parameters are the most common physicochemical properties used to develop predictive models [1].

The partition coefficient model involves calculation or measurement of the log of the ratio of concentrations of a compound which has partitioned between two liquid phases, usually octanol and water, at equilibrium and is known as the log P value using Eq. 2-1.

$$\log P_{\text{oct/wat}} = \log \left( \frac{[\text{solute}]_{\text{octanol}}^{\text{un-ionized}}}{[\text{solute}]_{\text{water}}^{\text{un-ionized}}} \right) \quad (2-1)$$

In Eq. 2-1 above, the concentration of the tested compound in the octanol phase ( $\log P_{\text{oct}}$ ) is divided by the concentration in the water phase ( $\log P_{\text{wat}}$ ) to create a ratio of the partitioning behavior of a given compound or material between these two phases. This value is often used as a measure of hydrophobicity. The log P of a gum matrix is calculated by, averaging the log Ps of all of the components of a given matrix, and normalizing by the composition of the matrix. The convention from this model is that non-polar flavor compounds with higher log P values would have an affinity for non-polar matrices with higher log P values and thus be retained in the gum [11]. This principal was further developed in terms specific to gum. In a gum system there are three phases gum, water and air and two partition coefficients the partitioning of flavor between gum and water ( $P_{\text{gw}}$ ) and the partitioning from water to air ( $P_{\text{aw}}$ ). The concentration of flavor released in water can be predicted using the relationship in Eq. 2-2.

$$C_w = C_g P_{\text{gw}} \quad (2-2)$$

Where the concentration in the water ( $C_w$ ) is equal to the concentration in the gas phase ( $C_g$ ) multiplied by the gum water partition coefficient ( $P_{\text{gw}}$ ). The concentration released into the air can be predicted using a similar formula. These relationships are useful to gum formulators however, they are valid in equilibrium conditions, which do not govern during

consumption. Experimental measurements of flavor release tend to be less different than those predicted by partition coefficients[10] indicating the need for more comprehensive approaches to understand flavor-matrix interactions.

Similar to the partition coefficient model the solubility parameter model was developed using calculated solubility parameters, Hildebrand (Eq. 2-3) or Hansen, for the gum matrix.

$$\delta = \sqrt{\frac{\Delta H_v - RT}{V_m}}$$

**H= Enthalpy, R=universal gas constant, T=Temperature, and V<sub>m</sub>=molar volume (2-3)**

Using this principle and assuming a mostly non-polar flavor, the gum matrices with higher solubility parameters promote faster flavor release and those with lower solubility parameters, slower flavor release [10]. This model is considered less predictive as it does not take the effects of all phases involved (gum, water and air) into account.

Both the partition coefficient and solubility parameter models consider the partitioning of flavor among phases at equilibrium but earlier research in the study of flavor release found differences that suggested that flavor release could not be described only in equilibrium conditions [12, 13]. A non-equilibrium partition model was developed that addressed the impact of mass transport, which was thought to be highly predictive of molecular

movement in non-equilibrium conditions. As gum is masticated the release of flavor from gum to saliva is not at equilibrium as saliva is continually renewed and gum is undergoing surface renewal. Mass transport is thought to occur during gum chewing driven by two types of diffusion static and eddy. During storage flavor would migrate within or out of the gum by static diffusion. But, the mechanisms of chewing facilitate eddy diffusion and this is thought to be primarily driven by surface renewal of the gum during mastication [13]. This model concludes that the single most important factor in the release of flavor from gum is increased surface renewal.

These models have been used to examine how changes in the gum matrix formulation might affect the release of flavor [14]. They generally predict changes in flavor release accompanying large changes to the gum matrix composition but are less effective with subtle formulation changes. And while the non-equilibrium model located an important contribution to flavor release mechanisms it did not produce a specific convention for chewing gum formulators to follow in order to increase flavor release.

## 2.4.2 Flavor Release Techniques

### 2.4.2.1 In vitro Techniques

Techniques which aim to study flavor release using in vitro methods generally fall into two categories. Those, which aim to understand and measure the physicochemical properties influencing a gum system and those, which attempt to, gain reliable data from simulating human mastication.

One such measurement of physicochemical properties is the gum to saliva partition coefficient. This special value was developed for the partition coefficient model to study the partitioning of flavor between gum matrix and water specifically [15]. This partitioning of a flavor between simulated saliva or water and gum matrix materials, represented as a log cP, can be measured using analytical techniques. In general, a sample gum matrix is combined with water and flavor in sealed vials and allowed to equilibrate. The residual flavor in the headspace of the vial is then sampled using solid phase micro extraction (SPME) and analyzed using gas chromatography mass spectrometry (GC-MS). Flavors which have high log cP values are highly affinitive to the gum matrix and vice versa for lower log cP values. The conclusions drawn from log cP measurements tend to align with flavor release profiles more than the physicochemical models alone.

Another study, which increased the understanding of physicochemical properties using in vitro methodologies, was conducted by Niederer *et al.* This study measured the partition coefficients of various flavor compounds to matrix materials using inverse gas chromatography and found that release of flavor is influenced by matrix composition and binding strength of flavor

to matrix could be calculated [14]. This study isolated both the matrix materials and flavor compounds to study the interaction in situ between a given matrix material and flavor. Albeit, the partitioning of flavor between more than one matrix material was not measured and a direct observation of the interaction between the matrix and the flavor was not provided.

Simulated chewing devices were also developed in order to study the impact of formulation changes on flavor release without the inherent variation involved with using human subjects. There are several oral parameters of mastication that are at a minimum uncomfortable and at a maximum impossible for a human subject to control. These include chewing rate, chewing force, frequency of breath, force of breath, swallowing, salivary flow and volume. And so, artificial chewing devices were developed in order to simulate mastication and gather flavor release data. Most simplistic devices have the ability to deliver a simulated chew that is temperature controlled, has simulated breath, saliva flow, consistent 'chew' action and the ability to interface with analytical equipment for real-time release measurements [16]. An example from Mielle et al. is shown in Figure 2-1 below[16].

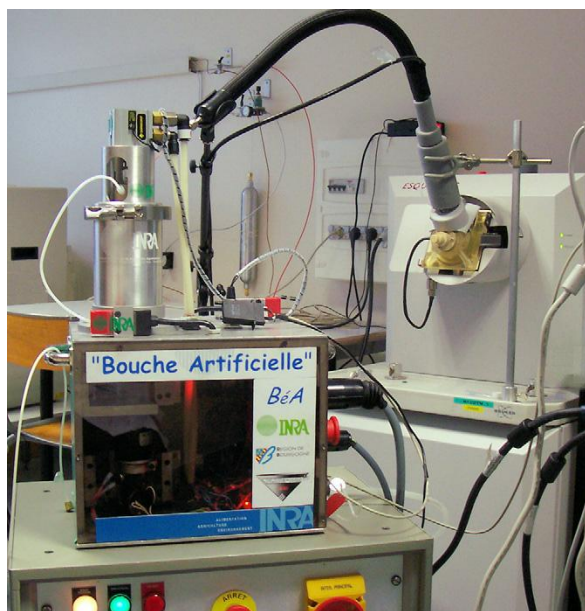


**Figure 2-1**The chewing machine coupled to an APCI-MS[16].

A more detailed diagram of how chewing devices themselves can be designed is from Krause et al. is shown in Figure 2-2 below[17].

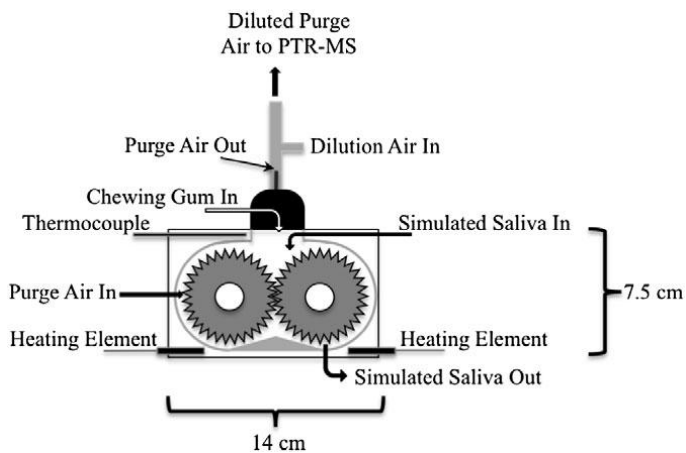


**Figure 2-2** Diagram of chewing device used to evaluate volatile and non-volatile compound release from chewing gum[17].

Most of the devices connect to proton transfer reaction mass spectrometers (PTR-MS) or atmospheric pressure chemical ionization mass

spectrometers (APCI-MS) and are able to record real-time aroma release profiles [15, 17]. While both PTR-MS and APCI-MS are ionization methods which are both lower fragmentation ionization methods, allowing for better real-time analysis, APCI-MS can handle higher flow rates than PTR-MS and also has the ability to ionize and detect more compounds as it does not rely on protonation for ionization. While there is not currently a published report of a device capable of collecting a real-time taste release profile; a fraction collector could be used to collect samples that would be comparable to in vivo taste release profiles [17]. There have been several types of artificial mouths developed in the past few decades and their designs continue to improve [6]. Along the same lines as artificial mouths, artificial noses have also been developed. These remain fairly limited and they need to be programmed for a discreet group of aroma molecules and they do not provide the ability to gather simultaneous aroma and taste profiles.

#### 2.4.2.2 In vivo Techniques

Human subjects have been integral to the study of flavor release for decades. Since gum is intended for human consumption evaluating the acceptability of gum using humans has been crucial. Artificial chewing devices mentioned above have an important place in flavor release study but they cannot reproduce all of the data that human subjects supply. In vivo

flavor release studies involve some combination of sensory evaluation, saliva sampling, gum cud sampling and breath analysis. In general, the techniques are divided by whether taste or aroma molecules are evaluated and whether or not the analysis is conducted in real-time during mastication.

Real-time analysis has remained a feasible option for the analysis of aroma molecules released from gum during chewing. These analysis involve interfacing the breath exiting the nose with analytical equipment as studies have linked sensory perception with in-nose concentration of aroma molecules [18] . Most studies of this nature use proton transfer reaction-mass spectrometry (PTR-MS) or atmospheric pressure chemical ionization-mass spectrometry (APCI-MS) [19, 20]. These methods continue to be advanced in order to increase sensitivity and reproducibility. Sensory analysis can also be considered a real-time analysis as the flavor, sweetness or other sensory perception can be gathered from subjects during chewing [19].

The remaining methods common to flavor release study are not considered real-time methodologies and are usually divided into volatile and non-volatile approaches. In order to quantify the non-volatile flavor components in gum, such as sweetener, saliva samples are collected at discreet time intervals as subjects chew the gum. The non-volatiles of interest are then extracted and analyzed primarily with high performance liquid chromatography (HPLC) coupled with an appropriate detection

methods, such as ultra violet (UV) or mass spectrometry (MS). Residual non-volatiles can also be extracted from gum cuds by dissolving the cud in a suitable solvent and extracting the non-volatiles into an aqueous or other relatively polar solvent prior to HPLC-MS analysis.

Volatiles, primarily aroma molecules, can be analyzed in a variety of ways. Saliva samples gathered in a manner similar to sampling for non-volatiles can be placed in sealed vials, equilibrated at a steady temperature and sampled via solid phase micro-extraction (SPME), static or dynamic headspace sampling and extracted from the saliva using solvent extraction techniques. The samples can then be analyzed via gas chromatography (GC) coupled to either a flame ionization detector (FID) or MS detector. While FID detectors had long been thought to be more stable and sensitive; advances in MS technology have made these techniques more comparable with respect to sensitivity and repeatability. The added bonus with the MS is that it provides mass spectra containing a wealth of structural information. Another more common method of flavor release analysis from gum involves collecting the remaining gum cud after discreet chewing time points. The residual flavor is then extracted from the gum by dissolving the residual matrix in chloroform and extracting the aroma molecules into a suitable solvent prior to GC analysis.

The varied techniques for determining the aroma or taste molecules released during the consumption of gum can be combined to attempt a more

comprehensive flavor release profile. For example, human subjects could chew a sample gum and provide saliva and cud samples at 30seconds, 1 minute, 3 minutes, 5minutes and 15 minutes. Sweeteners released in the saliva and residual aroma compounds in the gum cud could be quantified using the techniques mentioned above and the resulting sweetener and aroma release profile could be compared with sensory data collected at the same time points.

In vivo release methods continue to improve and generate useful data regarding flavor release kinetics. Often, the results of the release studies are compared with the predictions from physicochemical models and hypotheses are generated as to how flavor will be released from the product. When combined, these classical approaches have been somewhat effective in predicting flavor release from the gum matrix. However, this approach cannot adequately predict the mechanisms of flavor release. Traditional flavor analysis techniques can only provide quantitative data of flavor in the expectorated air, saliva or gum cud but no information can be derived regarding the interaction between the flavor and material in its native state. The molecular and physical interaction is destroyed during extraction of the flavor compounds from the gum matrix thus, hindering our understanding of the forces that govern its release and thus the ability to develop optimized formulations for improved flavor release and perception.

## 2.4.3 Flavor Release Conventions

### 2.4.3.1 Gumbase Composition

As previously mentioned the majority of research surrounding flavor release from chewing gum is patented or trade secret. Of the publically available studies many focus on the sweetener system and flavor formulation or encapsulation [21-23]. However, the contribution of gum matrix to flavor release has not been completely neglected.

Previous studies have evaluated the impact of changes to gum matrix composition, mainly increasing polarity of the matrix, on flavor release. Kruetzmann and Nielsen studied flavor release from combinations of elastomers and resins [24] and found that increased resin, particularly PVAc, facilitated flavor release. Similarly Haahr et al., varied the matrix composition and bulk sweetener in gums and found that release of flavor was greater from more polar gum matrices [25]. Both studies examined the overall gum matrix properties, such as polarity, at the system level and measured release behavior that can be compared with predictions from physicochemical models. However, it is expected that changes in gum matrix compositions would be coupled to textural changes. The impact of these changes on flavor release was not addressed and the interactions between flavor and gum matrix were not characterized. Overall, the convention established by

research regarding the composition of the gum base suggests that it should be hydrophilic and a greater proportion of the gum.

#### 2.4.3.2 Chewing Efficiency

While the composition of the gum and gumbase is certainly an important factor which determines the extent to which flavor has the potential to release; ultimately it is the mastication of the gum which provides the mechanism of release. To understand this mechanism the chewing of gum must be studied using human subjects. Work with in vivo measurement of aroma and taste release highlighted the inherent variation when using human subjects. Chewing rate, force of mastication, flavor perception and saliva production can vary greatly between two human panelists. This issue is so pronounced that flavor releaser profiles cannot be averaged between panelists but can be averaged for the same panelist. However, this aspect has been found to be very important as chewing efficiency has been linked to flavor release [12, 13, 25, 26]. In particular the softness of gum has been linked with improved flavor release and this was thought to be the result of increased chewing efficiency by panelists [27, 28].

One study examined the collective differences in chewing behavior and combined that information into a computer model [27]. The study combined measurement of chewing force with flavor release measurements via cud samples from panelists and combined that data with mass transfer

kinetics to develop the simulation program. The simulation was then compared to actual time intensity sensory data. This study concluded that while the simulation was able to return a similar time course for the flavor concentration it was not able to do so without neglecting possibly important factors. The simulation was not able to take breath patterns and data into account partially because there were not adequate methods available which could have generated that data [27].

Overall, since confectioners are not able to dictate the chewing efficiency of consumers the assumption is that if a gum has a soft enough texture it will be able to experience increased gum surface renewal during mastication even by less efficient chewers.

#### 2.4.3.3 Aroma and Taste Interactions

Aroma and taste are often described as two separate processes, the perception of aroma compounds in the nasal olfactory epithelium and the perception of the tastes by taste receptors in the mouth. However, there is now an overwhelming body of research that shows that aroma and taste are often intertwined and that the contributions of aroma and taste to flavor perception should not be overlooked[29]. One of the most important interactions between aroma and taste perception regarding flavor release from gum is the interplay between sweetness and overall flavor perception.

Flavor perception or the degree to which sensory panelists score the flavor intensity of a gum has been evaluated and compared to aroma and taste release profiles [23]. Davidson et al. found that flavor intensity closely followed the sweetener release profile rather than the aroma release profile. This suggests that a sweet taste is so closely associated with flavor perception that sensory panelists fail to recognize the impact of the release of aroma compounds, as indicated with real-time MS analysis, when sweeteners are no longer being released.

The study of the interplay between tastes and aromas during gum chewing is in itself complicated. While it is possible to train panelists and produce time intensity curves of specific attributes while at the same time recording aroma release it is very difficult[19]. Continued research which aims to enhance the technical capabilities for aroma and taste release monitoring is ongoing but still highly specific and tailored to model matrices and individual flavor compounds or very simple mixtures [30]. It would be ideal to have in vivo release curves for all aromas and taste active compounds of interest as well as time intensity sensory information; the combination of the release techniques available is not yet sufficient for elucidating anything but large trends in flavor release from chewing gum. As with other food matrices the focus is not on measuring any and all loss of flavor but in understanding what drives the release of the most impactful flavor molecules for the overall character of the gum [10].

#### 2.4.3.4 Matrix Design for Optimal Performance

The somewhat limited body of publicly available research regarding gum matrix design does indicate some main design guidelines with which to design chewing gum with favorable flavor release properties. However, some of these suggestions contradict each other and others are less feasible with respect to producing an economically feasible gum for the market. For example, it has been suggested that if a gum is sufficiently hard then the flavor release from said gum would be largely diffusion controlled and more efficient [31]. However, several studies have indicated that soft gums actually release flavor more efficiently through facilitating eddy diffusion through increased surface renewal [25, 26]. Also, it has been suggested that increasing the proportion of matrix to other ingredients in the gum would facilitate greater release of aromas. However, this would also require a much greater amount of flavor to be added to the gum and together these would not make economic sense to the manufacturer. In addition, a similar study on drug release from chewing gum actually concluded that a lower proportion of gum matrix contributed to increased drug release [32]. A less disputed suggestion is that gum matrices be largely hydrophilic in order to facilitate the release of primarily hydrophobic flavor systems such as peppermint oils [33]. In general, gum is a very difficult to formulate as it is a multiphase system which needs to balance hydrophobicity. This balance is necessary to provide

a pleasant experience that delivers sweetness, pleasant flavor perception, desirable texture and chewing performance.

While the larger trends regarding the impact of gumbase composition on flavor release are somewhat understood the interplay between flavor to matrix interactions and texture is not. In addition, gum is a highly specialized matrix which requires the ability to finely tune the physical properties of the gum without affecting the balance of hydrophobicity and hydrophilicity in the gum. There is yet to be an approach to understanding flavor release sensitive enough to investigate subtle structural differences between gum matrices.

## 2.5 The Work Presented

It has been suggested by several studies that the contribution of matrix to flavor interactions, in particular possible close associations of flavor compounds with the microstructures of the matrix, may play a large role in flavor release [20, 28, 34-36]. However, studies which investigated the role of matrix composition or texture in flavor release from gum matrix did not investigate the interaction in detail or examine the microstructures that might be present [20, 24, 26]. Increasing the fundamental understanding of flavor to matrix interactions would facilitate flavor release prediction and gum matrix optimization thus the aim of this study was to observe the interaction of flavor with the matrix in its native state.

Techniques for the study of the flavor to matrix interactions were developed using solid state nuclear magnetic resonance (ssNMR). These techniques were applied to understand the interaction of selected flavor compounds with conventional gum matrix materials. The information gained was compared to predicted values obtained using partition coefficient modeling. Next, a carbon-13 enriched model block copolymer matrix was used to investigate how flavor to matrix interactions were affected by changes in the texture of the matrix. Information gained from ssNMR was then compared to flavor release profiles, flavor release quantification and measurements of the partitioning of flavor to the model matrix. Lastly, ssNMR techniques were used to gain atomic level information about the intermolecular interactions between flavor and matrix materials in order to determine the strength and type of intermolecular interactions occurring. The ultimate goal of this work was to develop an analytical platform that would allow researchers to study flavor interactions in situ before and after release from the gum matrix and provide much needed insight for formulation optimization.

## **Chapter 3 Solid State Nuclear Magnetic Resonance as a Tool to Understand Flavor Release**

### **3.1 Background**

Nuclear magnetic resonance (NMR) is a physical phenomenon that has become a vital means of studying atomic nuclei and molecular information. Any isotope with an odd number of protons and/or neutrons can be observed but some are more naturally abundant and easier to observe than other isotopes. The most commonly studied isotopes are  $^1\text{H}$  and  $^{13}\text{C}$ . Sample materials are placed in a large magnetic field with varying electromagnetic pulses that result in frequencies which can be transformed into spectra for interpretation to define molecular dynamics [37]. Most chemists are familiar with its use to analyze materials in solution state in order to provide structural characterization and elucidation information. In addition NMR can be applied to study of the interaction among molecules (i.e. flavors with food matrix materials) and provide a deeper level of information about these interactions at the atomic scale. It is important to consider the types of NMR analysis available, mainly solution or solid state, and select the most appropriate technique for the study of flavor to matrix interactions. The most common type of NMR remains solution state.

Solution state NMR relies on the ability to dissolve sample material in a suitable solvent for analysis and is typically focused on the generation of

proton spectra. In a strong magnetic field such as those used in NMR each chemical bond experiences an uneven distribution of electrons, known as Chemical Shift Anisotropy (CSA)[38]. The strength of which depends on the orientation of the bond relative to the applied field. In addition, spatial proximity between atoms can cause the spin state of an atom to be affected by the spin state of a neighboring atom. This is known as dipolar coupling. CSAs and dipolar coupling can provide information regarding the orientation and spatial proximity of atoms enabling study of the dynamics of chemical bonds during NMR analysis[38]. Due to the solution state of the sample and the Brownian motion present, the orientation dependant anisotropic interactions are canceled out[37]. As such, solution state NMR is commonly used to gain structural and purity information, for example with flavor compounds and food matrix materials, but cannot gather information about the position of the chemical bonds in space. In addition, any interactions between flavor molecules and other species in the sample would be destroyed in preparation for solution state NMR analysis which requires that the sample be dissolved in a suitable solvent for analysis. Conversely, solid state NMR techniques possess the ability to retain and manipulate anisotropic interactions providing the ability to learn about how atoms are oriented in space with respect to each other and as a result gaining more specific information about molecular interactions.

### 3.2 Principles of Solid State NMR

Solid state NMR is a type of NMR which, as the name implies, has been optimized to analyze solid samples. Atoms in solids or other low mobility environments are not free to tumble in their local environment. This means that the CSAs of the chemical bonds and any dipolar coupling in the material are not averaged out as they are in solution state NMR. Historically, this resulted in ssNMR spectra which were broad and much less intense than solution state spectra[3]. The development of high resolution ssNMR (HR-ssNMR) techniques has greatly increased the resolution of ssNMR spectra[39]. In addition, HR-MAS techniques can regain anisotropic information by measuring residual dipolar couplings [39].

Development of HR-ssNMR has resulted in a catalog of techniques comparable to those available for solution state analysis[3]. Through the ability to increase signal resolution and retain anisotropic interactions HR-ssNMR can obtain molecular information from solid, gel or liquid samples providing structural, purity and dynamic information[39].

### 3.3 High Resolution-ssNMR Techniques

There are two main categories of ssNMR techniques which could be used to study flavor interactions, through space and through bond correlations [3, 39, 40]. How these techniques are implemented will determine the extent to which the flavor to matrix interactions can be characterized. These

techniques can be applied to investigate materials varying in rigidity, analyzed over a range of temperatures (-15°C to 45°C), and in more than one dimension Table 3-1. A brief description of these ssNMR techniques are listed below.

- Through Space Correlations: This class of experiments investigates the correlation of atoms that are not chemically bonded by measuring the dipolar couplings between them. The correlations between flavor and matrix components or even between matrix components can be defined.
- Through Bond Correlations: This class of experiments uses scalar or J-coupling to transfer magnetization through chemical bonds from one atom to its nearest neighbors to determine which atoms are bonded to each other. These techniques can be optimized to measure distances from one atom to atoms which are further neighbors as long as all of the atoms are connected by bonds.

**Table 3-1 Acronyms for solid state nuclear magnetic resonance (ssNMR) techniques.**

<b>Acronym</b>	<b>Technique</b>	<b>Brief Description</b>
MAS	Magic Angle Spinning	Process in which the chemical shift anisotropy is averaged out in an effort to achieve the same resolution and sensitivity observed in solution state NMR
DP-MAS	Direct Polarization-Magic Angle Spinning	Polarization of the sample resulting in a $^{13}\text{C}$ shift pattern which reflects all of the carbons present in the sample
CP-MAS	Cross-Polarization-Magic Angle Spinning	Polarization of protons transferred to carbons resulting in chemical shifts associated with carbons that are attached to protons only
INEPT	Insensitive Nuclei Enhanced Proton Transfer	1D or 2D spectra generated by through bond transfer, allows comparison between molecular interactions usually associated with the more mobile species in a system
TOBSY	Total Through Bond Correlation Spectroscopy	2D spectra generated by through bond transfer, can be used to sequentially assign a structure
NOESY	Nuclear Overhauser Effect Spectroscopy	2D spectra generated through space between proton within a molecule, especially helpful with very large biopolymers
HETCOR	Heteronuclear Correlation	Similar to COSY in solution state NMR, this technique generates a 2D spectra and can observe changes in shift associated with the less mobile species
DARR	Dipolar Assisted Rotational Resonance	2D experiment which can provide distance information regarding molecular interactions and can be used to determine the exact type of molecular interactions

**Table 3-2 Solid state nuclear magnetic resonance (ssNMR) techniques and applicability**

Experiment	Through Bond	Through Space	Mobile Species	Rigid Species	1D	2D
DP-MAS						
CP-MAS						
INEPT						
TOBSY						
NOESY						
HETCOR						
DARR						

### 3.3.1 Application of One-Dimensional ssNMR Techniques

The three main one-dimensional techniques common to ssNMR (DP-MAS, CP-MAS and INEPT, Table 3-2) are often used in combination to investigate molecular information. During HR-ssNMR analysis it is common to first analyze the sample using one-dimensional techniques before moving on to two dimensional techniques [3]. One-dimensional spectra, mostly carbon-13 spectra for ssNMR, can show whether there is enough resolution to study the target flavor compound(s), the matrix materials or both. Often, these techniques are optimized to increase resolution prior to beginning two-dimensional analysis. Once the resolution is optimized the one-dimensional spectra can furthermore be used to confirm the concentration of

sample components[41]. For example, if samples have been prepared to contain the same amount of a given small molecule then the peaks attributed to that molecule should be the same intensity across all DP-MAS spectra. These techniques can also confirm if the compounds in the sample mixture are behaving as mobile or rigid species in the sample mixture[42].

Considering a matrix which is thought to be rigid at analytical temperature with a liquid flavor it is expected that spectral peaks associated with the flavor and the matrix in would be observed in the DP-MAS spectra. However, the CP-MAS spectra (see Table 3.2) would be expected to show only peaks associated with the rigid matrix material. Whereas, the one-dimensional INEPT spectra (Table 3-2) would show primarily peaks associated with the mobile fraction of the flavor compounds. This method of combined experiments can be used to determine which matrix components are mobile at a given temperature and even hypothesize whether the flavor might be closely associating, possibly interacting with the matrix material. These approaches have also been used to examine crystalline versus amorphous blends of materials[43, 44]. In another example, if spectral peaks associated with the flavor are observed in the CP-MAS spectra this suggests that the flavor may be interacting 'closely' with matrix material and is no longer mobile. This suggests very close associations of the flavor with the matrix material.

The peak shape and line shape of the one-dimensional spectra can also be used to provide information about intermolecular interactions and molecular spin dynamics[45]. If a polymer matrix material is analyzed at two different temperatures, one below its glass transition temperature ( $T_g$ ) and one above, a difference in the line width of the ssNMR spectra is expected to be observed[46]. In this case if the peak broadening is observed in the spectra collected above the  $T_g$  this is thought to occur because the sample is more mobile and the global average of atoms that are observed is wider thus broadening the peak shape. A similar convention can be used to examine the impact of matrix on flavor spin dynamics. If the concentration of flavor in a mixture of flavor and matrix materials is kept constant and the matrix is altered there may be a difference in the line width of the flavor peaks. If the flavor is unaffected by the presence of the matrix materials it is expected that the flavor peaks have a line width and peak shape similar to when the flavor is analyzed without the presence of matrix material. If the line width or peak shape of the flavor is broadened this suggests that the flavor atoms are being influenced by the spin dynamics of the matrix materials suggesting a very close proximity in space.

In summary, one-dimensional spectra can be examined to gain information about the physical state (mobile or rigid), the impact of temperature and the interactions between a small molecule and matrix materials. However, one-dimensional analysis can lack the sensitivity needed

for the analysis of very minor constituents in food systems such as flavors, antioxidants, preservatives and some enzymes. For example, changes in the one-dimensional spectra of flavor and gum matrix would be observed when the flavor is added at a 25 w/w% concentration but not at 4 w/w%, a more common concentration of flavor for a commercial gum formulation. There are two common ways to increase the sensitivity of one-dimensional ssNMR. One, increase the number of scans and therefore the analysis time for the sample and two, isotopically label the compounds of interest. Two-dimensional analysis has the possibility to observe these interactions at a lower level of concentration.

### 3.3.2 Application of Two-Dimensional ssNMR Techniques

Two-dimensional ssNMR much like one-dimensional ssNMR often involves the use of several techniques to gain information about carbons and protons present in a mixture. The main goal of this study is to investigate interactions between small flavor molecules and polymeric matrix materials which may vary in texture. Several two-dimensional techniques can be employed to gain more information about the flavor molecules and the matrix components present in the sample. The added  $^1\text{H}$  dimension provides greater specificity, the ability to differentiate between carbons which might have very similar carbon-13 shifts. In two-dimensional analysis cross peaks

with unique  $^{13}\text{C}$  and  $^1\text{H}$  shifts are obtained for most atoms in the sample. This will provide site specific information for atoms belonging to the flavor as well as the matrix components. In addition, more detailed observations of flavor compounds and matrices may be gathered from two-dimensional analysis even if these changes may not be visible in the one-dimensional analysis due to the low concentration of flavor in the sample. As with the one-dimensional analysis, two-dimensional analytical technique can also be separated into techniques which focus on mobile or rigid species Table 3-2. The most appropriate two-dimensional techniques for the observation of rigid components of flavor and matrix mixtures would be HETCOR and DARR (Table 3-2)[47]. However, since one of the goals of this project is to advance the understanding of the flavor to matrix interactions in effort to further understanding of flavor release drivers; it may be more relevant to use techniques which observe the more mobile species[42, 48]. Whether through bond or through space methodologies are more appropriate for a system containing flavor molecules and polymer matrices should also be considered. Since it can be reasonably expected that flavor is not consistently and frequently covalently bonding with matrix materials, selecting through space two dimensional techniques which focus on the more mobile species in a sample is a more logical choice. INEPT and NOESY-INEPT (Table 3-2) were selected as the most appropriate techniques to obtain information about the flavor to matrix interactions[42, 48, 49].

### 3.4 Interpretation of INEPT signals

When a sample is analyzed using the INEPT technique, a one-dimensional experiment is completed prior to optimize the correct amount of scans and therefore time needed to perform the two dimensional spectra acquisition. The INEPT experiment is based on signal enhancement through the polarization of proton which is then transferred to adjacent carbons[50]. This means that no spectra will be produced for carbons without adjacent proton such as carbonyls. Next, a two dimensional spectra with  $^{13}\text{C}$  on the x-axis and  $^1\text{H}$  on the y-axis is obtained. Only the two dimensional cross peaks of mobile carbon species are visible. The studies undertaken in this thesis use mixtures of flavor and model matrix polymers to study the interactions of flavors with matrix materials. Both the flavor and some of the model matrix polymers are expected to be sources of mobile carbon species during INEPT analysis. However, the focus of the INEPT interpretation in this case will be the flavor compound cross peaks rather than the flavor and mobile matrix polymer cross peaks. This will focus the discussion on how two-dimensional ssNMR techniques might further understanding of how small molecules are impacted by changes to their surrounding matrix. Insight into the interaction of flavor and matrix materials will be gained through interpreting the intensity, shift[40], degree of shift, direction of shift and shape of these cross peaks. Each cross peak is examined independently.

### 3.4.1 Interpretation of INEPT cross peak intensity

When comparing the same cross peak between two different samples, differences in intensity can be attributed to two factors, the sample composition and differences in the dynamics the atom is experiencing. Before the intensities of either one-dimensional or two-dimensional INEPT peaks of a small molecule in different matrices can be compared the analyte concentration must be confirmed to be equal. DP-MAS spectra can be utilized to confirm equivalent analyte concentrations based on peak intensities and line widths. This step rules out sample composition as a source of change in cross peak intensity.

The INEPT experiments observe only mobile species in a sample and in general the intensity of INEPT peaks can be correlated to mobility. This means that if a small molecule is combined with sample matrices of the same chemical properties but different physical properties differences in mobility and therefore peak intensity may be observed[42].

Subsequently any changes in intensity of the INEPT peaks can be correlated to changes in mobility of the analytes in the sample. The intensity of the INEPT peaks can be plotted against the matrix type or composition to evaluate changes in mobility of the analyte. Larger intensities indicate greater mobility of the molecule in the sample matrix.

### 3.4.2 Interpretation of INEPT cross peak shifts

To investigate interactions of flavor molecules with matrix materials, the flavor could be first monitored by INEPT alone (in pure form) and then combined with matrix materials to the cross peaks compared. When the flavor is alone, the flavor molecule can freely tumble in space absent any other local magnetic environments which might affect their spin dynamics. If another molecular species is present and is close enough to disturb the local magnetic environment of the flavor molecule, generally less than nine angstroms, then the cross peak shifts[51]. The size and direction of this shift is dependent on the species that caused the shift such that a cross peak shift may be unique to the matrix in which the flavor is interacting. If a hypothetical system of a flavor and two polymer matrices A and B is considered several different scenarios in which a flavor cross peak shifts might be observed. For example, when the flavor is combined with polymer matrix 'A' a shift in one direction might be observed and when combined with 'B' another direction for a given cross peak such as in Figure 3-1 below. For further illustration, the flavor compound associated with the A domain is be termed + A or + B (associated with the B domain).

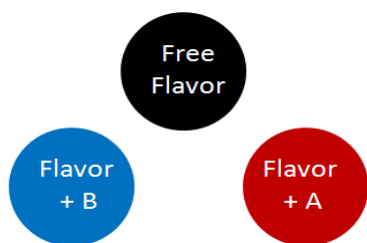


**Figure 3-1 Cross peak shift of flavor when free, combined with matrix A and combined with matrix B.**

These cross peak shifts are the average of all the interactions for this particular carbon atom. Thus this approach can provide insights into flavor interactions. For example, if the flavor compound in this binary mixture of polymers (A and B) has an observed cross peak shift closer to the A domain as in Figure 3-2, this suggests that this atom is largely interacting with polymer 'A'. Or moreover, the averaged observed signal for this crosspeak is experiencing a local magnetic environment resembling the 'A' domain.

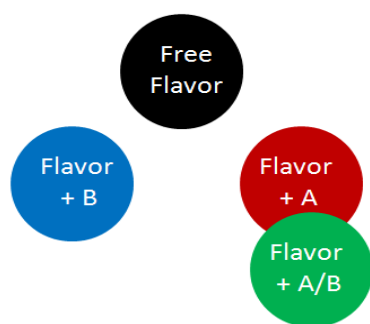


**Figure 3-2 Cross peak shift of flavor when free, combined with matrix A, matrix B and a combination of A & B near the A domain.**

Conversely if the cross peak shift is closer to the B domain seen in Figure 3-3, this suggests that this atom is largely interacting with polymer 'B'.

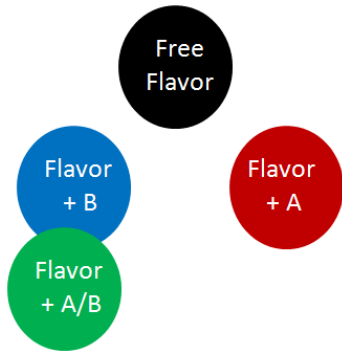


**Figure 3-3 Cross peak shift of flavor when free, combined with matrix A, matrix B and a combination of A &B near the B domain.**

Alternatively, if the cross peak is shifted between the A and B domains as in Figure 3-4, the interactions are less clear but suggest that some of the atoms are experiencing a local magnetic environment resembling the 'A' domain and some the 'B' domain such that the average of these interaction results in a cross peak between the two domains. This shift could also result from the interactions occurring at the interface between an 'A' domain and a 'B' domain.

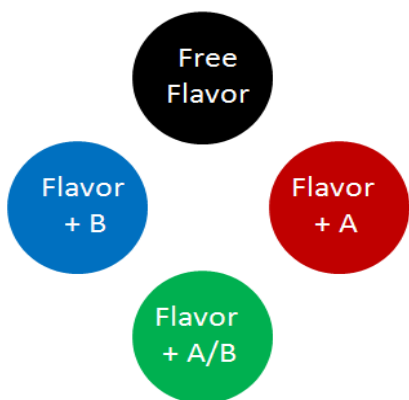


**Figure 3-4 Cross peak shift of flavor when free, combined with matrix A, matrix B and a combination of A &B.**

### 3.4.3 Interpretation of cross peak shape

The shape of the cross peak can also provide information as to the exchange phenomena being observed. Remember that the NMR spectra obtained in either a one or two dimensional analysis is the result of an average of all of the observed phenomena during the course of the experiment. The spectra obtained are a snapshot of the interactions occurring at a given time much like the shutter on a camera. For two dimensional cross peaks a classical circular peak shape implies that at the point at which the shutter opens the peak is in that position and most of the atom are in one position or domain as seen in Figure 3-4, referred to as selective exchange[51]. However, it could happen that sometimes the cross peak is closer to A domain and the next time the shutter is open the cross

peak is closer to the B domain. The average would resemble what is shown in Figure 3-5, where the atom is undergoing intermediate exchange phenomena.

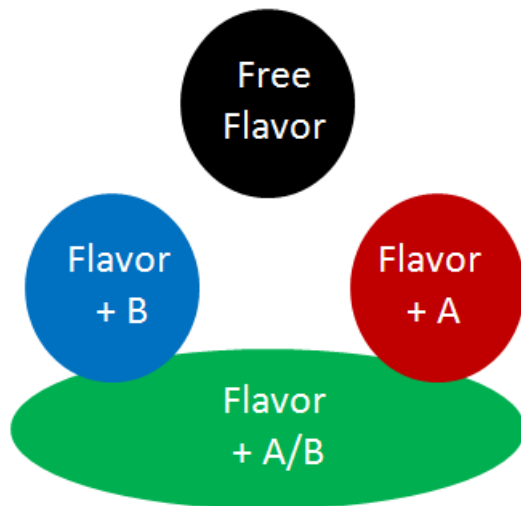


**Figure 3-5 Cross peak shift of flavor when free, combined with matrix A, matrix B and a combination of A & B experiencing non-selective exchange.**

#### 3.4.4 Interpretation of degree and direction of cross peak shift

Shifts in cross peak position can be the result of changes in the sample composition and do not indicate the preference of an atom for a particular domain. For example, if the mixture is largely made up of polymer matrix A then it is reasonable that the cross peak shift would be closer to the A domain. These phenomena are 'non-preferential interactions'. The cross peak is shifted to the A domain not because it prefers to associate with matrix A but, because the sample

matrix is largely composed of matrix A. If mixtures of flavor with blends of A and B ranging in composition were analyzed, the expected cross peak shifts would resemble Figure 3-6.

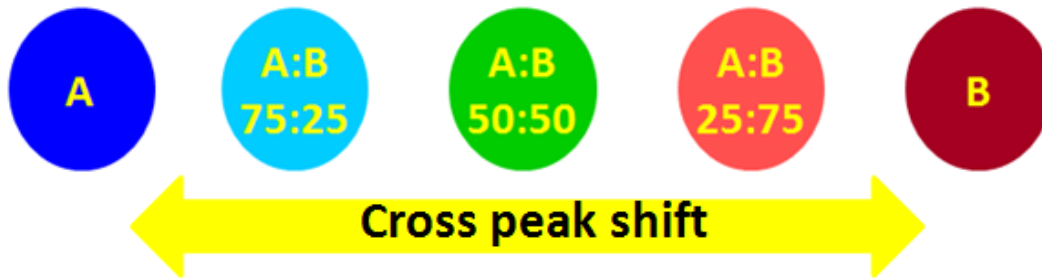


**Figure 3-6 Model of cross peak shifts experiencing non-preferential interactions with surrounding matrix.**

When the flavor is mixed with a 50:50 w/w% blend of A and B matrix materials and the flavor does not preferentially bind with either A or B the expected shift of the flavor cross peaks will reside halfway between the A and B domain. Likewise, if the flavor were mixed with a 75:25 w/w% blend of A and B respectively, then the flavor cross peak would be shifted closer to the A domain and further from the B domain proportional to the composition of the matrix blend. As such, non-preferential interactions between flavor and matrix materials can be determined using linear regression. Plotting the shift in the carbon-13 dimension against the composition of the matrix content would be expected to produce a linear relationship between the cross peak shift in the carbon-13 dimension and the matrix content Figure 3-7.

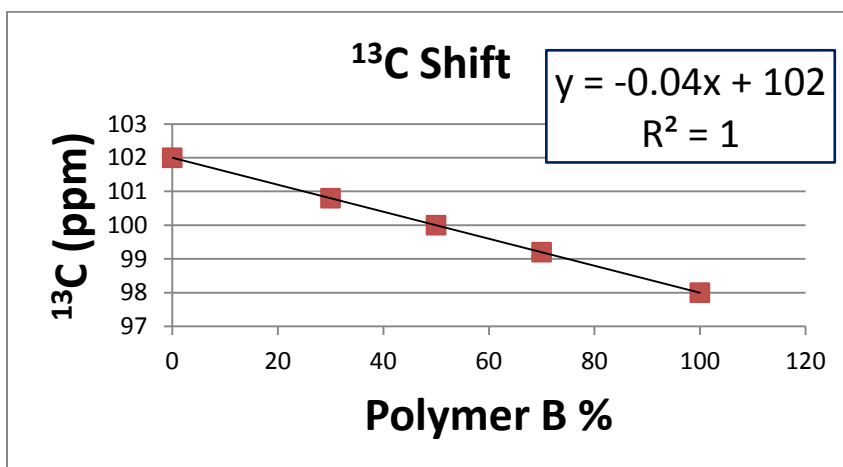


Figure 3-7 Model cross peak shifts plotted against matrix composition with a linear trendline applied, non-preferential interactions.

If however, the flavor prefers to interact with one type of polymer matrix over the other, for example with preference for polymer A domain over polymer B, shifts such as those displayed in Figure 3-8 would be observed.



Figure 3-8 Model of cross peak shifts experiencing preferential interactions with surrounding matrix component A.

Plotting the shift in the carbon dimension versus polymer B content in this case would result in cross peak shifts which no longer have a linear relationship with the matrix composition as shown in Figure 3-9.

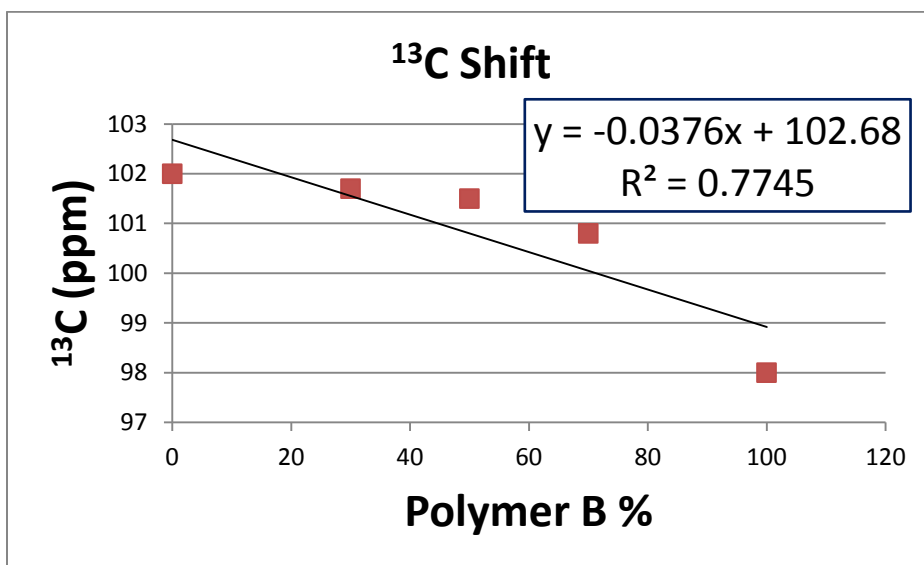


**Figure 3-9 Model cross peak shifts plotted against matrix composition with a linear trendline applied, preferential interactions.**

In yet another case, analysis of a flavor combined with polymer matrices having varying chemical compositions may not result in an apparent shift in the cross peak. Given the previous examples, it would be surmised that there are no interactions between the flavor and the matrices (close enough) to cause a shift in the cross peak. As such, the cross peaks of the flavor in the samples matrices would overlay with each other with no discernible shift as shown in Figure 3-10.

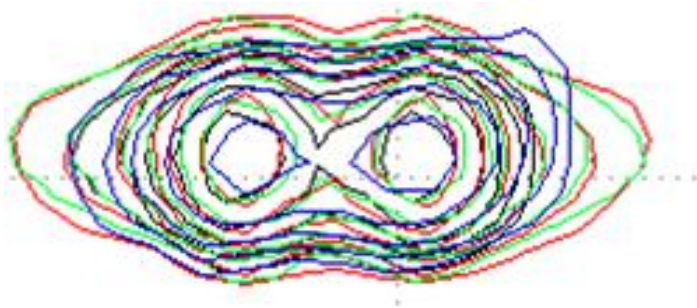


**Figure 3-10 Model of cross peak shifts where no cross peak shift is observed.**

Another potential aspect to consider is the degree to which the cross peaks shift in both the carbon (x-axis) and proton direction (y-axis) particularly as these dimensions do not have the same scaling and are difficult to combine without applying some conventions.

### 3.4.5 Quantification of Two -Dimensional INEPT Cross Peak Shifts

Chemical shift mapping is a technique familiar to the field of structural biology and is used to determine the binding site of a protein structure[52]. In order to determine the binding site, typically first an heteronuclear single quantum coherence spectroscopy (HSQC) experiment is performed on a <sup>15</sup>N labeled polymer. This results in a two-dimensional spectra of the N-H bonds in the protein which can be used as a 'fingerprint' of the protein at a given concentration, pH, temperature and solvent condition. Ligand is then titrated in and several more HSQC spectra obtained. Overall, some of the N-H peaks shifts while others do not, if no shifts are observed the ligand are not binding to the protein. Next, chemical shift mapping is used to determine the binding site of the ligand on the protein. Chemical shift perturbances (CSPs) are calculated using Equation 3-1 below.

$$\sqrt{[(\Delta^1\text{H})^2 + \{0.13(\Delta^{15}\text{N})\}^2]} \quad (3-1)$$

As shown in Eq. 3-1 this calculation accounts for the shift change ( $\Delta$ ) in both the proton and nitrogen dimensions. A weighting factor of 0.13 was used to account

for the differences between the  $^1\text{H}$  and  $^{15}\text{N}$  scales. The resulting values for each peak are then plotted against the amino acid structure with larger values implying greater movement in the protein as the ligand binds and therefore suggesting a binding site. These CSPs are mapped onto the protein structure to determine the binding site.

A similar analytical approach can be considered the analysis of flavor interacts with matrices. The two-dimensional INEPT spectra for flavor can be used as an analogous fingerprint similar to the HSQC of the  $^{15}\text{N}$  labeled protein[52]. Addition of matrix or mixtures of matrix materials perturbs the chemical shift if there is a very close interaction or conformational change. The proximity and strength of these shifts can also be used to determine where on the flavor molecule the interaction with matrix is occurring. Further, a weighting factor can be applied to combine chemical shift data from both nuclei into one measure to compare and quantify degree of chemical shift perturbation across a molecule[52].

There are a few differences between how CSPs and chemical shift mapping are used to study ligand to protein interactions and studying flavor to matrix interactions that need to be considered. With protein systems this process is based on examining the peaks for the protein or larger, less mobile species as a smaller more mobile species (ligand) is titrated into the mixture[53]. In the case of investigating flavor and matrix interactions, the primary goal is to examine how the small molecule, the flavor, is impacted by its surrounding larger, less mobile matrix. INEPT techniques were selected to best suit this observational goal. This investigation also employs non-isotopically labeled flavor and matrix materials

unlike the isotopically labeled amino acids and proteins common to studying protein systems. Lastly, where in protein studies they work from a discreet set of amino acids and are able to consistently label one bond type, N-H, in this study peaks are obtained from most of the carbons in the flavor molecule[53]. The INEPT technique primarily observes the cross peaks for carbons with adjacent protons and the flavor and matrix materials contain several types of carbons with adjacent protons. This means the INEPT technique will detect different types of carbons all containing C-H bonds such as benzene or aliphatic carbons. Similar to the protein analysis, a weighting factor can be applied and CSPs can be calculated using equation 3-2[52].

$$\sqrt{[(\Delta^{1}\text{H})^2 + \{0.185(\Delta^{13}\text{C})\}^2]} \quad (3-2)$$

As shown in Eq. 3-2 above this calculation accounts for the shift change ( $\Delta$ ) in both the proton and carbon dimensions between a given peak and a baseline or reference point. A weighting factor of 0.185 was used to account of the differences between the  $^1\text{H}$  and  $^{13}\text{C}$  scales[52]. These values can be used to determine which atom in the flavor molecule is most affected by the presence of matrix materials or changes to those matrix materials.

### 3.5 Interpretation of two-dimensional NOESY-INEPT cross peaks

The two dimensional nuclear Overhauser effect spectroscopy (NOESY)-INEPT experiment is a hybrid of high resolution solution and solid state NMR techniques. The strength of this technique is the ability to detect intermolecular interactions between atoms of different species through space that are less than 9Å apart[54]. Primarily this technique can be used to localize which atoms participate in intermolecular interactions from the direction of either participant. This technique has the ability to localize the interactions between any two atoms of any component in a given sample. For example, interactions between small molecules and a polymer matrix could be detected from the small molecule to the matrix and from the matrix to the small molecule[54].

#### 3.5.1 Identification of NOESY-INEPT generated cross peaks

The technical basis of the NOESY-INEPT is the ability to perform proton transfer from one species to another using NOESY and then INEPT to transfer from the receiving proton to an adjacent carbon. Identification of NOESY-INEPT peaks is initially similar to two-dimensional NOESY[55, 56]. Given a system of a small molecule and matrix there are two types of NOESY-INEPT cross peaks to identify; small molecule to matrix and matrix to small molecule. Matrix to small molecule interactions would be observed by proton transfer from a proton belonging to the matrix through space to a proton belonging to the small molecule using NOESY and

then transferrring from the small molecule proton to the small molecule carbon. This would result in a NOESY-INEPT crosspeak with a proton shift (y-axis) corresponding to a matrix proton resonance and a carbon shift (x-axis) corresponding to a small molecule carbon resonance. The opposite is true for small molecule to matrix NOESY-INEPT cross peaks which would have a proton shift (y-axis) corresponding to a small molecule resonance and a carbon shift (x-axis) corresponding to a matrix resonance. In order to identify the NOESY-INEPT cross peaks and separate them from the two-dimensional INEPT peaks present it is first necessary to record the two-dimensional INEPT proton and carbon resonances of each component in the sample. This makes screening two-dimensional NOESY-INEPT spectra for small molecule to matrix and matrix to small molecule cross peaks less complicated since the carbon and proton shifts can be predicted.

### 3.5.2 Interpretation of changes to NOESY-INEPT cross peaks

Since NOESY-INEPT involves the hybridization of techniques the interpretation of changes to these cross peaks is less well understood than the more classic techniques on which it is based[55, 56]. This technique is dependent on both the distance between the protons which are interacting and observed using NOESY and the dynamics which can typically be observed using INEPT[54]. It is difficult to deconvolute these two effects and the interpretation of this type of data is still somewhat unclear. In order to quantify the distance between to proton participating in an intermolecular interaction it would be necessary to run several NOESY-INEPT experiments with varying mixing times in the pulse programs.[55] Then , the build-

up of each peak would need to be examined to approximate the distance between the two protons[54].

As with most NMR techniques it is important to carefully consider the composition of the sample, if known, and evaluate the impact of any isotopic enrichment. For example, consider a system that is largely polymer matrix with 4% small molecule. A NOESY-INEPT experiment would create cross peaks representative of any intermolecular interactions between the two species. However, the matrix to small molecule interaction cross peaks would be expected to be much more intense than the small molecule to matrix interactions because the sample is 96% matrix and only 4% small molecule.

## **Chapter 4 Investigation of intermolecular interactions between flavor and conventional gum matrix materials using solid state nuclear magnetic resonance.**

### 4.1 Abstract

The interaction of flavor molecules with gum matrix materials is relatively uncharacterized. Solid state NMR(ssNMR) shows promise as an analytical tool that could be used to provide site-specific insight into the dynamics of flavor to matrix interactions. Melonal and ethyl propionate were combined with model gum matrix materials, polyisobutylene (PIB) and polyvinyl acetate (PVAc). The interaction of these flavors with the model gum matrix as the chemical composition of the matrix changes was studied. Water to gum matrix partition coefficients, termed  $\log c_P$ , were measured for each flavor in the model matrices. However, there were not clear significant differences between  $\log c_P$  values of flavor in different model matrices. One dimensional ssNMR experiments clearly identified the flavor and model matrix components and observed some information on the flavor and matrix dynamics. Cross polarization magic angle spinning (CP-MAS) determined that the rigid component of the matrix was PVAc. In sensitive nuclei enhanced by proton transfer (INEPT) determined that melonal and PIB were more mobile components of the flavor and matrix mixtures. Further, two dimensional INEPT experiments showed that melonal preferentially binds

with PIB over PVAc and ethyl propionate preferentially binds with PVAc over PIB. Lastly, chemical shift perturbances were calculated for most of the carbon positions of melonal. These values determined that the carbonyl carbon was the most altered, suggesting it drives the interaction of melonal with the model gum matrix. This work and the development of this approach revealed that preferential interactions exist between flavors and a model matrix materials and that these interactions can be studied by ssNMR even when they have been overlooked by the measurement of partition coefficients.

## 4.2 Introduction

The interactions between flavor compounds and their surrounding food matrix are important yet relatively uncharacterized phenomena. These interactions are key to understanding the forces that govern flavor release. Deeper understanding of these forces can provide tools to improve flavor release from food matrices.

Past research has sought to understand the mechanisms of flavor release by examining the overall affinity or 'liking' of flavor to matrices[8]. Solubility parameters and partition coefficients have been used to investigate the likelihood of flavor release from food matrices[1]. Conventions that predict flavor release from food matrices regarding other release drivers

have been investigated. Sostmann et al. sub-divided flavor release behavior into three groups dependent on the polarity of the chewing gum matrix material[26]. Unfortunately, these physicochemical models do not provide in depth information about the type or nature of interaction(s) occurring, nor adequate predict the release of flavor. The physicochemical models cannot determine whether interactions between flavor and matrix are occurring primarily between the flavor and one of a few of the matrix components. Rather, the physicochemical models study the matrix as a whole neglecting that the matrix may be composed of several components, some of which are much more favorable to the formation of intermolecular interactions with flavor than others. Also, since the physicochemical models involve indirect study of these interactions they do not possess the ability to characterize the interaction identifying the interaction participants and the type of intermolecular binding present. In addition, studies have shown that the physicochemical models cannot accurately predict release especially in cases where intermolecular interactions and texture effects modify the flavor release dynamics[15, 35]. .

The measurement of gum base-to-water partition coefficients ( $\log cP$ ) has been widely used as an estimate of flavor release but has limited sensitivity to subtle changes in matrix composition[15]. Predictive models have been related to flavor release profiles generated during consumption or from model 'mouth' systems, monitored by analytical equipment[15, 17, 19].

Together these approaches are currently the best methods employed to understand flavor release. However, what is predicted using physicochemical models and partition measurements does not always match what is observed in flavor release profiles during consumption[57]. This may be due to lack of sensitivity to formulation changes in the physicochemical models, variability inherent to flavor release profiles gathered from human subjects and inability to gather in situ information regarding the interactions between flavor and matrix materials.

Solid state nuclear magnetic resonance (ssNMR) has been used to characterize interactions of small molecule ligands with complex proteins and membranes[48, 53]. These techniques generate observations of the interactions between small molecules and larger macromolecules on the atomic scale. They have been used to locate binding sites of ligands on enzymes and determine which amino acids form the binding site[53]. They are even sensitive enough to observe changes in the dynamics of the intermolecular interactions[58-60]. Based on these prior findings, this analytical technology shows promise to investigate how the intermolecular interactions between flavor molecules and gum matrix materials, specifically, are affected by changes to the matrix composition.

Two dimensional insensitive nuclei enhanced by proton transfer (INEPT) can be used to obtain a 'fingerprint' of the atoms of the flavor molecules. This 'fingerprint' can then be examined for shift changes as matrix

materials are added to the flavor individually and combined into mixed matrix materials simulating a simple model gum matrix.

The overall goal of the current study is to examine the interaction of selected flavor compounds with a model matrix system. Melonal and ethyl propionate will be combined with polyisobutylene (PIB) and polyvinyl acetate (PVAc), both common components of gum matrix[8], as well as mixtures of PIB and PVAc. The log cP values for the selected flavors in PIB, PVAc and mixtures of PIB and PVAc will be measured and compared to what is observed using ssNMR. One dimensional direct polarization magic angle spinning (DP-MAS), cross polarization-magic angle spinning (CP-MAS) and INEPT will be performed to confirm peak identity, evaluate the peak shapes and look for changes in the dynamics of the flavor and matrix materials and optimize ssNMR parameters. Two dimensional INEPT will be employed to evaluate the affect of matrix composition on the intermolecular interactions between the selected flavor molecules and the matrix materials. Each atomic position in the flavor compounds will be examined to determine how the dynamics of the atom in the matrix mixture are impacted by changes to the matrix composition.

### 4.3 Materials and methods

**Model matrix materials.** Polyvinyl acetate (PVAc) 10 to 15kDa, Polyisobutylene (PIB) 400kDa and blends of PVAc and PIB (30:70, 50:50 and 70:30 w/w%) were obtained by an industrial partner. Melonal (2,6 dimethyl heptenal), ethyl propionate, and methyl hexanoate were obtained from Sigma (Sigma Aldrich, St. Louis MO). Hexanes and acetone were from Fisher Scientific (Fisher Scientific, Pittsburgh, PA)

**Measurement of Gum to Water Partition Coefficients (Log cP).** Matrix materials were processed into pieces of less than 2 cubic mm with either a razor blade or cryo-grinding with a blender and liquid nitrogen. Only materials which were processed to be less than 2 cubic mm were used for log cP and ssNMR analysis.

Stock solutions of ethyl propionate and Melonal were prepared at 10 w/w% in methanol. An internal standard solution of methyl hexanoate 100ppm in hexane:acetone 90:10 vol/vol was also prepared.

Processed materials (0.4 g) were placed in 20mL vials, 2mL of deionized distilled water were added. Aliquots of Melonal (30uL) and ethyl propionate (30uL) were added to individual vials of material and water. Vials were sealed with air-tight screw caps and equilibrated at 38°C in a shaking water bath for 72hours. Portions of the aqueous phase (1.5mL) were

removed from the sample vials and transferred to microfuge tubes via 0.22  $\mu\text{m}$  nylon syringe filtration. Extraction solvent containing the internal standard (0.3mL methyl hexanoate 100ppm in hexane:acetone 90:10 vol/vol) was added to each aqueous portion and extracted by shaking and vortexing for 1 minute. Extracted samples were centrifuged for 5min at 10000rpm and the hexane:acetone portion was removed to an auto sampler vial for GC/MS analysis. Samples were prepared in quadruplicate.

A standard curve was constructed for each flavor compound by aliquoting stock solution into 100ppm methyl hexanoate in hexane:acetone 90:10 vol/vol and analyzed via GC/MS along with the sample extracts.

**Gas Chromatography Mass Spectrometry(GC/MS).** Extracted flavor compounds in hexane:acetone 90:10 vol/vol were quantified by GC/MS, each replicate was injected in duplicate. Analysis was performed on a Agilent 7890B Series GC equipped with a 5977 mass selective detector, autosampler (HP 7673) and a fused-silica capillary column (DB-5, 60 m, 0.25 mm i.d., 0.25  $\mu\text{m}$  film thickness, Agilent Technologies, CA). The GC/MS operating conditions were as follows: inlet temperature was 220  $^{\circ}\text{C}$ , oven program was 40  $^{\circ}\text{C}$  for 0.5min, then increased at 10  $^{\circ}\text{C}/\text{min}$  to 230  $^{\circ}\text{C}$  and held for 3 min; constant flow of 1.0 mL/min (He); 1  $\mu\text{L}$  of sample was injected in split mode(1:20). Mass selective detector was operated in scan mode ranging from 30 to 300amu with a solvent delay of 5.5min. Samples were analyzed

alongside flavor standards and corrected using the internal standard.

Corrected peak areas from duplicate injections were averaged. Linear regression was employed to calculate the concentration of flavor in the extracted sample and adjusted to reflect the concentration in the aqueous phase.

#### **Calculation of gumbase/matrix to water partition coefficients (Log cP).**

Log cP values were calculated according to Eq. 4-1 below.

$$\log cP = \log \left( \frac{\text{mg flavor/g gumbase}}{\text{mg flavor/g aqueous solution}} \right)$$

**(4-1)**

Log cP values for duplicate injection were averaged. The average of the quadruplicate analysis of the samples was then average to obtain a single log cP value for each flavor molecule in each matrix mixture evaluated.

#### **Solid-state Nuclear Magnetic Resonance (ssNMR) of Flavor and Matrix Mixtures.**

Materials processed to less than 2mm with either a razor blade or cryo-grinding with a blender and liquid nitrogen were combined with flavor compounds. Melonal and ethyl propionate were added at approximately 17 w/w% to processed materials in sealed vials and equilibrated for more than

24 hours at room temperature. After equilibration, materials and flavor compounds were physically mixed to achieve a homogenous mixture. The material and flavor mixture was packed into 3.2mm torlon solid state NMR rotor.

**Solid-state NMR Analysis.** Materials, flavor and mixtures of materials and flavors were analyzed using techniques common to ssNMR. Analysis was performed by a trained operator on a Bruker 7002, 700 MHz spectrometer equipped with a 4mm high resolution magic angle spinning (HRMAS) probe of Z-gradient in cooperation with the Minnesota NMR Center. Samples were analyzed at a probe temperature of 38°C and a spinning rate of 12 kHz. One dimension techniques; direct polarization magic angle spinning (DP-MAS), cross polarization magic angle spinning (CP-MAS) and insensitive nuclei enhanced by proton transfer (INEPT); were applied to the samples. Two-dimensional INEPT was also performed for each sample.

**Chemical Shift Perturbance.** The chemical shift perturbation values were calculated for flavor atoms visible in two-dimensional INEPT spectra using Eq. 4-2 below.

$$\sqrt{[(\Delta^1\text{H})^2 + \{0.185(\Delta^{13}\text{C})\}^2]}$$

## (4-2)

Where  $\Delta^1\text{H}$  is the shift change in the proton dimension of the flavor atom from its position when analyzed alone to its position when combined with matrix material; likewise,  $\Delta^{13}\text{C}$  is the shift change in the carbon dimension.

**Statistical Analysis.** The average of the quadruplicate analyses, 95% confidence intervals were calculated using Excel (Ver. 2007, Microsoft). Statistical differences were detected using single factor analysis of variance (ANOVA),  $\alpha \leq 0.05$ , followed by Tukey Honest Significant difference (HSD) to determine differences between samples also calculated using Excel.

### 4.4 Results and Discussion

**Matrix to Water Partition Coefficients.** The partitioning behavior of flavor compounds in a model polymer matrix varying in hydrophobicity can be hypothesized by examining the predicted log P values of the flavor compounds[26, 61]. Flavors with higher log P values are expected to partition to the more hydrophobic polymer (PIB) and those with lower log P values to the more hydrophilic polymer (PVAc). Melonal with a predicted log P value of 3.00 is expected to partition primarily to PIB, whereas ethyl propionate with a predicted log P value of 1.24 is expected to partition to PVAc[62]. The analytical measurement of the partitioning of flavor between water and gum matrix materials, termed log cP, is thought to increase the understanding of flavor partitioning behavior in gum systems[26]. The log

cP matrix to water partition coefficients for Melonal and ethyl propionate were measured for PIB, PVAc and mixtures of PIB:PVAc are listed in Table 4-1 below.

**Table 4-1** Matrix to water partition coefficients for flavor compounds in model polymer matrices.\*

<b>Sample Code</b>	<b>Melonal<sup>1</sup></b>	<b>Ethyl Propionate<sup>1</sup></b>
<b>PIB</b>	2.07 ( $\pm 0.03$ ) <sup>b</sup>	1.04 ( $\pm 0.06$ ) <sup>a</sup>
<b>PIB:PVAc 70:30</b>	2.06 ( $\pm 0.03$ ) <sup>b</sup>	1.06 ( $\pm 0.04$ ) <sup>a</sup>
<b>PIB:PVAc 50:50</b>	2.21 ( $\pm 0.07$ )	1.06 ( $\pm 0.04$ ) <sup>a</sup>
<b>PIB:PVAc 30:70</b>	2.10 ( $\pm 0.13$ ) <sup>a</sup>	1.14 ( $\pm 0.09$ ) <sup>a</sup>
<b>PVAc</b>	2.07 ( $\pm 0.06$ ) <sup>b</sup>	1.12 ( $\pm 0.05$ ) <sup>a</sup>

<sup>1</sup> Different letters indicate statistically significant difference determined by oneway ANOVA analysis and Tukey's test ( $\alpha = 0.05$ ). <sup>a</sup>: not significantly different. <sup>b</sup>: significantly different from PIB:PVAc 50:50. \* Average of quadruplicate analysis  $\pm 95\%$  confidence intervals.

Overall, the magnitude of the log cP values reflect what was predicted from the log P values, i.e. the log cP values were higher for Melonal than ethyl propionate in the PIB:PVAc matrices. The Log cP values for Melonal did show some significant differences in partitioning behavior as the composition of the matrix changed. The log cP value for Melonal in 50:50 PIB:PVAc was significantly different ( $p < 0.05$ ) from most of the PIB:PVAs matrix blends with the exception of the 30:70 PIB:PVAc blend ( $p = 3.26$ ). However, while log P predicted differences between partitioning of Melonal in PIB versus PVAc the log cP values did not confirm the predicted difference (by log P) in partitioning behavior.

No significant differences were reported for the log cP values of ethyl propionate ( $p=0.112$ ) among polymer samples. A very slight increasing trend toward was noted for mixtures rich in PVAc (the more polar matrix polymer) as expected based on the calculated log P value. However, examination of the confidence intervals and lack of significance did not confirm a trend.

In summary, the Log cP measurements did not confirm what is predicted from estimation of partitioning behavior based on log P values. While there were significant differences in the partitioning of Melonal between the 50:50 PIB:PVAc blend and some PIB:PVAc matrices, furthermore there were no trends between sample matrix composition and log cP values.

**Solid State NMR-One Dimensional Analysis.** Mixtures of flavor and the sample matrices in Table 4-1 were further analyzed using one dimensional ssNMR techniques. One-dimensional techniques are typically performed prior to two dimensional or more advanced high resolution ssNMR techniques (chapter 3). These analyses are used to identify which sample component is assigned to a given NMR spectral signal, confirm the composition of the sample, and unlike solution state NMR, utilized to provide valuable information regarding the rigidity and mobility of sample analytes. The signal assignment and conformation of the sample composition was

confirmed through direct polarization magic angle spinning (DP-MAS). The rigid components of the flavor and matrix mixtures were identified using cross polarization magic angle spinning (CP-MAS) and the mobile components of the mixtures identified using insensitive nuclei enhanced by proton transfer (INEPT).

Direct polarization magic angle spinning (DP-MAS) is a common one-dimensional ssNMR technique that as the name suggests directly polarizes all of the carbons in the sample (chapter 3). It can be used to determine if all of the carbon-13 signals that need to be observed are present in the spectra. If not, the sensitivity is often optimized. Once the sensitivity is optimized and satisfactory spectra is achieved the spectral peaks are assigned. This technique can also be used to confirm the sample composition by qualitatively examining the intensity of the peaks from each sample component relative to another. The DP-MAS spectra from Melonal combined with the model gum matrices are overlaid and displayed in Figure 4-1 below.

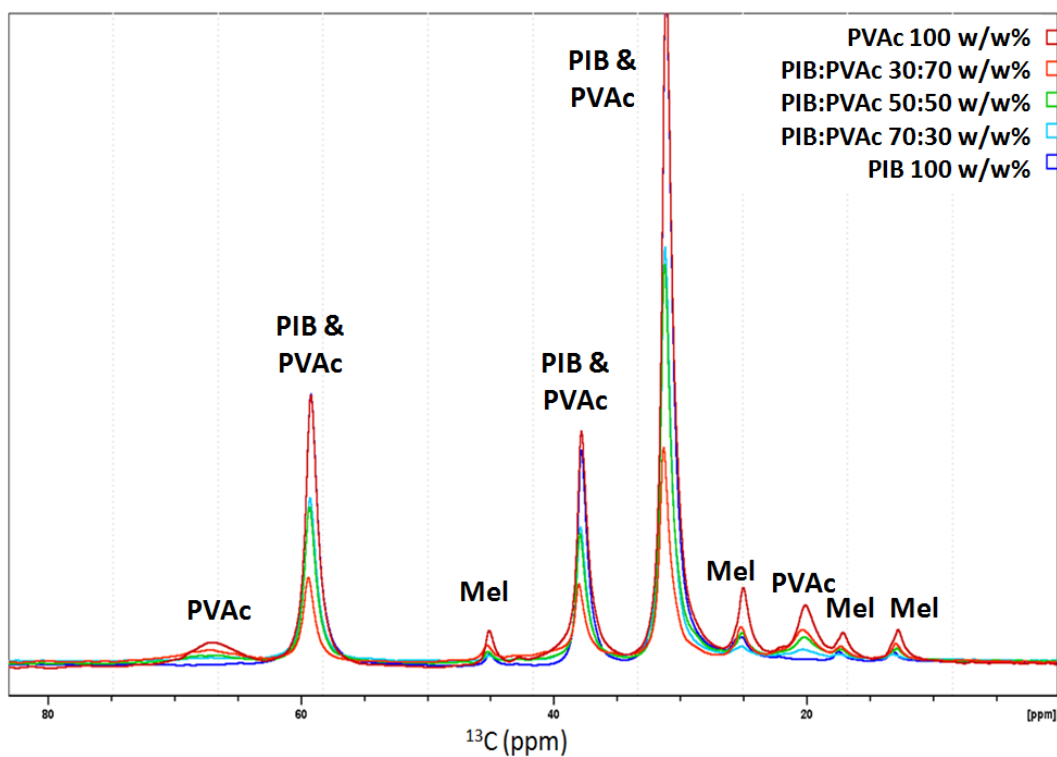
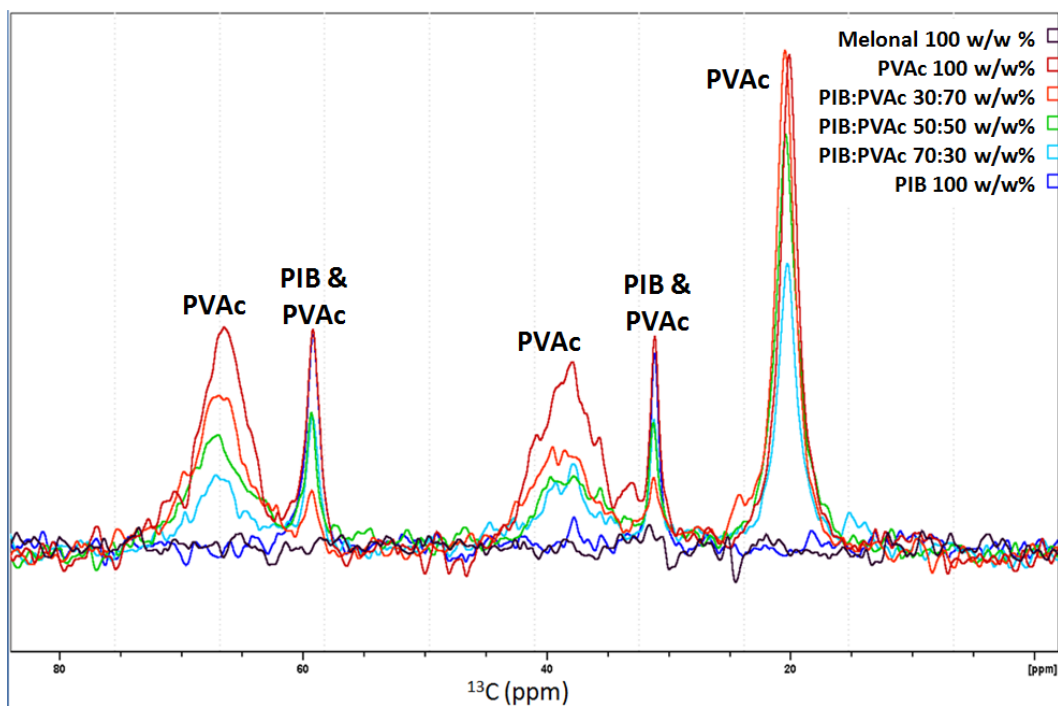


Figure 4-1 Direct polarization-magic angle spinning (DP-MAS) spectra of Melonal in model polymer matrices.

Excellent resolution of the Melonal, PIB and PVAc present in the sample was obtained and the peaks assigned as labeled in Figure 4-1 above. The DP-MAS spectra also confirmed the chemical composition of the sample. Peaks attributed to the Melonal, added at 17 w/w%, were less intense than the matrix peaks. The peaks attributed to PVAc, at 20 and 70 ppm increased in intensity as the PVAc content in the samples increased. For example, the PVAc peaks in the 100 w/w% PVAc and Melonal mixture had greater qualitative intensity than in the PIB:PVAc 50:50 w/w% and Melonal mixture. DP-MAS spectra for ethyl propionate in the PIB and PVAc sample matrices

also achieved good resolution enabling peak assignment. Qualitative examination of the intensity of the DP-MAS peaks for ethyl propionate and matrix mixtures also confirmed the differences in chemical composition of the samples.

Cross polarization magic angle spinning (CP-MAS) is a one-dimensional ssNMR technique which enhances the sensitivity and resolution of one dimensional spectra from ssNMR by polarizing the nearest proton to an adjacent carbon-13 and transferring that polarization to the carbon-13 (chapter 3). While initially used as a optimization method to reduce the broad peaks common to ssNMR this technique gained traction as a excellent tool for observation of the dynamics of sample, particularly rigidity. Rigid species, but not mobile species, will be present in the CP-MAS spectra. Among the rigid species detected by CP-MAS, the intensity can be examined to qualitatively determine the chemical composition of the sample as was described with DP-MAS above. Also peaks shape can be used to qualitatively examine spectra and provide observations of the molecular dynamics at play. Broader peak shapes indicating changes to the spin dynamics of that component indicative of greater mobility. The mixtures analyzed by DP-MAS were also analyzed by CP-MAS. CP-MAS spectra for mixtures of Melonal in model gum matrices are overlaid and displayed in Figure 4-2 below.



**Figure 4-2 Cross polarization-magic angle spinning (CP-MAS) spectra of Melonal in model polymer matrices.**

Peaks displayed in the figure above consist only of the resonances from the matrix polymers (PIB and PVAc); no peaks originating from Melonal were visible. Similarly, in the ethyl propionate and matrix samples spectra for ethyl propionate were also not reported (data not shown). This confirms that PIB and PVAc were the rigid components of the matrix and Melonal and ethyl propionate were the mobile components of the mixtures.

Differences in peak intensity are qualitatively observed across the flavor and matrix samples for both Melonal and ethyl propionate. As shown in the DP-MAS spectra, the differences in peak intensity are due to

differences in the chemical composition of the matrix. Peaks corresponding to PVAc were more intense in sample matrices containing more PVAc.

Peak shape was also qualitatively evaluated for the flavor and matrix mixtures. The peaks assigned only to PVAc were much broader than the peaks assigned to both PIB and PVAc. This indicated a change in the mobility of PVAc that is not visible in the unresolved PIB/PVAc spectra. This change in spin dynamics may be explained by examining the physical property transitions of PVAc and PIB and the analysis temperature. The glass transition temperatures ( $T_g$ ) of PVAc and PIB are 30 to 35°C and -65 to -63°C, respectively and the analysis temperature was 38°C. This taken into consideration it follows that PVAc experiences an increase in molecular motion and spin dynamics at the ssNMR analysis temperature as it is very close to the  $T_g$  for PVAc. PVAc is useful in gum applications because its  $T_g$  is close to human body temperature and it undergoes physical property changes at product use temperature[63]. CP-MAS was able to directly observe this phenomena.

Insenitive nuclei enhanced by proton transfer (INEPT) is also a technique used both for the enhancement of signal sensitivity and observation of sample dynamics. It is often employed prior to two-dimensional INEPT experiments in order to optimize sensitivity. The INEPT experiment is focused on observing the mobile species in a sample. Changes in intensity of INEPT signals are either due to changes in the chemical

composition of the samples, as with DP-MAS and CP-MAS, or changes in sample mobility. If the concentration of a given sample component, such as flavor, is held constant and differences in intensity of the flavor peaks are observed, greater intensity is due to greater mobility of the flavor in that sample. Intensities between sample components where their concentration is not held constant cannot be compared. The flavor and PIB/PVAc matrix mixtures were analyzed by one-dimensional INEPT in order to determine the mobile component of the samples and to observe any changes in sample mobility. Overlaid one-dimensional INEPT spectra of Melonal in combination with blends of model matrix are displayed in Figure 4-3 below.

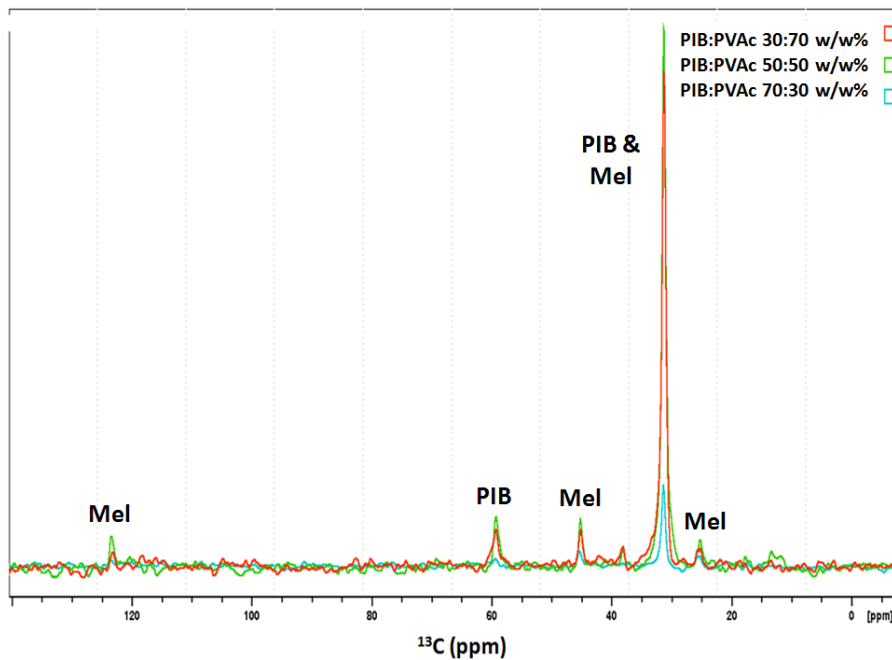


**Figure 4-3 INEPT spectra (one-dimensional) for Melonal in model matrix mixtures.**

Peaks attributed to Melonal and PIB were visible in Figure 4-3 but no peaks from PVAc were visible. Similarly for the mixtures of PIB/PVAc matrix and

ethyl propionate; only the ethyl propionate and PIB peaks were visible. The one-dimensional INEPT spectra confirms that PIB and the flavor compounds were the more mobile components of the flavor and PIB/PVAc sample mixture. Since the concentration of Melonal was held constant the intensities of the Melonal peaks could be qualitatively compared across the blended PIB/PVAc materials. Melonal has greater peak intensity and therefore mobility in the PIB:PVAc 30:70 w/w% and 50:50 w/w% blends as opposed to the PIB:PVAc 70:30 w/w% blend.

In summary, one-dimensional ssNMR analysis was utilized to confirm peak identity and good resolution of each model matrix polymer and flavor mixture were obtained by DP-MAS. CP-MAS confirmed that the model matrix polymers were the rigid species in the flavor and model matrix mixtures and that this technique can be used to suggest which matrix material experiences more dynamic molecular movement. INEPT one-dimensional analysis confirmed the more mobile species in the flavor and matrix mixtures to be the flavor compounds and PIB.

**Solid State NMR - Two Dimensional Analysis.** In order to probe the interaction of flavor with the model gum matrix mixtures further two dimensional ssNMR analysis was necessary. Two-dimensional analysis allows for detailed information to be gathered for most of the carbons in the flavor molecules. One of the goals of this study was to understand how flavor

molecules are impacted by changes to their surrounding model gum matrix. Since, one-dimensional analysis determined that the flavor is a mobile species, a two-dimensional method suited to observing mobile species was selected. Two-dimensional INEPT analysis can be used to gather a two-dimensional spectra of the mobile species in a sample mixture. First, a two-dimensional INEPT spectra of Melonal without added model matrix materials was obtained. The resultant spectra for pure Melonal is shown in Figure 4-4; a molecular structure of Melonal with the corresponding carbon number is superimposed.

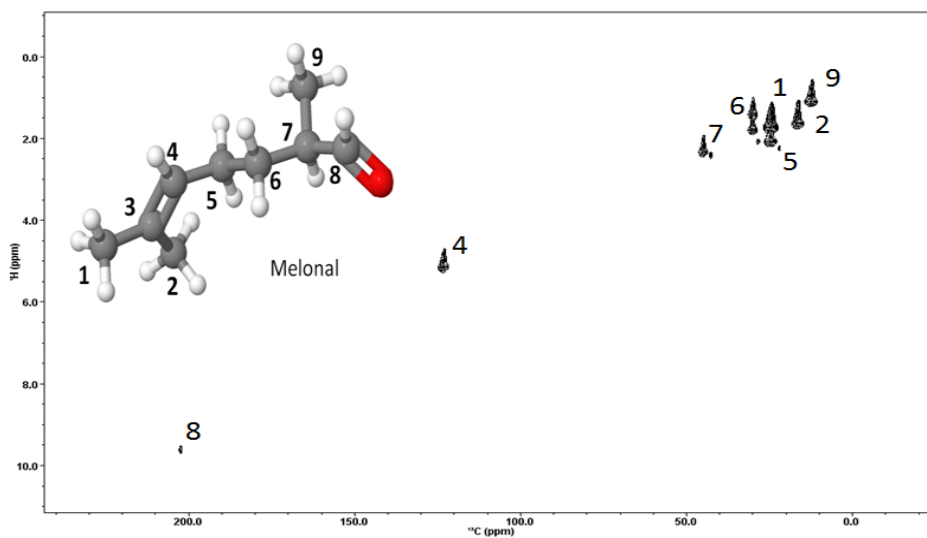


**Figure 4-4 Two-dimensional INEPT spectra for Melonal with corresponding number assignments.**

The corresponding cross peaks for carbon atoms directly bonded to a hydrogen in Melonal were observed. This molecular ‘fingerprint’ can be applied to investigate how the dynamics of the flavor molecules were

affected by the addition of model matrix and changes to the chemical composition of that matrix. This spectra of Melonal alone will be referred to as 'free' Melonal as the flavor is not interacting with another species, besides itself. Changes in the shift of this 'fingerprint' were further evaluated as Melonal was combined with PVAc, a model gum matrix component. The two-dimensional spectra for Melonal combined with PVAc with an overlaid with the 'free' Melonal spectra (Fig 4-4) is shown in Figure 4-5.

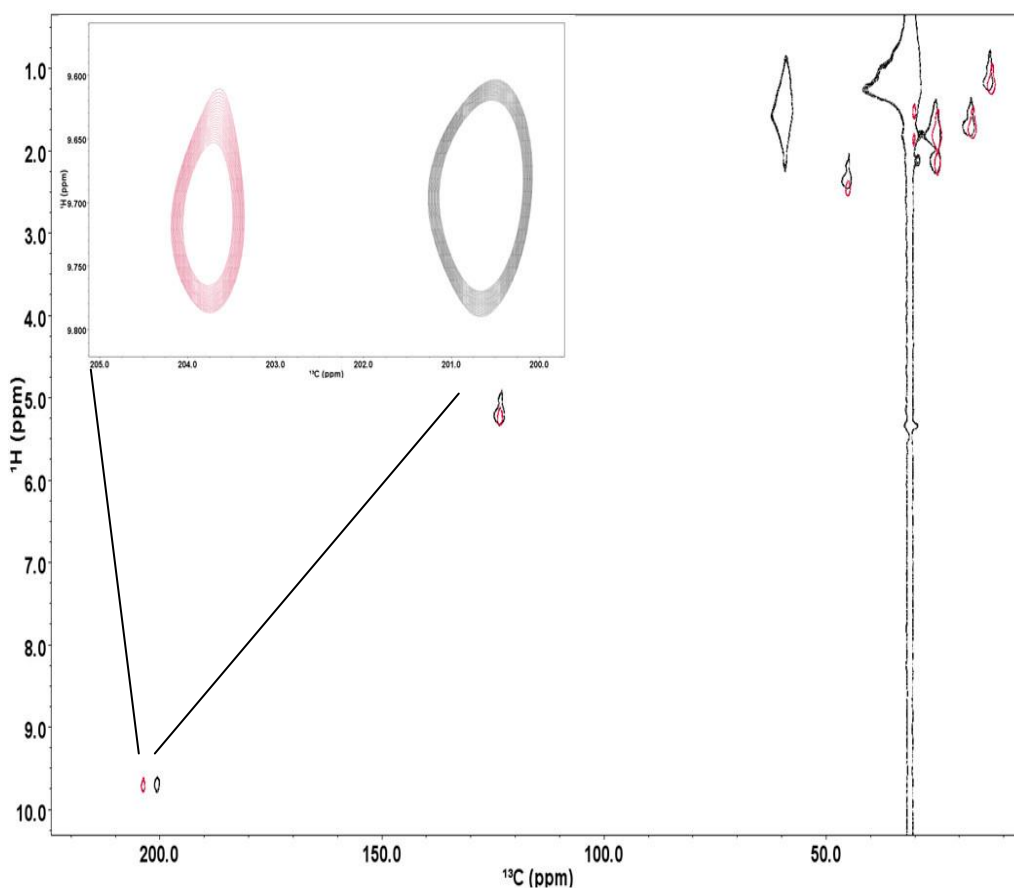


**Figure 4-5** Two-dimensional INEPT spectra for Melonal (black) overlaid with two-dimensional INEPT spectra for Melonal with PVAc (red). Resonance of the carbonyl carbon enlarged to show detail.

When the cross peaks of the melonal and PVAc mixture (red) are inspected and compared to the free Melonal (black) a shift of the cross peaks is observed. In order to overcome the spatial resolution of the entire two-dimensional spectra and observe this shift, the carbon cross peak at approximately 200ppm is zoomed and superimposed. As discussed in chapter 3 this shift indicates an intermolecular interaction is occurring between the flavor compound and the polymer. The location of this shift when a flavor molecule interacts with a matrix component can be referred to as a domain. The cross peak for the carbonyl carbon in Melonal (zoomed in region) in Figure 4-5 (red) is the PVAc domain for Melonal. The PIB domain for Melonal was also located from two-dimensional INEPT spectra. Mixtures of Melonal and both PIB and PVAc were analyzed by two-dimensional INEPT and the positions of these cross peaks in reference to the PIB and PVAc domains were investigated. Both the degree and direction of the cross peak shifts varied across the Melonal molecule in both the carbon and proton dimensions as the composition of the matrix changes. The shift in the carbon dimension was the largest shift reported of the cross peaks. The shift in the carbon dimension can be plotted against the PIB content of the polymer matrix, specifically carbon 9 (Figure 4-4) is shown in Figure 4-6.

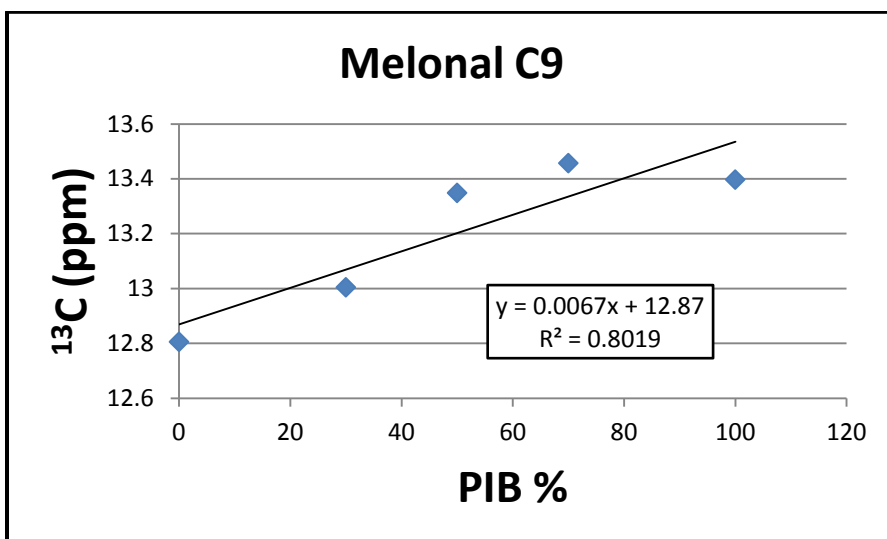


Figure 4-6 <sup>13</sup>C chemical shift for one of the methyl carbons (C9) belonging to Melonal plotted against polyisobutylene (PIB) content with linear trendline applied.

As discussed in chapter 3, a linear trendline can be applied to determine if an atom belonging to a small molecule is experiencing a preferential interaction with a matrix component. The linear regression trendline applied to Figure 4-6 shows a correlation coefficient of 0.8019 which suggests a preferential interaction between Melonal and PIB over PVAc. The carbon-13 shifts for most carbons in Melonal were also plotted against PIB content and the linear trendline and correlation coefficients are displayed in Table 4-2 below.

**Table 4-2 Linear trend lines for <sup>13</sup>C shifts for Melonal versus PIB content**

<b>Carbon #</b>	<b>ppm</b>	<b>Functional Group</b>	<b>Linear Trendline</b>	<b>R<sup>2</sup></b>
9	12.5	CH3	$y = 0.0067x + 12.87$	0.8019
2	16.7	CH3	$y = 0.0059x + 17.24$	0.7006
1	24.7	CH3	$y = 0.0066x + 25.202$	0.8282
5	24.9	CH2	$y = 0.0017x + 25.078$	0.2887
7	45.1	CH	$y = 0.0003x + 45.212$	0.0217
4	123.4	=CH	$y = -0.0008x + 123.58$	0.1862
8	202.4	C=O	$y = -0.0097x + 201.52$	0.8572

Examination of the correlation coefficients in Table 4-2 showed variance in the measured preference of each atom in Melonal for PIB. Atoms which showed less correlation between the chemical shift and the content of PIB in the matrix are thought to have a stronger preferential interaction with PIB than those with higher R<sup>2</sup> values. The sign of the slope of the linear trendline can also provide information regarding the interaction. When the crosspeak shifts upfield with respect to the cross peak of the free melonal the sign of the slope is positive and vice versa for shifts downfield. It is not entirely clear what implication the direction of shift, either upfield or downfield has for the interaction dynamics of flavors with model gum matrix materials. Chemical

shifts present in NMR are in general correlated to shielding of a given atom from the magnetic field by other structural features in the molecules.

The carbon-13 shifts for ethyl propionate were similarly plotted against the matrix composition and the linear trendlines and correlation coefficients are displayed in Table 4-3 below.

**Table 4-3 Linear trend lines for <sup>13</sup>C shifts for ethyl propionate versus PVAc content**

<b>Carbon #</b>	<b>ppm</b>	<b>Functional Group</b>	<b>Linear Trendline</b>	<b>R<sup>2</sup></b>
1	8	CH3	y = -0.0034x + 8.9339	0.8467
5	13.2	CH3	y = -0.0046x + 14.191	0.9296
2	26.5	CH2	y = -0.0007x + 26.957	0.0142
4	59	CH2	y = 0.0052x + 59.061	0.8231

As with Melonal, ethyl propionate experiences local interaction phenomena that vary across the molecular structure. Ethyl propionate also experiences differences in the direction, degree and linear relationship of cross peak shift with matrix composition across the ethyl propionate molecule.

In order to account for the shifts of the cross peaks in both the proton and carbon dimensions the chemical shift perturbances (as described in chapter 3) of Melonal in the model matrices were calculated using Eq. 4-2 below.

$$\sqrt{[(\Delta^1\text{H})^2 + \{0.185(\Delta^{13}\text{C})\}^2]}$$

(4-2)

These CSP values were plotted against the Melonal carbon position for each matrix material and plotted in Figure 4-7 below.

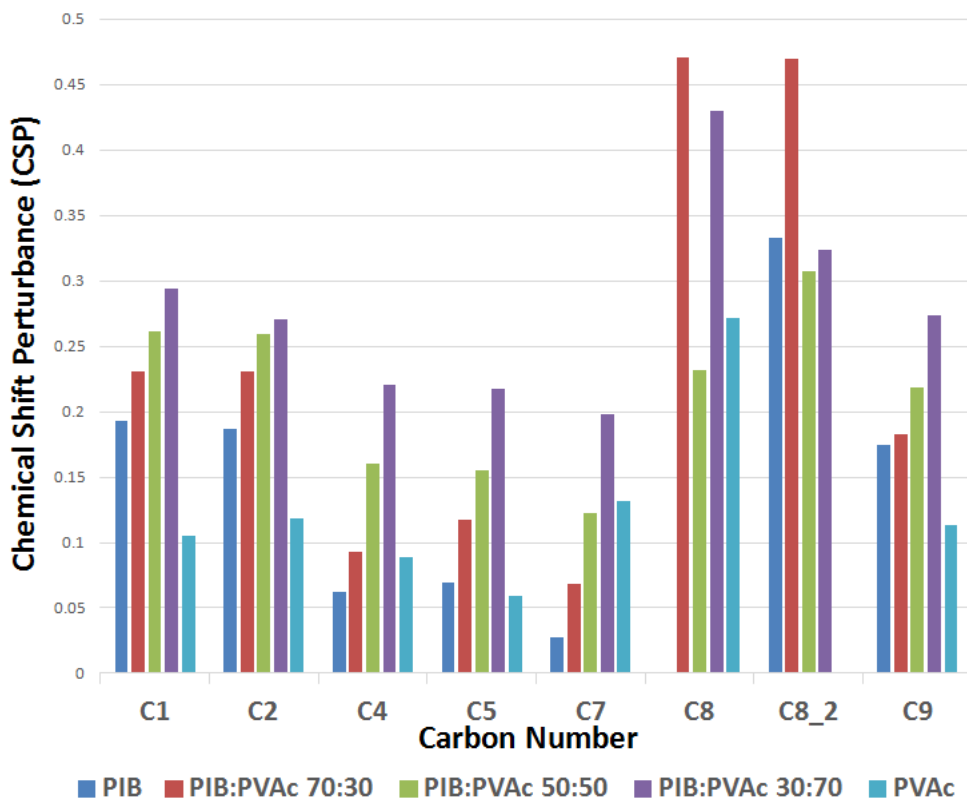


Figure 4-7 Chemical shift perturbances for Melonal in model polymer matrices.

The CSP values provide an indication of which atomic position on the flavor molecule experiences the largest shift in response to changes to the model matrix. The carbonyl carbon of Melonal (C8) displayed more than one cross peak for the matrices containing both PIB and PVAc. This indicated there were carbonyl cross peaks observed near both the PIB and PVAc domains in Melonal. Correspondingly, two CSP values were calculated; one for the PVAc

domain (C8) and one for the PIB domain (C8\_2) in Figure 3-7 above. The magnitude of the CSP change for Melonal as the matrix composition was altered, from PIB to PVAc, follows a similar pattern for most positions in Melonal (C1, C2, C4, C5, C7 and C9). This pattern suggests that Melonal is mostly perturbed from its 'free' position when the surrounded by a model matrix mixture that is higher in PVAc content but not when it is surrounded by only PVAc. The largest CSP values were experienced by the carbonyl carbon especially when combined with a mixture of PIB:PVAc 70:30 w/w% for both the PIB and PVAc domains and also when combined with PIB:PVAc 30:70 w/w% for the PVAc domain. Interpretation of these values is theoretical however, these values do indicate that the most active part of the flavor compound with respect to matrix interactions is the carbonyl carbon. The values also indicated that the remaining aliphatic carbons respond to changes to the matrix in a similar manner. If the functional groups of Melonal are considered, it followed that the highest source of electro negativity, the carbonyl carbon, experienced the largest perturbances. For the PVAc domain, the CSP values calculated were the largest for both mixtures high in PIB and PVAc which can be related to hydrophobic moieties on the flavor molecule. These moieties would prefer the PIB components in the polymeric matrix. The CSP for Melonal in the PIB domain for C8 was the highest when the matrix is mostly PVAc. This is again due to the fact that most of the molecule prefers the PIB components but the electronegative carbonyl is predicted to

prefer the PVAc material. As such, when there is a small amount of PVAc present the affinity of the carbonyl is strong enough to result in a perturbed cross peak.

The carbonyl was also reported to display some differences in cross peak shape, related to exchange behavior as discussed in chapter 3. When the shape of the cross peak in the various model matrices was examined, (Figure 4-8 below), both rounded, elongated and elliptical shapes are apparent.

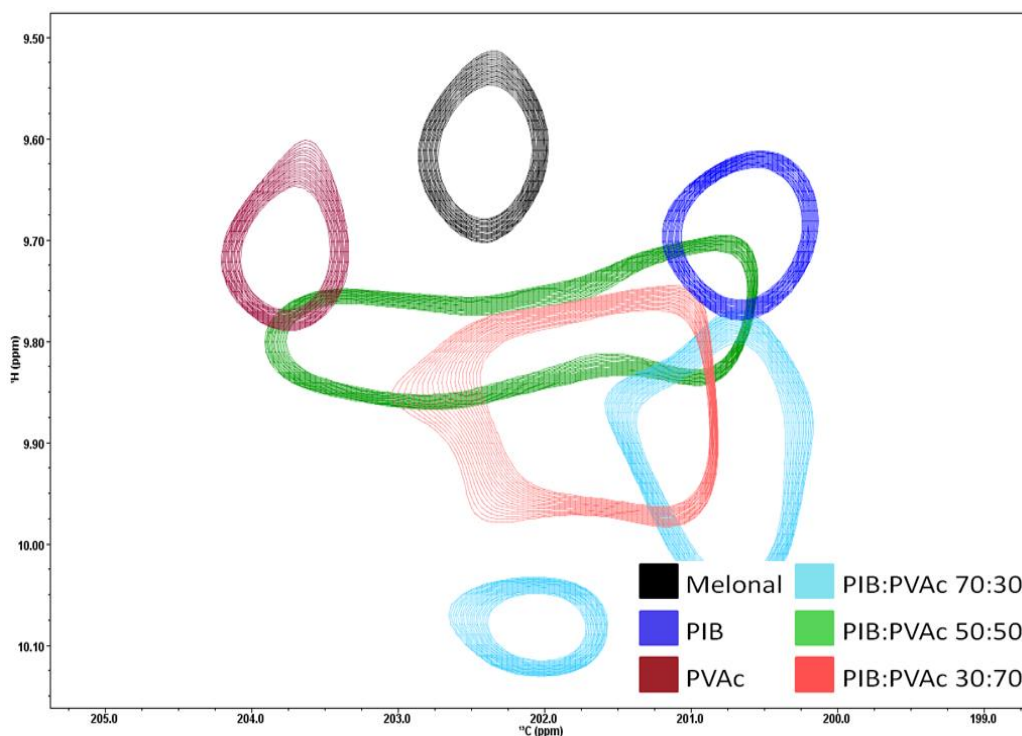


**Figure 4-8 Two-dimensional INEPT cross peak for the carbonyl carbon of Melonal in various model matrices**

The rounded shape of the carbonyl cross peak when Melonal was combined with PIB 100 w/w%, PIB:PVAc 70:30 w/w% and PVAc 100 w/w% indicated selective exchange with the matrix and stronger preference for those

domains. The elongated elliptical shapes of the carbonyl cross peak when Melonal was combined with PIB:PVAc 30:70 w/w% and especially 50:50 w/w% indicate that it is undergoing intermediate exchange dynamics with the model matrix materials. This means that it doesn't overwhelmingly prefer the PIB or PVAc domains. As the Melonal molecules were observed by the Two-dimensional INEPT experiment there was movement of the carbonyl carbon between those domains resulting in an elliptical cross peak (chapter 3). Review of the remaining C-H cross peaks shown in the two-dimensional INEPT spectra for Melonal more closely resemble a round shape as shown for Melonal combined with PVAc (red) or PIB (blue) in Figure 4-8 above. The round cross peaks shape (chapter 3) indicates a more selective interaction exchange (with each polymer) between the flavor molecule and matrix. This means that these positions in Melonal more strongly prefer either PVAc or PIB.

The combined knowledge gained from the use of two-dimensional ssNMR techniques has provided evidence of preferential interactions between flavor compounds and the polymeric matrix components investigated. This lends credence to the idea of affinity as an important factor in prediction of flavor release from food matrices. In addition, the ability to develop a quantitative value of interaction between flavor and matrix materials, the CSP, provides information about what functional groups participate in and perhaps drive the intermolecular interactions between

flavor molecules and food matrix materials. Lastly, the intermolecular interactions between flavors and matrix materials were observed in situ and without the need for isotopic enrichment of either the matrix or flavor molecule. In summary, this two-dimensional ssNMR technique showed promise for increasing the fundamental understand of how flavor molecules interact with food matrices and provide information as to which intermolecular forces drive these interactions.

## Chapter 5 Influence of texture on flavor release dynamics

### 5.1 Abstract

Previous studies regarding the dynamics of flavor release from gum matrices have identified texture effects as important contributors to flavor release. Solid state NMR (ssNMR) was utilized to investigate flavor (acetophenone) interactions in model gum systems consisting of two polymer blocks decalactone(D) /polylactide (L) ranging in molecular weight . The texture of the model matrices ranged in hardness but had identical chemical composition. Water to matrix partition coefficients,  $\log cP$ , did not indicate differences in partitioning of acetophenone to the model matrices. However flavor release profiles monitored from an artificial mouth coupled to a APci-MS showed qualitative differences from short MW 'soft' matrices releasing more acetophenone than long MW 'firm' matrices. Furthermore, quantification of acetophenone released during artificial chewing confirmed that more acetophenone released from short MW 'soft' model matrices. Additionally the flavor release was greater from blends of short MW 'soft' and long MW 'firm' than from either the short or long MW matrices alone. Two-dimensional INEPT analysis confirmed that acetophenone participates in weaker intermolecular interactions when combined with blended short and long MW matrices making it more available for release from the matrix.

## 5.2 Introduction

Physicochemical models have been previously developed to predict flavor release[1]. These models involve examining the chemical properties of flavor and food matrix components and predicting how closely a given flavor compound will associate with a given component. This is often referred to as the 'affinity' of the flavor to the food matrix. Flavor release from more complex mixtures, such as gum bases, have been modeled by using weighted averages for each component[11, 26] . Chewing gum matrix is often composed of fairly characterized mixture of polymers that provide a physiochemical base to model flavor release [10]. In general, more hydrophobic flavors are thought to have greater release from more polar gum base matrices and vice versa.

Flavor release profiles from chewing gum can also be analytically monitored and have been compared to release prediction models[17, 57]. These models do not typically adequately predict the flavor release profiles and deviations from predictions are thought to result from differences in texture or surface renewal of the gum during chewing[15, 17, 57, 64]. However, there is a lack of understanding regarding the mechanistic impact of these texture changes and the nature of the flavor-matrix interactions involved.

Previous studies have suggested altering gum base formulations to change the texture of the gum as a method to alter flavor delivery [24, 28]. Softer gums are suggested to release more flavor than harder gums[28]. Texture of gum base has been correlated to various flavor release phenomena by the confectionary industry but any details of the mechanisms of this increased release appear to be trade secrets[10]. However, often modifications to the texture of the gum must not disturb the balance of hydrophobic and hydrophilic components released in order to maintain the flavor quality of the product. Increased understanding of gum base textural properties and knowledge from polymer chemistry has enabled confectioners to modify the texture of the gum bases without adjusting the overall chemical properties of the gum base[63]. This approach provided the ability to modify the texture properties of gum without disturbing the crucial balance of hydrophobic and hydrophilic. Alternation of the polymer molecular weight of the gum base materials has enabled the creation of gums whose physical properties can be adjusted to achieve the desired textural effects such as extensibility and bounce but retain favorable flavor release conditions [63]. However, designing gum base materials to tailor specific flavor release has been more challenging. Further, this method of gum matrix optimization has created challenges for the prediction of flavor release using traditional methods.

Using modern chewing gum formulating techniques two gum bases could be created with very similar chemical properties but very different textures. In this case the physicochemical properties would be the same in both gum bases and predictions of flavor release based on physicochemical properties would also be equal; providing a base to further understand the impact of texture changes on flavor partitioning and release. Further examination of the physical properties of specific polymers forming the gum matrix could further provide information with which to form a hypothesis regarding flavor release.

Changes to the size of polymers used in gum matrices can affect large changes in the texture properties of the gum base. The molecular weight of entanglement ( $M_e$ ) for a given polymer for example, is a physical phenomena which could be examined for indicators of release modifying behavior. This phenomena uses calculated values to determine the point at which the molecular weight has increased to the point where different chains of a polymer can experience entanglement with each other [65, 66]. This entanglement may entrap small molecules such as flavor molecules. This phenomena would lead to a decrease in flavor release from matrices experiencing entanglement. Traditional flavor release methodologies could examine whether correlations exist between  $M_e$  values for gum matrix polymers and flavor release. However, current flavor release methodologies

cannot observe if the dynamics of the flavor compounds are different in matrices above or below the  $M_e$  of the gum matrix polymers.

Solid state NMR has been shown to be a useful analytical technique for the investigation the interactions between flavor compound and gum matrix polymers (chapter 4). This approach can be used to investigate the impact of matrix texture changes on flavor to matrix interactions even when there are no chemical differences in the matrix mixtures. One-dimensional ssNMR technique direct polarization magic angle spinning (DP-MAS) can be used to confirm the composition of a flavor and matrix mixtures. The two-dimensional ssNMR technique known as insensitive nuclei enhanced by proton transfer (INEPT), can be used to evaluate how the flavor molecule is affected by physical rather than chemical property changes in the matrix. Changes in the dynamics of the model matrices can also be observed using Two-dimensional INEPT.

The main goal of this study was to utilize model polymer matrices composed of poly-epsilon decalactone (D)/polylactide (L) block copolymers ranging in molecular weights above and below the  $M_e$  for the polymers. This will result in a short DL diblock which will be 'soft' and a long MW DL diblock which will be 'firm'. These polymers can then be used to create model matrices of varying textures. Both classical flavor release methodologies and ssNMR techniques will be employed to study the impact of texture changes on flavor release dynamics. The water to matrix partition coefficients, termed

log cP, of a model flavor in these model matrices will be measured as well as flavor release profiles using a chewing device. The flavor released from these matrices will be quantified and the interaction of flavor with these matrices as the physical properties of the matrices changes will be monitored using ssNMR techniques; specifically DP-MAS and two-dimensional INEPT.

### 5.3 Materials and Methods

**Selection of Model Polymer Matrix Materials.** Sustainable block copolymers having elastomeric properties have been developed using green chemistry techniques and thoroughly characterized[67, 68]. The texture of these materials is tunable by adjusting the molecular weights of the polymers rather than the ratio of the polymers[67-69]. This means that diblock copolymers composed of two polymers (poly-epsilon decalactone and polylactide) can be designed to have a soft gel-like consistency or a firmer paraffin-like consistency. These block copolymers would also be suitable for the production of environmentally compatible chewing gum base as they contain both elastomeric and extensible mechanical properties[67]. The synthesis and characterization of these diblock copolymers is well understood and two diblocks both containing 50 w/w% for each polymer type can be produced [68, 70]. One diblock having molecular weights over the molecular weight of entanglement ( $M_e$ ) and one below[66]. These diblock copolymers would have very different textures and can be used study

differences in polymer matrices where chemical properties remain the same but texture properties vary. Hamad et. Al. used a similar approach to study the differences in protein partitioning between diblock copolymer containing different microstructures but identical composition[71]. Diblocks which contained carbon-13 enrichment could also be produced. This enrichment is not necessarily required to study these materials via ssNMR but would dramatically reduce the analysis time needed for high resolution ssNMR observations.

**Materials.** Poly-epsilon decalatonone:polylactide diblock copolymers in varying molecular weights both with and without carbon-13 enrichment of the polymers were obtained from Ortec Inc (Piedmont, SC.). Acetophenone and methyl hexanoate were obtained from Sigma Aldrich (St. Louis, MO.). Isotopically enriched  $^{13}\text{C}_8$  Acetophenone was obtained from Isotec (Miamisburg, OH.) Hexanes, acetone, methanol and isopropanol were obtained from Sigma Aldrich (St. Louis, MO.) Physical properties were obtained from the manufacturer and are displayed in Table 5-1 below. Molecular weights for D and L were obtained using gel permeation chromatography (GPC) protocols common to the synthetic polymer industry. glass transition temperature ( $T_g$ ) was obtained via differential scanning calorimetry (DSC) also using protocols common to the industry.

Table 5-1 Physical properties for model polymer matrices.

Sample	Weight (%)	Molecular Weight D Block (kDa)	Molecular Weight L Block (kDa)	Molecular Weight of Entanglement D Block (kDa)	Molecular Weight of Entanglement L Block (kDa)	Glass Transition Temperature D Block (°C)	Glass Transition Temperature L Block (°C)
<b>DL Short</b>	100	4.0	2.6	5.9	9.2	-47.0	43.5
<b>DL Short</b>	70	4.0	2.6	5.9	9.2	-47.0	43.5
<b>DL Long</b>	30	21.9	14.6	5.9	9.2	-46.4	54.1
<b>DL Short</b>	50	4.0	2.6	5.9	9.2	-47.0	43.5
<b>DL Long</b>	50	21.9	14.6	5.9	9.2	-46.4	54.1
<b>DL Short</b>	30	4.0	2.6	5.9	9.2	-47.0	43.5
<b>DL Long</b>	70	21.9	14.6	5.9	9.2	-46.4	54.1
<b>DL Long</b>	100	21.9	14.6	5.9	9.2	-46.4	54.1
<b>D*L* Short</b>	100	4	2.7	5.9	9.2	-47.0	52.2
<b>D*L* Short</b>	70	4	2.7	5.9	9.2	-47.0	52.2
<b>D*L* Long</b>	30	23.5	15.7	5.9	9.2	-45.6	53.3
<b>D*L* Short</b>	50	4	2.7	5.9	9.2	-47.0	52.2
<b>D*L* Long</b>	50	23.5	15.7	5.9	9.2	-45.6	53.3
<b>D*L* Short</b>	30	4	2.7	5.9	9.2	-47.0	52.2
<b>D*L* Long</b>	70	23.5	15.7	5.9	9.2	-45.6	53.3
<b>D*L* Long</b>	100	23.5	15.7	5.9	9.2	-45.6	53.3

\*Indicates presence and position of <sup>13</sup>C isotopic enrichment

**Matrix and Flavor Blend Preparation.** In order to evaluate changes in flavor release related to texture change it was necessary to create blends of short and long diblocks. Mixtures of short and long diblocks in ratios of 30:70, 50:50 and 70:30 w/w % were prepared by weighing desired amounts of polymer into vials, sealing the vials and placing the mixtures in an oven at 64°C for at least 2 hours. After heating for two hours the polymers were mixed thoroughly with a dental probe until a visually homogeneous mixture was obtained. Separate portions of short and long diblocks were also heated and mixed similarly to the short and long mixtures to control for any differences that might result from the mixing process. After heating and mixing the polymers and mixtures were stored at room temperature in sealed vials and protected from light.

Diblock copolymers which were isotopically enriched with carbon-13 were labeled either on the poly-epsilon decalactone (D) block or the poly-lactide (L) block. As such, in order to maximize the increased sensitivity of ssNMR analysis mixtures of short and long diblocks containing both enriched D and L blocks were created. Short diblock with carbon-13 enriched D block was combined with short diblock having carbon-13 enriched L block in a vial at 50/50 w/w%, sealed and heated in an oven at 64°C for at least two hours before being mixed until homogeneous with a dental probe. The same type of mixture was prepared using long diblocks with carbon-13 enriched D and L blocks. This results in a mixture of short diblocks with both D and L block carbon-13 enriched (short enriched) and a mixture of long diblocks with both D and L carbon-13 enriched (long enriched).

Mixtures of short and long enriched diblock were prepared in ratios of 30:70, 50:50 and 70:30 w/w% as above with the unlabeled short and long diblocks.

**Measurement of gumbase/matrix to water partition coefficients (Log cP).**

Non-isotopically enriched short, long and mixtures of short and long diblocks were processed into pieces of less than 2 cubic mm with a razor blade. Only materials which were processed to be less than 2 cubic mm were used for log cP and ssNMR analysis.

A stock solution of acetophenone was prepared at 10 w/w% in methanol. An internal standard solution of methyl hexanoate 100ppm in hexane:acetone 90:10 vol/vol was also prepared.

Processed materials (0.4 g) were placed in 20mL vials, 2mL of deionized distilled water were added. Aliquots of acetophenone (5uL) were added to individual vials of material and water. Vials were sealed with air-tight screw caps and equilibrated at 38°C in a shaking water bath for 72hours. A portion of the aqueous phase (1.5mL) was removed from the sample vial and transferred to a microfuge tubes via 0.22 µm nylon syringe filtration. The aqueous portion was extracted by shaking and vortexing with 0.3mL methyl hexanoate 100ppm in hexane:acetone 90:10 vol/vol. Extracted samples were centrifuged for 5min at 10000rpm and sample extracted into the hexane:acetone portion was removed to an auto sampler vial for GC/MS analysis. Samples were prepared in quadruplicate. A

standard curve was constructed for acetophenone by aliquoting stock acetophenone solution into 100ppm methyl hexanoate in hexane:acetone 90:10 and analyzed via GC/MS along with the sample extracts.

**Gas Chromatography Mass Spectrometry(GC/MS).** Extracted acetophenone in hexane:acetone 90:10 vol/vol were quantified by GC/MS, each replicate was injected in duplicate. Analysis was performed on a Agilent 7890B Series GC equipped with a 5977 mass selective detector, autosampler (HP 7673) and a fused-silica capillary column (DB-5, 60 m, 0.25 mm i.d., 0.25  $\mu\text{m}$  film thickness, Agilent Technologies, CA). The GC/MS operating conditions were as follows: inlet temperature was 220  $^{\circ}\text{C}$ , oven program was 40  $^{\circ}\text{C}$  for 0.5min, then increased at 10  $^{\circ}\text{C}/\text{min}$  to 230  $^{\circ}\text{C}$  and held for 3 min; constant flow of 1.0 mL/min (He); 1  $\mu\text{L}$  of sample was injected in split mode(1:20). Mass selective detector was operated in scan mode ranging from 30 to 300amu with a solvent delay of 5.5min. Samples were analyzed alongside flavor standards and corrected using the internal standard. Corrected peak areas from duplicate injections were averaged. Linear regression was employed to calculate the concentration of flavor in the extracted sample and adjusted to reflect the concentration in the aqueous phase.

**Calculation of gumbase/matrix to water partition coefficients (Log cP).** Log cP values were calculated according to the following equation:

$$\log cP = \log \left( \frac{\text{mg flavor/g gumbase}}{\text{mg flavor/g aqueous solution}} \right) \quad (5-1)$$

Log cP values for duplicate injection were averaged. The average of the quadruplicate analysis of the samples was then average to obtain a single log cP value for each flavor molecule in each matrix mixture evaluated.

### **Flavor Release from Model Matrix Materials.**

Non-enriched short diblock, long diblock and mixtures of short and long diblock (30:70, 50:50 and 70:30 w/w%), 250mg, were combined with acetophenone, 12.5 $\mu$ L in sealed vials. The model matrix and acetophenone mixtures were placed in an oven at 64°C for two hours before being removed and mixed until homogeneous with a dental probe. Polymer and flavor mixtures were stored at room temperature and protected from light for at least 18 hours before analysis.

### **Measurement of Flavor Released from Model Matrix during Simulated Chewing.**

A portion, 150mg, of each model matrix and flavor mixture was removed and placed in the cylinder of an artificial chewing device (Appendix A) which was pre-heated to 37.8°C. Nano-pure water (0.5mL) was added to the cylinder and the top piston of the chewing device was placed into the cylinder. Nano pure water at 37.8°C was supplied to the chewing device at a flow rate of 0.5mL/min via an Shimadzu LC-10AD HPLC binary gradient pump and drawn from the device using a

Masterflex L/S reversible drive peristaltic pump (Cole Palmer Instrument Co., Vernon Hills, IL) operating at 2.5mL/min. Air flow was directed into the device at 50mL/min and out of the device at 49mL/min through a small section of deactivated fused silica capillary column 0.5mm i.d.(Agilent Technologies, Santa Clara, CA.). The articulation of the device was operated at 60rpm. The chewing device was operated for 20 minutes during each sample run. Each model matrix and flavor mixture was analyzed in duplicate during the same operating period.

**Atmospheric Pressure Chemical Ionization Mass Spectrometry(APCI-MS).** A flavor release profile was generated by sampling the air expelled from the artificial chewing device during simulated chews of mixtures of model matrix polymers and acetophenone. Acetophenone released from the matrix and therefore in the air from the chewing device is drawn into the APCI source by connecting the capillary exiting the chewing device to a capillary extending from the APCI source and detected using mass spectrometry.

**Calibration of the APCI-MS.** A mixture of 5 w/w% acetophenone in acetone was used to calibrate the APCI-MS prior to sample analysis. In brief, an aliquot of acetophenone calibration std was added to a sealed water jacketed vessel (1L) and allowed to equilibrate in the sealed vessel for 30 sec prior to sampling the vessel by connecting a capillary extending from the vessel to a capillary sampling into the APCI-MS source. The vessel is connected and disconnected in order to achieve three measurements of abundance. This process is repeated with increasing aliquots of

calibration standards, any residual acetophenone is removed from the vessel between standard runs with the use of a heat gun. The averaged abundances for these standards is plotted against the concentration of the acetophenone in the calibration vessel to obtain a calibration curve for acetophenone in air sampled by APcI-MS.

**APcI-MS Operating Conditions.** Analysis was performed using a Waters micromass Quattro Micro. Air flow was drawn into the source at a rate of 125mL/min through a fused silica capillary column 0.5mm i.d. (Agilent Technologies, Santa Clara, CA.) using a transfer line heated to 75°C. The source, fitted with an APcI probe, was operated in select ion recording (SIR) mode with a source temperature of 120°C and a probe temperature of 150°C. The source was operated in positive ionization mode at a corona discharge of 4kV. Acetophenone was monitored at 117.0(M-H<sub>3</sub>), 120.90 (M+H) and 179.00 (2M - 2OCH<sub>3</sub> +H) m/z with a dwell time of 0.050 sec between scans.

#### **Quantification of Flavor Released from Model Matrix after Artificial Chewing.**

Each model matrix and flavor mixture was sampled for quantification before and after artificial chewing. A portion, 50mg, of each non-enriched polymer and flavor mixture was removed and placed in a microfuge tube, 2.0mL. Chloroform (1.0mL) and methyl hexanoate (100ppm in isopropanol, as internal standard, 1.0mL) were added to the sample and the mixture was vortexed for 60sec to solubilize the polymer and extract the acetophenone from the polymer matrix. The

solubilized sample was removed to an autosampler vial and analyzed for acetophenone content via GC/MS. Aliquots of 10 w/w% acetophenone in methanol were added to chloroform (1.0mL) and ISTD mixture in isopropanol (1.0mL) and analyzed with the extracted samples to form a standard curve.

**Gas Chromatography Mass Spectrometry(GC/MS).** Analysis was performed on a Agilent 7890B Series GC equipped with a 5977 mass selective detector, autosampler (HP 7673) and a fused-silica capillary column (DB-5, 60 m, 0.25 mm i.d., 0.25  $\mu$ m film thickness, Agilent Technologies, CA). The GC operating conditions were as follows: inlet temperature was 220 °C, oven program was 40 °C for 0.5min, then increased at 10 °C/min to 230 °C and held for 3 min; constant flow of 1.0 mL/min (He); 1  $\mu$ L of sample was injected in split mode(1:20). Mass selective detector was operated in scan mode ranging from 30 to 300amu with a solvent delay of 5.5min.

Acetophenone content was calculated using linear regression from a standard curve and was internal standard corrected. Duplicate samples before and after artificial chewing were injected in triplicate along with standard calibration curve, these injections were averaged to produce the final values.

### **Solid-state Nuclear Magnetic Resonance (ssNMR) of Flavor and Matrix Mixtures.**

**Solid State Nuclear Magnetic Resonance (ssNMR) Analysis.** Both short and long enriched diblocks as well as mixtures of short and long enriched diblock were

combined with acetophenone at 4.8 w/w% and placed in an oven at 64°C for two hours. The heated diblock and acetophenone mixtures were removed from the oven and immediately stirred until homogenous using a dental probe. Stirred diblock and acetophenone mixtures were stored at room temperature and in the absence of light for at least 18 hours prior to ssNMR analysis. Immediately prior to analysis enriched diblock and acetophenone samples were packed into 3.2mm zircon rotors and weighed to record sample weight listed in Table 5-2 below.

**Table 5-2 Sample weights for samples analyzed by ssNMR.**

<b>Sample</b>	<b>Weight (%)</b>	<b>Sample Weight (mg)</b>
<b>D*L* Short</b>	100	34.8
<b>D*L* Short</b>	70	37.7
<b>D*L* Long</b>	30	
<b>D*L* Short</b>	50	39.8
<b>D*L* Long</b>	50	
<b>D*L* Short</b>	30	43.1
<b>D*L* Long</b>	70	
<b>D*L* Long</b>	100	46.1

Differences in physical properties, primarily MW, resulted in differences in the weight of sample analyzed by ssNMR due to the sample rotor being a fixed volume (Table 5-2). Shorter polymers have greater free volume than longer diblocks that resulted in lower sample weight for ssNMR analysis. Analysis was performed by a trained operator on a Bruker 7002, 700 MHz spectrometer equipped with a 4mm high resolution magic angle spinning (HRMAS) probe of Z-gradient in cooperation

with the Minnesota NMR Center. Samples were analyzed at a probe temperature of 38°C and a spinning rate of 12 kHz. One dimensional direct polarization magic angle spinning (DP-MAS) and insensitive nuclei enhanced by proton transfer (INEPT); were applied to the samples. Two-dimensional INEPT was also performed for each sample.

**Statistical Analysis.** The average of the triplicate analyses, 95% confidence intervals were calculated using Excel (Ver. 2007, Microsoft). Statistical differences were detected using single factor analysis of variance (ANOVA),  $\alpha \leq 0.05$ , followed by Tukey Honest Significant difference (HSD) to determine differences between samples also calculated using Excel.

## 5.4 Results and Discussion

### **Measurement of gum base/matrix to water partition coefficients (Log cP).**

Model matrices composed of short and long MW DL diblocks, mixed at three ratios 70:30, 50:50 and 30:70 w/w%, were combined with acetophenone and the log cP values for acetophenone in DL short, DL long and mixtures of short and long DL were measured. The log cP values for the model matrices are show in Table 5-3 below.

**Table 5-3 Matrix to water partition coefficients for acetophenone in model matrix mixtures\*.**

<b>Sample Code</b>	<b>Log cP Acetophenone</b>
<b>DL Short</b>	2.20 ( $\pm 0.03$ )
<b>DL Short: Long 70:30</b>	2.21 ( $\pm 0.02$ )
<b>DL Short: Long 50:50</b>	2.20 ( $\pm 0.03$ )
<b>DL Short: Long 30:70</b>	2.22 ( $\pm 0.04$ )
<b>DL Long</b>	2.18 ( $\pm 0.02$ )

\*Average of triplicate analysis  $\pm 95\%$  confidence intervals, D=poly-epsilon decalactone, L=poly lactide

There were no significant differences between the DL short, DL long or any of the DL short and long blended model matrix mixtures. This is not unexpected as the chemical composition of the matrices does not change even though the physical properties of the matrices are different. Given these results a change in the predicted release of acetophenone from these matrices, based on physicochemical models, would not be predicted[1].

### **Flavor Release from Model Matrix Materials.**

The model matrix system constructed from the short and long DL diblock copolymers results in five matrices which vary in texture from soft (short diblock) to firm (long diblock) but have the same chemical composition[70]. Partitioning and solubility parameter theory does not further predict any difference in flavor release between these materials[1]. It should be noted, there is also a lack of data related to

predicting flavor release from texture differences where the chemical compositions of the matrices are the same. It was hypothesized previously that the molecular weight of entanglement may be somewhat predictive. Given these model matrices with molecular weights both above and below the  $M_e$  for the matrix polymers (Table 5-1) matrices rich in short diblocks would be expected to release more flavor than those rich in long diblocks. This somewhat correlates to observations that conclude soft gum base materials release more flavor than firmer gum bases[63]. However, in those studies the modification of the gum texture was achieved by changing the composition of the gum [17, 28, 57, 63] and based on classical analytical techniques.

#### **Measurement of Flavor Released from Model Matrix during Simulated**

**Chewing.** The release of acetophenone into the air under simulated 'chewing' conditions was measured to determine if there were any apparent differences in kinetic release from these model matrices. The mixtures of acetophenone with short and long DL matrices were processed using an artificial chewing device (Appendix A). Flavor release profiles for acetophenone from the five model matrices were obtained and are overlaid in Figure 5-1 below.

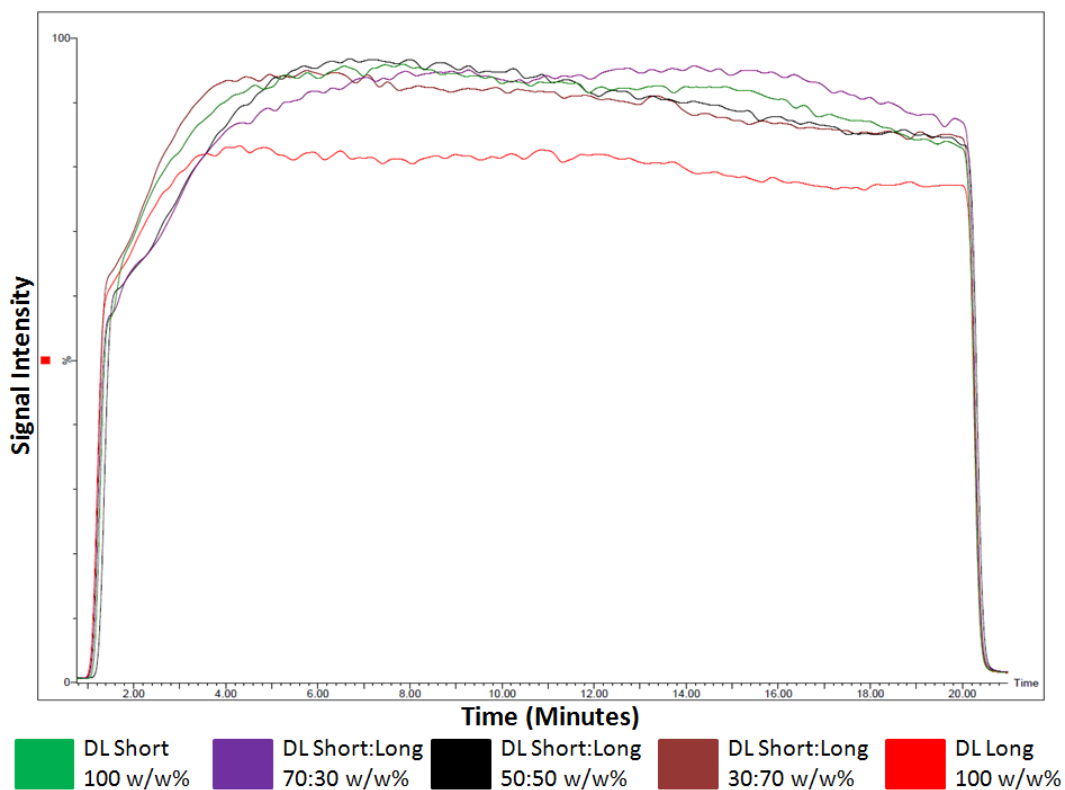


Figure 5-1 Acetophenone release profiles from model matrices

Overall there is a noted difference in intensity of acetophenone release profile between the DL short matrix (green) and the DL long matrix (red) indicating that less acetophenone is released from the longer MW matrix. The differences in release profiles for the blended matrices were less dramatic but generally indicated a decrease in acetophenone release as the matrix contains more long MW material. Since the flavor release profiles are relatively close together and can be difficult to visualize; the peak intensity of the release profile at its maximum height and the corresponding concentration of acetophenone being released at that time were also recorded. The concentration of acetophenone released at the maximum intensity of

the flavor release profile was calculated by linear regression from the standard curve generated during calibration of the APCI-MS. Examination of the maximum intensity of the flavor release profiles and concentration of acetophenone being released in Table 5-4 below to provide a quantitative understanding of the differences in the flavor release profiles.

**Table 5-4 Maximum peak intensities and acetophenone concentration for flavor release profiles generated by APCI-MS.<sup>a</sup>**

<b>Sample Code</b>	<b>Maximum Peak Intensity</b>	<b>Acetophenone <math>\mu\text{g/L}</math></b>
<b>DL Short 100 w/w%</b>	2.18E+08	225.9
<b>DL Short: Long 70:30 w/w%</b>	2.26E+08	245.0
<b>DL Short: Long 50:50 w/w%</b>	2.22E+08	236.2
<b>DL Short: Long 30:70 w/w%</b>	2.08E+08	200.4
<b>DL Long 100 w/w%</b>	2.04E+08	189.1

<sup>a</sup> = mean of duplicate, D = poly-epsilon decalactone, L = polylactide

There were no significant differences between the maximum intensities which refutes the presence of any strong trend. Examination of the average maximum flavor release peak intensities showed that the flavor release profile was greatest for the DL short:long 70:30 mixture followed closely by the DL 50:50 blend and the DL short diblock mixture. Conversely the peak intensity decreased as the mixture becomes largely DL long diblock (DL short:long 30:70) followed by the DL long diblock mixture. The concentration of acetophenone projected to be released during this time agrees with this trend. The release profiles suggested that the short and long blended materials increased flavor release.

### **Quantification of Flavor Released from Model Matrix after Artificial Chewing.**

The flavor load in the flavor and matrix mixtures before artificial chewing and flavor remaining after artificial chewing were also measured. These values provide a further quantitative measure of the flavor released during chewing. Solvent extraction were analyzed by GC/MS analysis. A small portion matrix was analyzed prior to simulated chewing and also removed from the artificial chewing device after 20 minutes of artificial chewing. The flavor content in the matrix before and after artificial chewing and the percent of flavor released as a result of this process are displayed in Table 5-5 below.

**Table 5-5 Flavor content in model matrix mixtures before and after artificial chewing.**

<b>Sample Code</b>	<b>Acetophenone in matrix w/w%</b>	<b>Acetophenone in matrix w/w% after simulated chewing</b>	<b>Acetophenone released %</b>
<b>DL Short 100 w/w%</b>	5.0 (±0.1)	4.0 (±0.2)	20.1 (±4.1)
<b>DL Short: Long 70:30 w/w%</b>	5.0 (±0.1)	3.6 (±0.2)	28.4 (±2.5)
<b>DL Short: Long 50:50 w/w%</b>	5.2 (±0.0)	3.9 (±0.8)	23.8 (±14.9)
<b>DL Short: Long 30:70 w/w%</b>	5.1 (±0.3)	4.0 (±0.4)	20.7 (±1.7)
<b>DL Long 100 w/w%</b>	4.7 (±0.3)	4.2 (±0.3)	9.6 (±0.8)

\*Average of duplicate analysis, triplicate injections, corrected using an internal standard and calculated using linear regression from calibration standards. Margin of error between duplicate samples in parentheses. D = poly-epsilon decalactone L = polylactide

Statistical analysis did not show significant difference present when the release from all five matrix mixtures were compared (p=0.098). However, the flavor release

and quantification could only be performed in duplicate due to limited amount of the model matrix materials. Acetophenone was released to the greatest extent from the DL short:long 70:30 matrix mixture followed by the 50:50 mixture then the 30:70 mixture which released just slightly more than the DL short diblock on its own. Again, the 100 w/w% short MW matrix releases more flavor than the long MW matrix which is consistent with what was observed during real-time release via APCI-MS. The DL short:long 30:70 blend released more flavor than the intensity of the flavor release profile would suggest. Overall, The release of acetophenone was increased in the blended short and long matrices over the short or long matrices separately.

With both the flavor release profiles and the flavor release quantification, DL short:long 70:30 released more than DL short:long 50:50 which released more than DL short:long 30:70. The DL short:long blends also released more flavor than either the DL short or DL long polymer alone. This suggests a synergistic effect is present in which the mixture of short and long diblock copolymers released more flavor than either the short or long diblocks on their own. This suggests texture effects that are more nuanced than the proportion of soft (DL short MW) versus firm (DL long MW) would predict. This shows that the relationship between texture changes and likelihood of flavor release is not well understood. Similar trends to those shown in the flavor release profiles between the extremes of the matrices (short vs. long) are observed. Short MW polymers released more flavor than long MW polymers.

## **Solid-state Nuclear Magnetic Resonance (ssNMR) of Flavor and Matrix Mixtures.**

**Solid State Nuclear Magnetic Resonance (ssNMR) Analysis.** For enhanced sensitivity isotopically enriched model matrix materials were combined to recreate the mixtures of DL short and DL long diblocks which contain varying amounts of DL short and DL long diblocks as shown in Table 5-1 above. Labeled diblock mixtures were combined with carbon-13 labeled acetophenone and analyzed using one and two-dimensional ssNMR experiments.

One dimensional DP-MAS is a common foundational ssNMR technique during which all of the carbons in the sample are polarized to generate a carbon spectra. It is commonly performed in order to confirm sample suitability, instrument sensitivity and the chemical composition of the sample (chapter 3). DP-MAS was performed on the mixtures of acetophenone and DL short, DL long and mixtures of DL short and long to confirm that the concentration of acetophenone is comparable across the model matrices.

Spectra resulting from one-dimensional DP-MAS analysis were interpreted to determine if the acetophenone content in the diblock mixtures were comparable. The overlaid DP-MAS spectra of acetophenone in the model matrices is shown in

Figure 5-2 below.

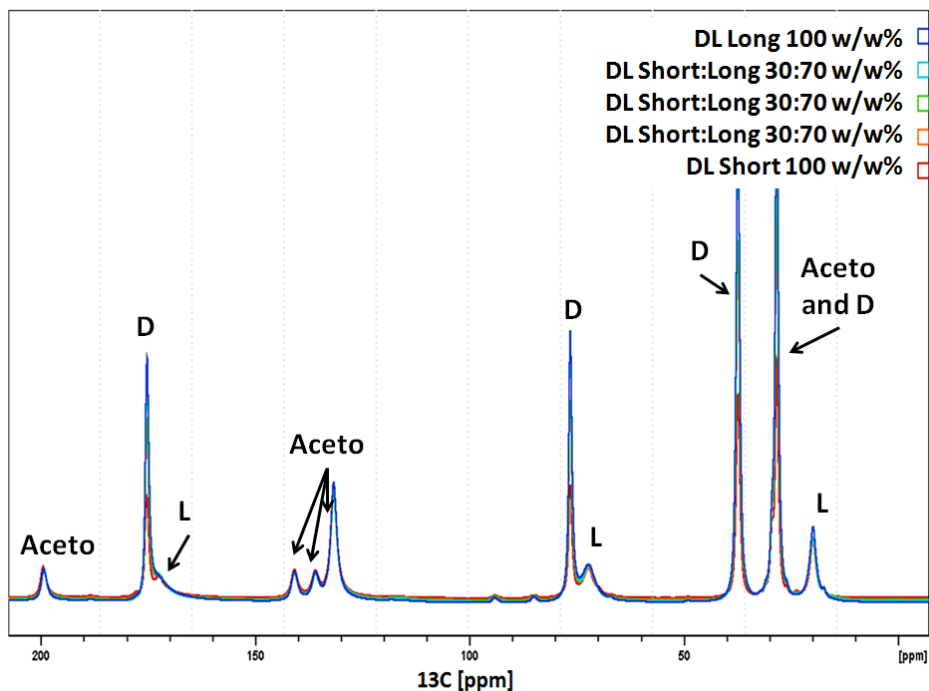


Figure 5-2 Overlay of one-dimensional DP-MAS spectra for mixtures of acetophenone in model matrices. Aceto=acetophenone, D=polyepsilon decalactone, L=polylactide

Examination of the spectra shows peaks at resonances corresponding to the matrix and acetophenone marked in the figure above. Peak identities were confirmed by comparison to DP-MAS analysis of each of the component individually, acetophenone, polyepsilon decalactone and polylactide. The peaks corresponding to the matrix vary in intensity according to the weight of sample analyzed. The long diblock and mixtures rich in long diblock have a higher intensity than the shorter diblocks corresponding to the higher sample weights for the matrix mixtures higher in long diblock (Table 5-2). However, the acetophenone peaks visible have nearly

identical peak intensity. This confirms that the sample matrix mixtures contained the same amount of acetophenone.

Two dimensional INEPT is a common ssNMR techniques used to both increase resolution of ssNMR spectra and for the observation of mobile species in samples. In the current study, this technique was used to evaluate the impact of physical property rather than chemical composition changes on the dynamics of a model flavor compound, acetophenone. As mentioned in chapter 3 when no changes to the chemical composition are present, cross peaks shifts are less likely. DP-MAS analysis confirmed that all of the sample matrices contain the same concentration of acetophenone. As such, any changes in the intensity of the acetophenone peaks are due to changes in dynamics of acetophenone as previously observed by the two-dimensional INEPT technique (chapter 3).

Two dimensional INEPT spectra were obtained for the acetophenone and matrix mixtures. Resonances assigned to both the polymer matrix and acetophenone are visible in the two-dimensional spectra overlaid in Figure 5-3.

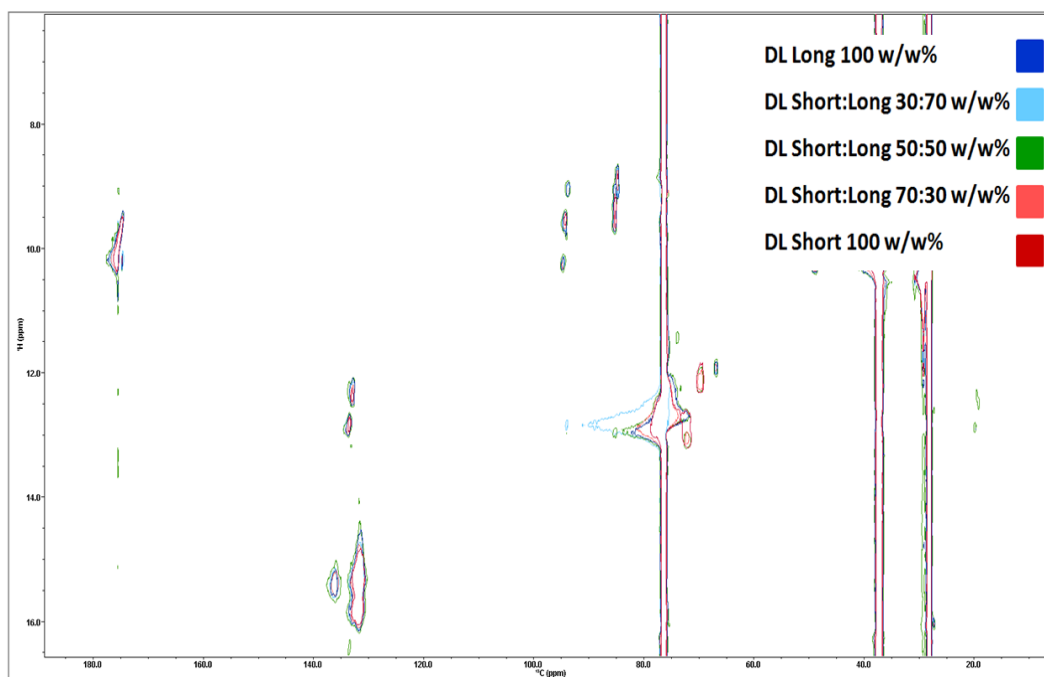


**Figure 5-3** Overlay of two-dimensional INEPT spectra for mixtures of acetophenone in model matrices.

INEPT experiments observe the mobile species in a given mixture. As such, the cross peaks shown Figure 5-3 above are largely resonances attributed to poly-D and acetophenone. Polylactide is the most rigid component of the system with glass transition temperatures above the analysis temperature of 38°C (Table 5-1) and as such most peaks from L were not visible in one or two-dimensional INEPT experiments. However, a cross peak at 20ppm attributed to L was visible, and likely in part due to the carbon-13 isotopic enrichment of the model matrices, shown in Figure 5-4.

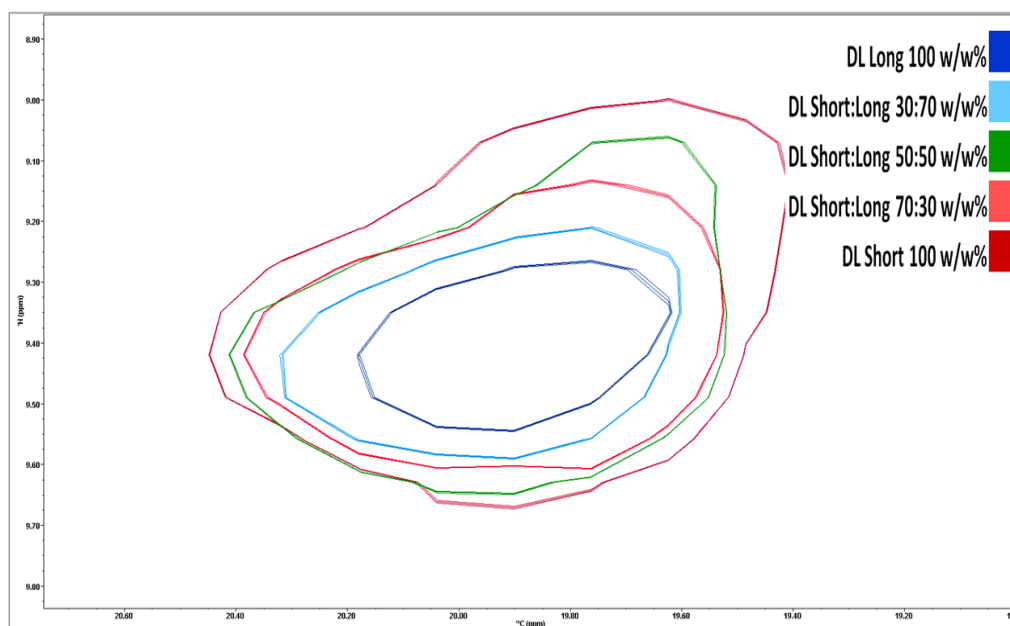


**Figure 5-4** Overlay of the two-dimensional INEPT cross peak from polylactide in mixtures of acetophenone and model matrices.

In general differences in the size of the cross peak were observed from acetophenone and model matrix mixtures. Representations of two-dimensional NMR data resemble a topographic map, with a larger cross section or area of the cross peak representing a larger/more intense peaks. The signal of each spectrum was normalized when the samples were overlaid to ensure that observed differences in intensity are not artifacts of the two-dimensional signal display. When the areas or intensities of these cross peaks were examined the intensity was correlated with the molecular weight content of the matrix. Model matrices with greater DL short content displayed greater intensity. Increased intensity observed in INEPT experiments is indicative of greater mobility of the given cross peak in the sample. Model matrices with greater DL short content therefore showed greater

mobility. This increased mobility is not unexpected as the physical properties of the L blocks, such as glass transition temperature ( $T_g$ ) in particular, are decreased when the MW of the L block is decreased (from 53.3°C to 52.2°C) Table 5-1. Since the analytical temperature was 38°C for this analysis, the DL Short diblock is closer to its  $T_g$  and therefore is more mobile. Similar effects were seen with polyvinyl acetate in chapter 4. These observed changes in L block peak intensity provide evidence that the physical properties of the matrix mixtures do vary and the ssNMR technique employed is sensitive to these changes.

When the acetophenone cross peaks were examined differences in cross peaks intensity were observed and are visible in Figure 5-5 below.

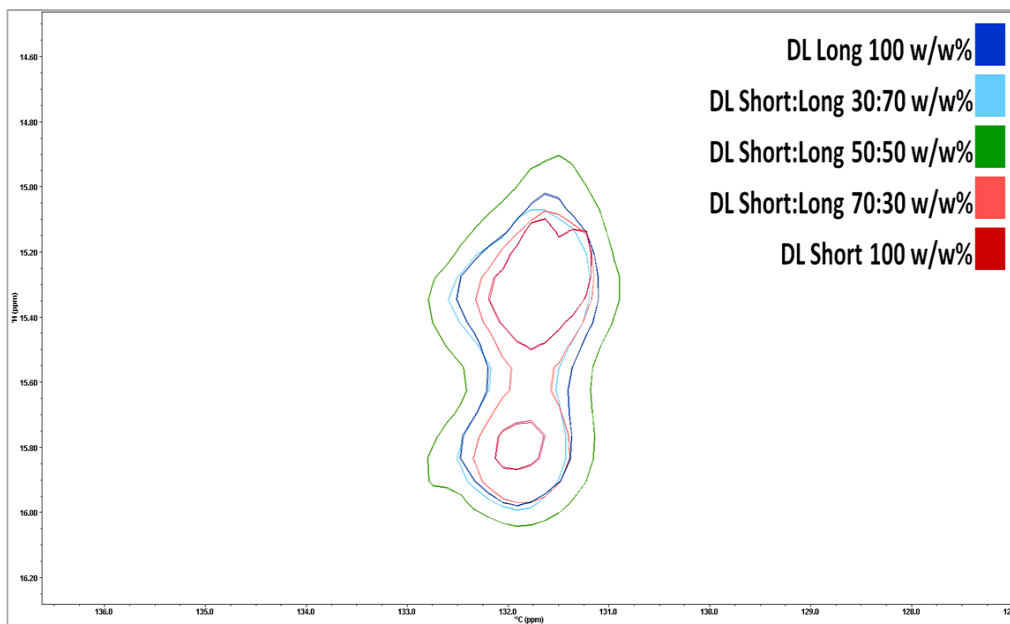


**Figure 5-5** Overlay of two-dimensional-INEPT acetophenone cross peaks for acetophenone in model matrices.

Acetophenone in the DL short:long 50:50 mixture has the greatest intensity, the largest peak area in Figure 5-5 above. This suggests that the acetophenone is most mobile when combined with the DL short:long 50:50 matrix and therefore less likely to be participating in close intramolecular interactions with the matrix materials. The intensity values for the cross peaks were plotted to provide a more quantitative approach towards comparing the intensities of the acetophenone cross peaks. The intensities of each acetophenone cross peak were plotted for each sample mixture in Figure 5-6 below.

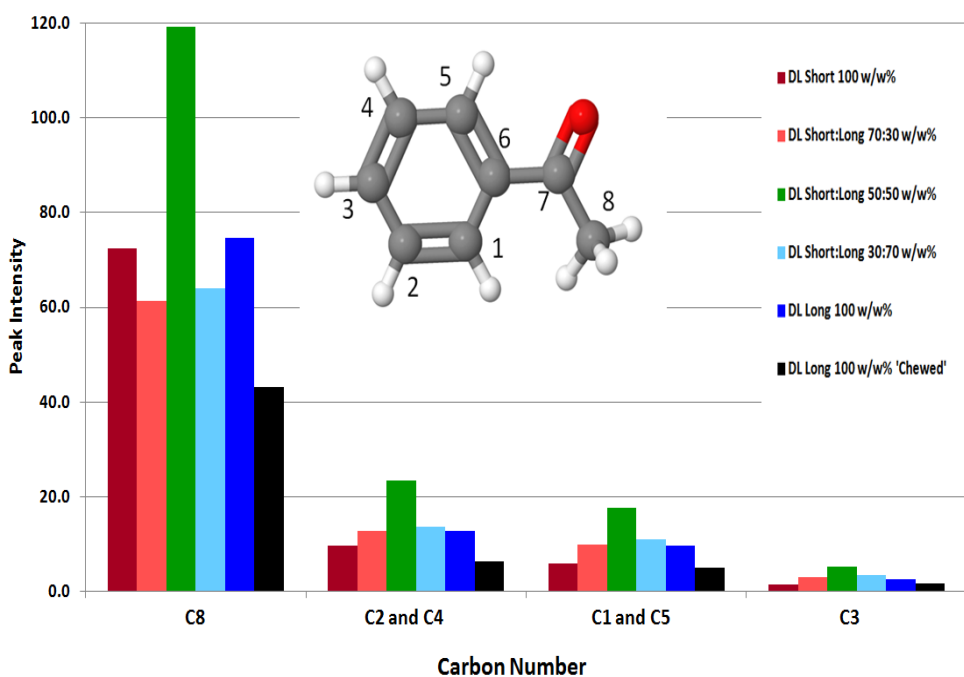


Figure 5-6 Acetophenone cross peak intensities in various model matrices plotted against carbon position.

As shown in Figure 5-6 above the methyl carbon, C8 in the figure above, shows the highest intensity and therefore mobility across all sample matrices followed by the cyclic carbons. The less mobile cyclic carbons suggest they have a

much stronger intramolecular interaction with the sample matrix than the methyl carbon. Examination of the impact of the matrix composition on the interaction reveals two patterns. One, the methyl carbon is most mobile in the DL short:long 50:50 matrix followed by the DL long, DL short and then the other blended materials. Two, for the cyclic carbons, the DL short:long 50:50 is also the most mobile followed by the other blended matrices, DL long and finally the DL short diblock. This data suggests that release is the most probable from the DL short:long 50:50 matrix followed by the DL short:long blended matrices.

In general, the pattern of mobility for the cyclic carbons was similar to the acetophenone release profiles and the quantification of the flavor release during artificial chewing from these model matrices. Where blended DL short and long matrices are thought to release more flavor than either DL short or long alone. Again, similar to the traditional methodologies, the two-dimensional INEPT results do not show a linear relationship between DL short:long matrix composition and projected flavor release. There may be some antagonistic effects between acetophenone and the DL short:long 50:50 matrix mixture causing the acetophenone to be more mobile and available to release from the matrix. This data again highlights that the relationship between matrix texture and release is not straightforward.

A mixture of the DL long matrix with acetophenone was also analyzed after simulated chewing and the intensity of the acetophenone cross peaks is also plotted in Figure 5-6. A pronounced decrease in peak intensity was observed, in this case

indicating that there is less flavor remaining in the matrix. Further analysis of the remaining acetophenone and DL short:long matrix mixtures after simulated chewing could help determine if the observations from two-dimensional INEPT might predict the release behavior across more subtle matrix composition changes. This was not undertaken as part of this study due to limited amounts of matrix material.

This study concludes that while the log cP values did not predict differences in flavor release; kinetic release profiles and flavor release quantification did show differences in flavor release. Differences in kinetic flavor release were most pronounced between the DL short and long diblocks. DL short released more acetophenone than DL long as observed in the flavor release profile and the quantification of flavor released via GC/MS. The blended DL short:long matrices released more flavor than either the DL short or DL long.

The two-dimensional INEPT ssNMR experiments indicated slightly increased mobility of acetophenone in the long MW diblock as compared to the short MW diblock. This suggests that there are stronger intramolecular interactions in the short diblock. Most interestingly, examination of acetophenone two-dimensional INEPT cross peak intensities show greater mobility, and therefore predicted release, from the DL short:long blended matrix materials than either the DL short or long for the cyclic carbons in acetophenone. This observation was in agreement with the results for the APcI-MS release and residual quantitation from gum during consumption.

The increased mobility of the acetophenone in the DL short:long blended materials and increased kinetic release observed suggest synergistic effects between the short and long diblocks with regard to flavor release. Examination of measured partition coefficients and consideration of the texture changes to the matrix using traditional flavor release conventions were not able to predict this phenomena. However, observations gathered from ssNMR analysis were able to suggest greater opportunity for release from the blended materials. The changes in free volume of the polymer matrices and moderate physical properties of blended matrix materials results in phase separated materials which appear to encourage flavor release from the matrix[69].

These results highlight the importance of ssNMR as a technique for the investigation of flavor to matrix interaction behavior as a predictor of release behavior. Direct observation of the intramolecular interactions using these techniques was able to obtain information about the impact of physical property changes even when the chemical composition of the model food matrix did not change.

## **Chapter 6 Investigation of intermolecular interactions between flavor molecules and model matrix polymers using solid state nuclear magnetic resonance**

### 6.1 Abstract

Solid state NMR techniques were used to investigate and characterize interactions between a model flavor molecule and model polymer matrix system. The model matrix system was composed of homopolymers and diblock copolymers of polyepsilon decalactone (D) and polylactide (L) in varying molecular weights. Model diblock copolymers (DL) were selectively carbon-13 enriched on either the D or L block to assist with targeting regions of the polymer to analyze. Water to flavor partition coefficients, termed  $\log cP$ , were measured for the flavor compound acetophenone in polyepsilon decalactone (D) and polylactide(L) homopolymers as well as a DL diblock copolymer. The  $\log cP$  value for acetophenone in L was significantly different from D and DL polymers suggesting that the D block is influential to partitioning behavior. One-dimensional ssNMR analysis confirmed the efficacy of selective carbon-13 labeling of model DL diblocks and equivalent concentration of acetophenone across the various model matrix mixtures. Acetophenone and the D blocks of the model matrix system were confirmed to be the mobile components and L blocks the rigid component in the sample mixtures using one-dimensional ssNMR techniques. Selective labeling and cross polarization magic angle spinning (CP-MAS) found that while L blocks appear to interact with acetophenone slowing its molecular dynamics, the D block did not interact with

acetophenone in this manner. One and two dimensional insensitive nuclei enhanced by proton transfer (INEPT) experiments further indicated that acetophenone experienced more molecular mobility when combined with longer MW DL diblocks suggesting greater flavor release from these materials. Lastly, two dimensional nuclear Overhauser effect spectroscopy (NOESY)-INEPT confirmed the presence of through space correlations between acetophenone and matrix polymers indicating close intermolecular interactions. Further, these interactions were found to be sensitive to physical properties of the model matrices.

## 6.2 Introduction

The intermolecular interactions between flavor and food matrices are key to understanding flavor release from a matrix during mastication and consumption. Until recently study of these interactions was complicated due to lack of application of analytical techniques possessing the ability to make direct observations of flavor molecules in food matrices. Instead, flavor scientists have characterized food matrices to the best of their abilities based on what is known or assumed about their chemical properties[1, 11, 72].

Physicochemical models have been developed to model flavor interactions to various matrices based on their chemical structure[1]. The hypotheses these models were based on use the chemical composition of the food matrix to predict flavor release from foods[14, 24, 25]. However, these methods could not account for

differences in the physical properties of food matrices. A common physical property that varies between food matrices but does not often alter the chemical properties is the degree of polymerization of the matrix. Carbohydrates, proteins and other polymers are common to many food matrices and changes to the physical properties of these polymers can have important ramifications with regard to flavor release[73]. In addition, several recent studies have concluded that further understanding of the intermolecular interactions between flavors and microstructures is necessary [4, 5, 34-36]. Since many traditional predictive flavor release models and analytical techniques rely on examining chemical differences there have not been great strides recently in the development of techniques capable of studying flavor to matrix interactions in situ in chemically similar matrices.

The main research goal of this study was to examine the use of several ssNMR techniques to investigate the chemical and physical properties of a flavor and polymer model mixture. A diblock copolymer system suitable for use as a chewing gum base (as reported in chapter 5) was further investigated to understand flavor to matrix interactions(chapter 5). This system composed of a polyepsilon decalactone (D) homopolymer covalently bound to a polylactide (L) homopolymer forming a diblock copolymer[68]. The synthesis is well understood and characterized[68]. Specifically, changes in sample and flavor mobility as the matrix undergoes physical property changes as well as direct evidence of intermolecular interactions between flavor and matrices will be confirmed through the use of nuclear Overhauser effect spectroscopy (NOESY)-INEPT. The impact of physical

property changes to the model matrices on these intermolecular interactions, if present, will be also be examined.

### 6.3 Materials and Methods

**Selection of Model Polymer Matrix Materials.** Evaluation of the many ways that ssNMR techniques can be used to study interactions between flavor molecules would benefit from a highly characterized and controlled model matrix. As mentioned in chapter 5 sustainable block copolymers have been developed using green chemistry techniques and thoroughly characterized. These model matrix materials provide the ability to study the interaction of flavor with separate polymers, mixtures or polymers of various lengths. In addition, selective isotopic enrichment of the matrix materials allows for reduced sample analysis time and the ability to enhance segments of a model matrix in a controlled manner.

**Materials.** Poly-epsilon decalactone ( $\epsilon$ -DCL) and poly-lactide (L) homopolymers as well as poly-epsilon decalactone:poly-lactide (DL) diblock copolymers in varying molecular weights both with and without carbon-13 enrichment of the polymers were obtained from Ortec Inc (Piedmont, SC.). Acetophenone and methyl hexanoate were obtained from Sigma Aldrich (St. Louis, MO.). Isotopically enriched  $^{13}\text{C}_8$  Acetophenone was obtained from Isotec (Miamisburg, OH.) Hexanes, acetone, and methanol were obtained from Sigma Aldrich (St. Louis, MO.) Physical properties were obtained from the manufacturer and are displayed in Table 6-1 below.

Molecular weights for D and L were obtained using gel permeation chromatography (GPC) protocols common to the synthetic polymer industry. Glass transition temperature ( $T_g$ ) was obtained via differential scanning calorimetry (DSC) also using protocols common to the industry.

**Table 6-1 Physical properties for model matrix materials.**

<b>Sample</b>	<b>Molecular Weight D Block (kDa)</b>	<b>Molecular Weight L Block (kDa)</b>	<b>Molecular Weight of Entanglement D Block (kDa)</b>	<b>Molecular Weight of Entanglement L Block (kDa)</b>	<b>Glass Transition Temperature D Block (°C)</b>	<b>Glass Transition Temperature L Block (°C)</b>
<b>D Long</b>	24.5		5.9	9.2	-50.3	-
<b>L Long</b>		15.7	5.9	9.2		49.1
<b>DL Long</b>	21.9	14.6	5.9	9.2	-46.4	54.1
<b>D* Short</b>	4.6		5.9	9.2	-52.7	
<b>L* Short</b>		2.7	5.9	9.2		40.8
<b>D*L Short</b>	4.0	2.7	5.9	9.2	-47.5	50.3
<b>DL* Short</b>	4.0	2.6	5.9	9.2	-46.4	54
<b>D*L Long</b>	23.5	15.7	5.9	9.2	-46.2	53.5
<b>DL* Long</b>	23.4	15.6	5.9	9.2	-44.9	53.1

\*Indicates presence and position of <sup>13</sup>C isotopic enrichment, D=poly-epsilon decalactone L=poly lactide

**Measurement of gumbase/matrix to water partition coefficients (Log cP).** Non-isotopically enriched long D homopolymer, long L homopolymer and long DL diblock copolymer were processed into pieces of less than 2 cubic mm with a razor blade. Only materials which were processed to be less than 2 cubic mm were used for log cP measurement.

A stock solution of acetophenone was prepared at 10 w/w% in methanol. An internal standard solution of methyl hexanoate 100ppm in hexane:acetone 90:10 vol/vol was also prepared.

Processed materials (0.4 g) were placed in 20mL vials, 2mL of deionized distilled water were added. Aliquots of acetophenone ( $\mu\text{L}$ ) were added to individual vials of material and water. Vials were sealed with air-tight screw caps and equilibrated at 38°C in a shaking water bath for 72hours. A portion of the aqueous phase (1.5mL) was removed from the sample vial and transferred to a microfuge tubes via 0.22  $\mu\text{m}$  nylon syringe filtration. The aqueous portion was extracted by shaking and vortexing with 0.3mL methyl hexanoate 100ppm in hexane:acetone 90:10 vol/vol. Extracted samples were centrifuged for 5min at 10000rpm and sample extracted into the hexane:acetone portion was removed to an auto sampler vial for GC/MS analysis. Samples were prepared in triplicate. A standard curve was constructed for acetophenone by aliquoting stock acetophenone solution into 100ppm methyl hexanoate in hexane:acetone 90:10 and analyzed via GC/MS along with the sample extracts.

**Gas Chromatography Mass Spectrometry(GC/MS).** Extracted acetophenone in hexane:acetone 90:10 vol/vol were quantified by GC/MS, each replicate was injected in duplicate. Analysis was performed on a Agilent 7890B Series GC equipped with a 5977 mass selective detector, autosampler (HP 7673) and a fused-silica capillary column (DB-5, 60 m, 0.25 mm i.d., 0.25 µm film thickness, Agilent Technologies, CA). The GC/MS operating conditions were as follows: inlet temperature was 220 °C, oven program was 40 °C for 0.5min, then increased at 10 °C/min to 230 °C and held for 3 min; constant flow of 1.0 mL/min (He); 1 µL of sample was injected in split mode(1:20). Mass selective detector was operated in scan mode ranging from 30 to 300amu with a solvent delay of 5.5min. Samples were analyzed alongside flavor standards and corrected using the internal standard. Corrected peak areas from duplicate injections were averaged. Linear regression was employed to calculate the concentration of flavor in the extracted sample and adjusted to reflect the concentration in the aqueous phase.

**Calculation of gumbase/matrix to water partition coefficients (Log cP).** Log cP values were calculated according to the following equation:

$$\log cP = \log \left( \frac{\text{mg flavor/g gumbase}}{\text{mg flavor/g aqueous solution}} \right)$$

**(6-1)**

Log cP values for duplicate injection were averaged. The average of the triplicate analysis of the samples was then average to obtain a single log cP value for each flavor molecule in each matrix mixture evaluated.

**Solid-state Nuclear Magnetic Resonance (ssNMR) of Flavor and Matrix Mixtures.**

**Solid State Nuclear Magnetic Resonance (ssNMR) Analysis.** Carbon-13 enriched long D and L homopolymers as well as short and long DL diblocks differentially labeled with carbon-13 on either the D or L block were combined with acetophenone at 3.8 w/w% and placed in an oven at 64°C for two hours. The heated model matrix and acetophenone mixtures were removed from the oven and immediately stirred until homogenous using a dental probe. Stirred model matrix and acetophenone mixtures were stored at room temperature and in the absence of light for at least 18 hours prior to ssNMR analysis. Immediately prior to analysis enriched matrix and acetophenone samples were packed into 3.2mm zircon rotors and weighed to record sample weight listed in Table 6-2 below.

**Table 6-2 Sample weights for samples analyzed by ssNMR.**

<b>Sample</b>	<b>Sample Weight (mg)</b>
<b>D* Short</b>	31
<b>L* Short</b>	42
<b>D*L Short</b>	36
<b>DL* Short</b>	23
<b>D*L Long</b>	36
<b>DL* Long</b>	45

\*Indicates presence and position of 13C isotopic enrichment, D=poly-epsilon decalactone L=polylactide

Analysis was performed by a trained operator on a Bruker 7002, 700 MHz spectrometer equipped with a 4mm high resolution magic angle spinning (HRMAS) probe of Z-gradient in cooperation with the Minnesota NMR Center. Samples were analyzed at a probe temperature of 38°C and a spinning rate of 12 kHz. One dimension techniques; direct polarization magic angle spinning (DP-MAS), cross polarization magic angle spinning (CP-MAS) and insensitive nuclei enhanced by proton transfer (INEPT); were applied to the samples. Two-dimensional INEPT and nuclear Overhauser effect spectroscopy (NOESY)-INEPT were also performed for each sample.

**Statistical analysis.** The average of the triplicate analyses, 95% confidence intervals were calculated using Excel (Ver. 2007, Microsoft). Statistical differences were detected using single factor analysis of variance (ANOVA),  $\alpha \leq 0.05$ , followed by Tukey Honest Significant difference (HSD) to determine differences between samples also calculated using Excel.

## 6.4 Results and Discussion

### **Measurement of gumbase/matrix to water partition coefficients (Log cP).**

The non-isotopically enriched long D and L homopolymers and the long DL diblock were combined with acetophenone and their partition coefficients were measured and are shown in Table 6-3 below.

**Table 6-3 Gumbase/matrix to water partition coefficients for acetophenone in model matrix materials.**

<b>Sample Code</b>	<b>Molecular Weight (kDa)</b>	<b>Acetophenone<sup>1</sup></b>
<b>DL</b>	22/15	2.12 ( $\pm 0.021$ )a
<b>D</b>	24	2.10 ( $\pm 0.004$ )a
<b>L</b>	16	1.62 ( $\pm 0.077$ )b

<sup>1</sup> Different letters indicate statistically significant difference determined by oneway ANOVA analysis and Tukey's test ( $\alpha = 0.05$ ). <sup>a</sup>: not significantly different. Average of triplicate analysis  $\pm 95\%$  confidence intervals. **D= poly-epsilon decalactone L=poly lactide.**

The partition coefficients showed significantly difference ( $p = 3.04 \times 10^{-13}$ ) with Tukey HSD showing significant difference between D and L homopolymers ( $p < 0.01$ ) as well as between the DL diblock and L homopolymer ( $p < 0.01$ ). However, there was no significant difference between the DL diblock and the D homopolymer. This suggests that when combined as a diblock copolymer the D block is more influential to the partitioning behavior of the diblock than the L homopolymer.

### **Solid-state Nuclear Magnetic Resonance (ssNMR) of Flavor and Matrix Mixtures.**

#### **One-dimensional-Solid State Nuclear Magnetic Resonance (ssNMR) Analysis.**

Direct polarization magic angle spinning (DP-MAS) is a common one dimensional ssNMR technique in which all of the carbons in the sample are polarized and a carbon-13 spectra generated. It is commonly employed to confirm the identity of peaks in samples spectra and optimize the sensitivity of the instrument prior to other ssNMR analysis (chapter 3). In this study it was also used to confirm that the

selective labeling of some of the DL diblock on either the D or the L block was successful.

The acetophenone and model matrix materials were analyzed using DP-MAS to confirm the peak identities and flavor content of the mixtures. The D and L homopolymers were combined with acetophenone, analyzed by ssNMR and their DP-MAS spectra is overlaid in Figure 6-1 below.

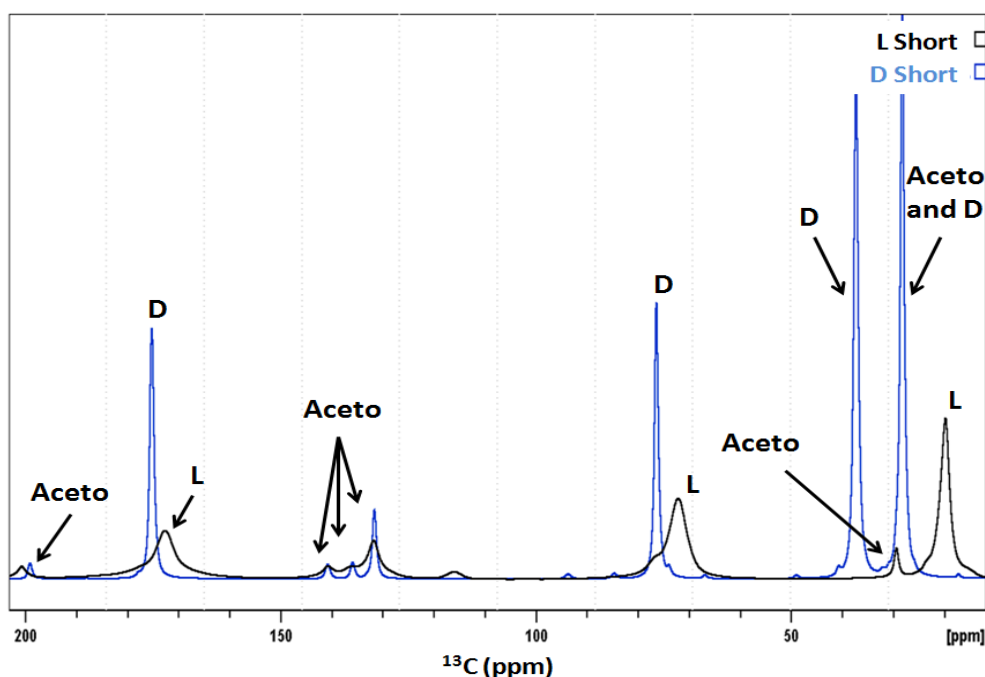


Figure 6-1 DP-MAS spectra for short D and L homopolymers with acetophenone 4 w/w%.

We can see in Figure 6-1 above resonances for acetophenone, D and L with little signal overlap with the exception of the 29ppm resonance of acetophenone and 28ppm resonance of D. The flavor content between the samples was confirmed to be very similar given the similar signal intensity of the acetophenone peaks. The diblock copolymers with either the D or L block enriched in both short and long MW

were also combined with acetophenone at 4w/w%, analyzed by DP-MAS and are displayed in Figure 6-2 below.

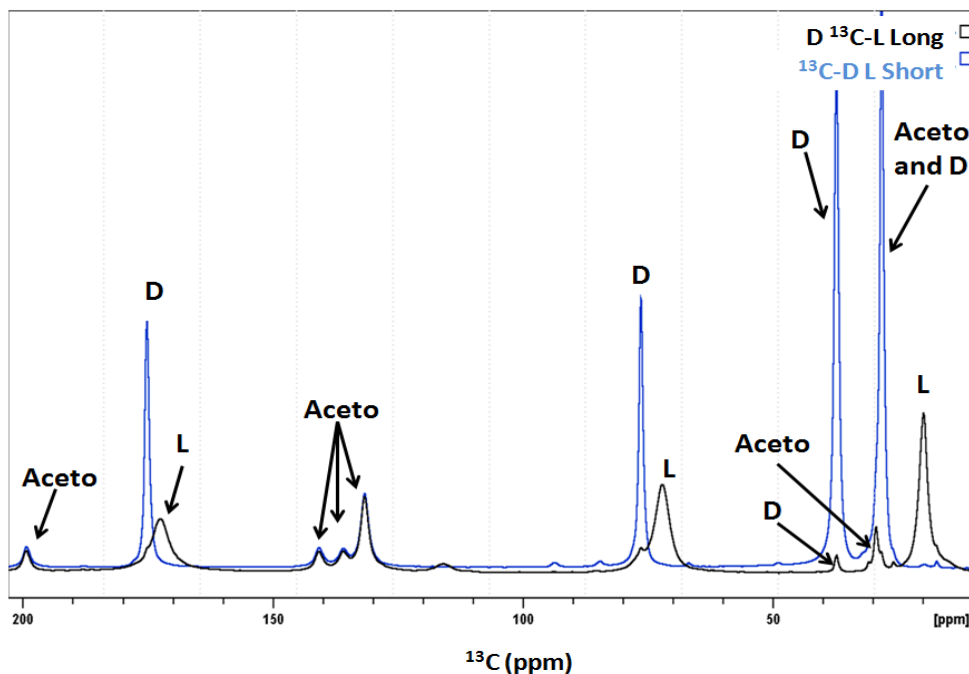


Figure 6-2 DP-MAS spectra for  $^{13}\text{C}$ -DL short MW (blue) and D  $^{13}\text{C}$ -L Long MW (black) with acetophenone 4 w/w%.

The matching signal intensity of the acetophenone peaks confirms that the acetophenone content in both mixtures was comparable. Both the D and L polymers were present in each mixture however the carbon-13 enrichment varied. The spectra from the D enriched diblock contains resonances attributed to D and acetophenone but does not show peaks from the L block due to the lack of enrichment. However, the spectra from the L enriched diblock contained resonance attributed to L, acetophenone and small peaks attributed to D. These spectra show

that the selective enrichment was successful and provided the ability to focus on one component of the matrix when both components are present.

Cross polarisation magic angle spinning (CP-MAS) is another common one-dimensional ssNMR technique. Initially used as a signal enhancement technique the CP-MAS technique is often used in more recent work to focus on the rigid components in a sample mixture (chapter 3). CP-MAS was used in this study to determine which components in the acetophenone, D and L model matrix system are behaving as rigid species. Interpretation of intensity changes in CP-MAS signals can also be used to observed changes in mobility of small molecules which suggest very close associations with the matrix. Adjustments to the analytical conditions, primarily probe temperature, of the CP-MAS technique were also used to increase the resolution of mobile matrix components.

Mixtures of enriched homopolymers and diblocks in short or long MW mixed with carbon-13 acetophenone, also at 4w/w%, were analyzed by CP-MAS. The CP-MAS spectra for short MW D and L with acetophenone are overlaid below in Figure 6-3.

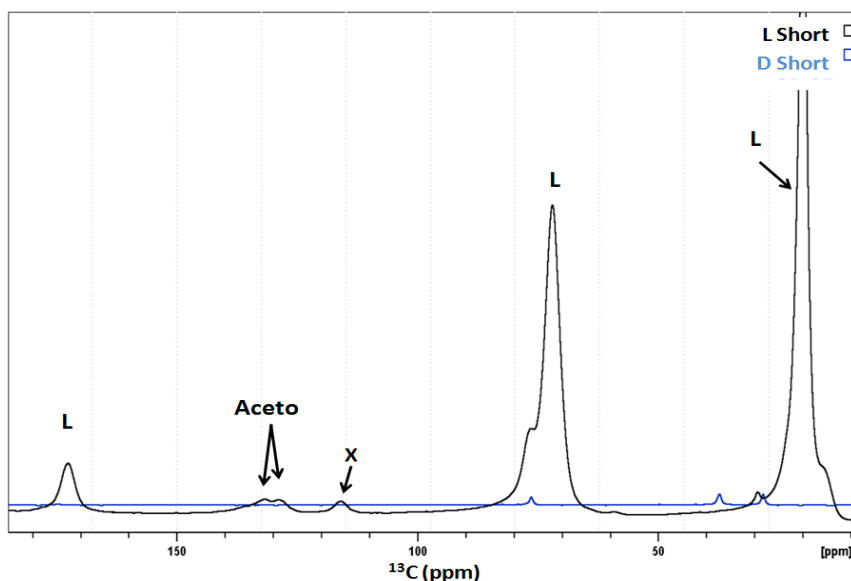


**Figure 6-3 CP-MAS spectra for short D and L homopolymers with acetophenone 4 w/w%, x=spinning side band irregularity.**

Peaks assigned to L were visible in the CP-MAS spectra but the peaks associated with D were very small and the acetophenone peaks were only visible when combined with L. These results confirm that L is the more rigid matrix material in a system composed of D, L and acetophenone. The appearance of acetophenone peaks in the CP-MAS spectra for the mixture of acetophenone at 4w/w% in L suggests that the acetophenone may be interacting with the L. The interaction of the acetophenone with L would impede the mobility of the acetophenone thus increasing its rigidity and signal intensity in the CP-MAS experiment. Acetophenone peaks were not observed in the mixture of 4w/w% acetophenone in D. CP-MAS spectra was also collected for the mixture of D and acetophenone at -14°C rather than the typical 38°C to determine if lowering the analysis temperature would increase the rigidity of the D and increase the signal intensity of the CP-MAS spectra.

The CP-MAS spectra for D with acetophenone 4w/w% analyzed at 38°C and -14°C are overlaid in Figure 6-4 below.

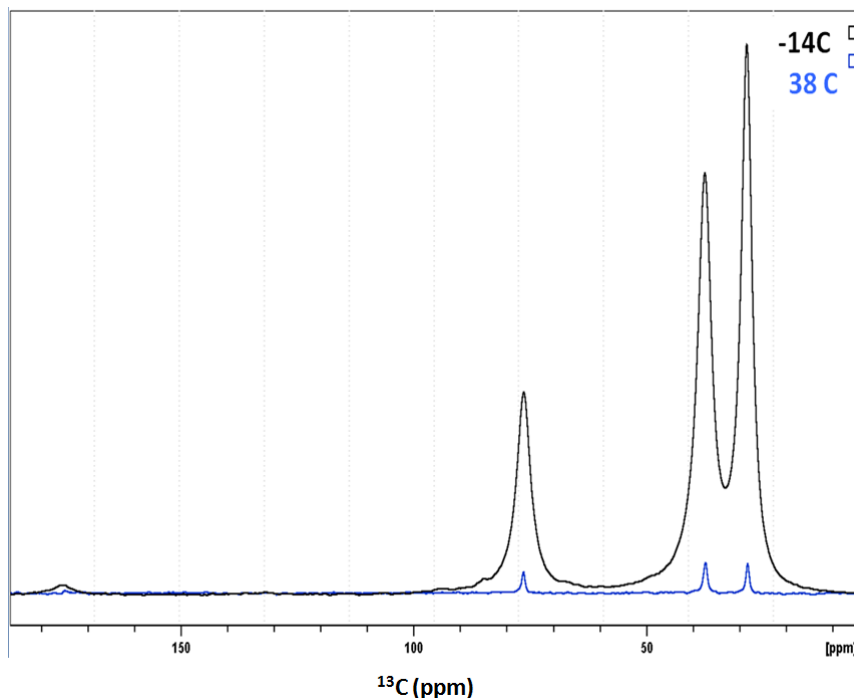


Figure 6-4 CP-MAS spectra for D with acetophenone, 4 w/w% at -14 (black) and 38°C (blue).

Lowering the probe temperature during the analysis was able to increase the sample intensity to a range comparable to the L however, even at adequate signal intensity there were no peaks belonging to acetophenone visible in the CP-MAS spectra for D and acetophenone. There was no evidence of entanglement of acetophenone in D.

The diblock copolymers with either the D or L block enriched, both short and long MW, were also combined with acetophenone at 4w/w%, analyzed by CP-MAS and are displayed in Figure 6-5 below.

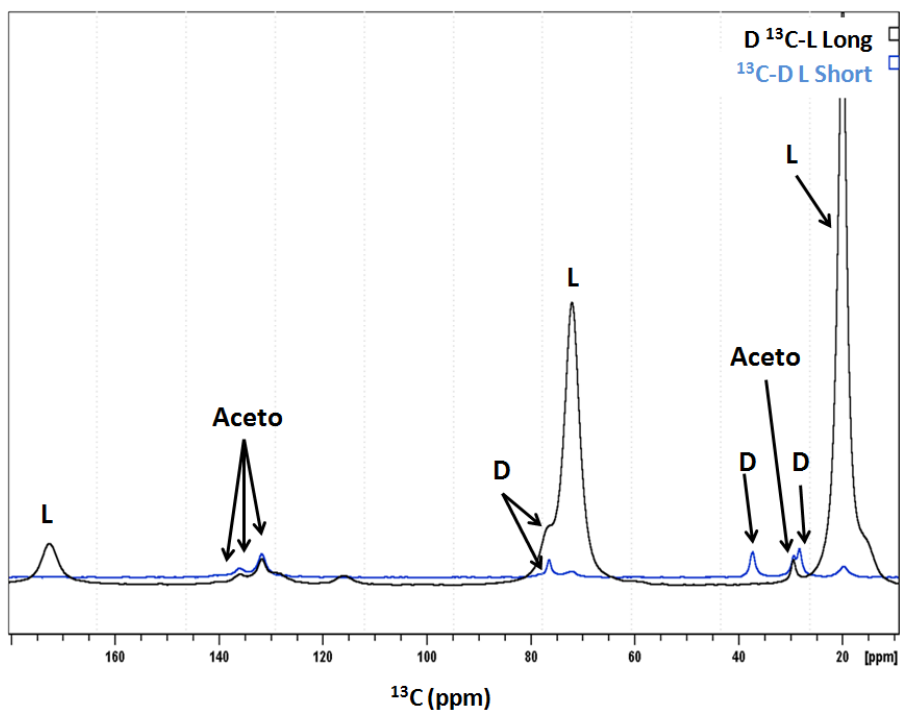


Figure 6-5 CP-MAS spectra for  $^{13}\text{C}$ -DL short MW (blue) and  $\text{D } ^{13}\text{C}$ -L Long MW (black) with acetophenone 4 w/w%.

Examination of the CP-MAS spectra of the selectively enriched diblocks showed resonances corresponding to the enrichment location and rigidity of the enriched block. The diblock with enriched D block (Blue trace in Figure 6-5 above) had a much lower intensity due to its lack of rigidity at  $38^\circ\text{C}$  but did contain resonance associated with D, L and acetophenone. While acetophenone resonances were not observable by CP-MAS in the mixture of D homopolymer and acetophenone (Figure 6-4) they were visible when D was combined with L as a diblock. This indicates that the presence of the more rigid L was necessary to decrease the mobility of acetophenone in the matrix. The diblock enriched on the L block (black trace in Figure 6-5 above) combined with acetophenone shows resonances for L,

acetophenone and only one resonance associated with D, 76ppm, indicating that D was not entangled or experiencing increased rigidity due to the presence of L. If this would have occurred we would have seen an increase in the intensity of peaks assigned to D. Examination of the differences between the signal intensity of acetophenone in short versus long MW diblocks was examined. The CP-MAS spectra for short and long D enriched diblocks are overlaid in Figure 6-6 below.

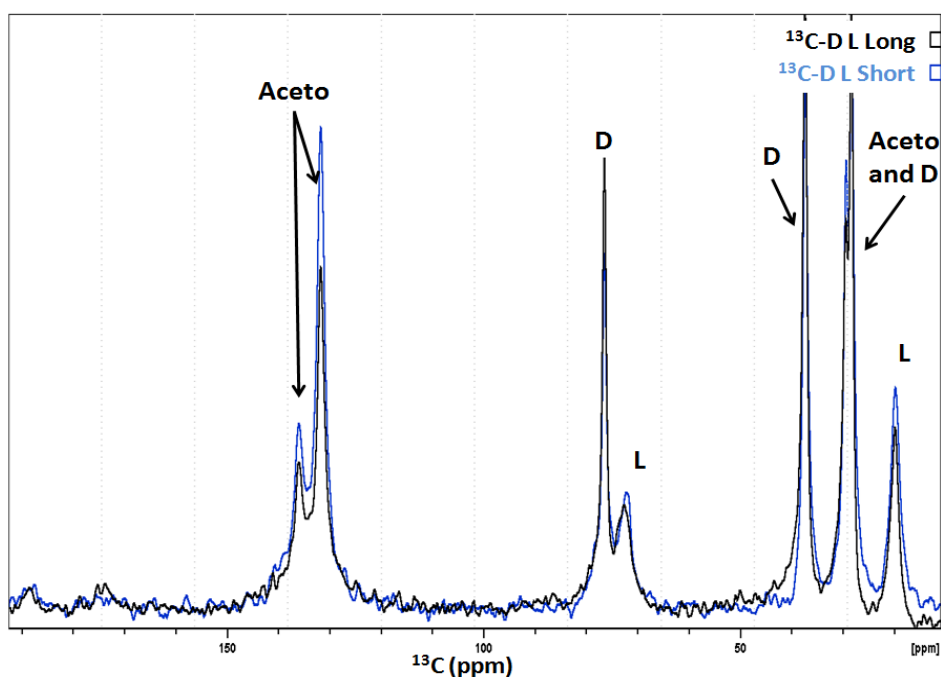
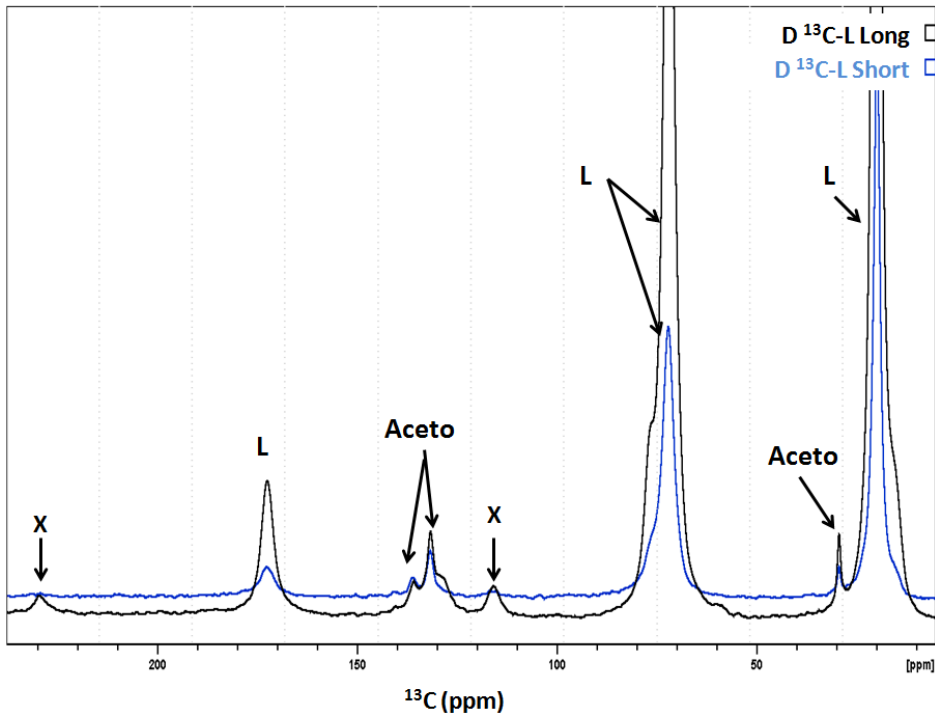


Figure 6-6 CP-MAS spectra for  $^{13}\text{C}$ -DL short MW (blue) and  $^{13}\text{C}$ -DL Long MW (black) with acetophenone 4 w/w%.

The overall signal for this CP-MAS is much lower than other CP-MAS spectra evident by examining the increased baseline noise. This is due to the placement of the carbon-13 enrichment in these samples. The D block and acetophenone were enriched in these samples. Since they are mobile components of the matrix mixtures the signal in CP-MAS is very low even with carbon-13 enrichment. As such,

no conclusions regarding the impact of MW on the mobility of acetophenone were drawn from examining this spectra. For the diblocks enriched on the L block and combined with acetophenone the CP-MAS spectra are overlaid in Figure 6-7 below.



**Figure 6-7 CP-MAS spectra for  $\text{D}^{13}\text{C-L}$  short MW (blue) and  $\text{D}^{13}\text{C-L}$  Long MW (black) with acetophenone 4 w/w%, x=spinning side band irregularities.**

Examination of the CP-MAS showed greater intensity overall for the polymer matrix and acetophenone peaks when combined with longer MW materials. Given that the acetophenone peaks are of the same intensity in the DP-MAS, the increased intensity observed in the CP-MAS spectra indicated that the acetophenone was less mobile when combined with longer diblocks. This suggests that flavor is more likely to release from shorter DL diblocks.

CP-MAS experiments have confirmed that L was indeed the more rigid component in the model matrix. Increased intensity and therefore reduced mobility was observed when acetophenone was combined with L as opposed to D. This suggests that L rather than D interacts very closely with acetophenone, decreasing its mobility. Control of the CP-MAS experimental parameters was able to increase the signal intensity of the mobile matrix component, D. However, even when the D homopolymer was analyzed in a less mobile state, acetophenone peaks were still not visible, suggesting D blocks do not affect the mobility of the acetophenone molecules. When diblocks of DL in combination with acetophenone were analyzed, the acetophenone peaks were visible independent of which block was carbon-13 enriched. This suggests that the presence of the L block enables a decrease in mobility of the acetophenone molecules. While the presence of L does impact the mobility of acetophenone, there was no evidence to indicate that the presence of L has an impact on the mobility of the D blocks. The dynamics of acetophenone were also compared between the L-enriched short and long diblocks. Increased CP-MAS spectral signal in long DL diblocks indicated that acetophenone was less mobile when combined with long MW diblocks. This suggests that shorter MW diblocks promote flavor release.

InSENSITIVE NUCLEI ENHANCED BY PROTON TRANSFER (INEPT) is a one-dimensional ssNMR technique that is often used for signal enhancement but is also a valuable tool for the study of mobile sample components (chapter 3). It was used in this study to determine which sample components are more mobile and interpret changes to

that mobility as the matrix composition and properties change. It is also necessary to gather one dimensional first before two dimensional INEPT spectra in order to best optimize the two dimensional experiments. Mixtures of enriched homopolymers and diblocks in short or long MW with enriched acetophenone were analyzed by INEPT. The one-dimensional INEPT spectra for acetophenone combined with short D and short L are overlaid in Figure 6-8 below.

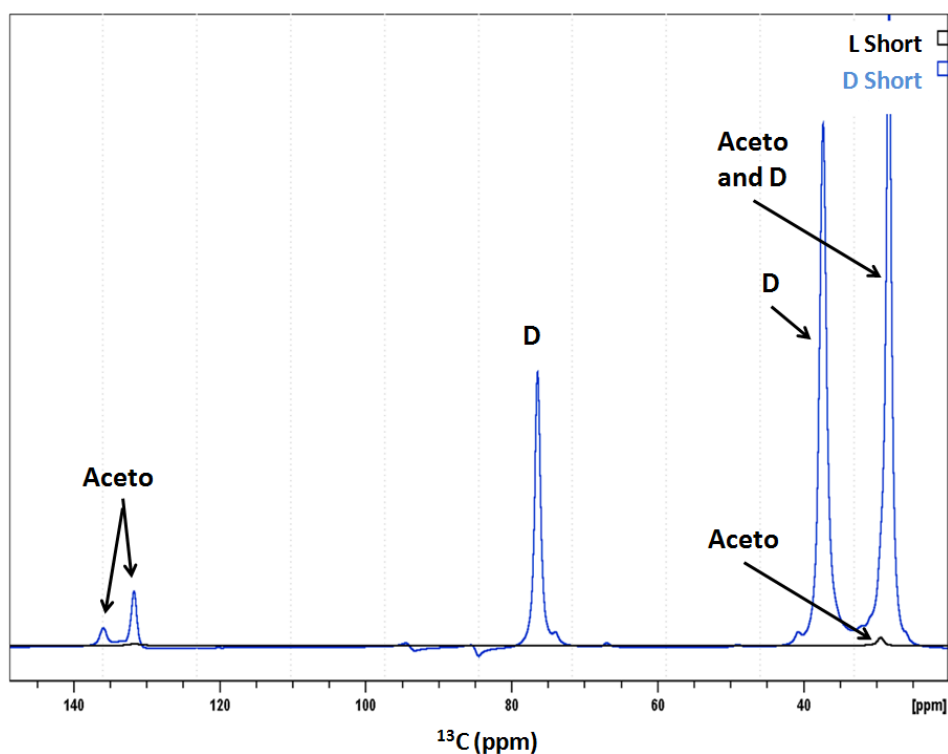


**Figure 6-8 One-dimensional INEPT spectra for short D (blue) and L (black) homopolymers with acetophenone 4 w/w%.**

The intensity of the acetophenone with short D is much greater than the short L homopolymer and acetophenone peaks are visible in both spectra. This confirms that both acetophenone and D homopolymer were mobile species. Resonances belonging to the L homopolymer were not observed due to its rigidity.

Combinations of acetophenone with differentially labeled DL diblocks were also analyzed. The overlay of acetophenone in short MW  $^{13}\text{C}$ -DL and long MW  $\text{D}^{13}\text{C}$ -L are shown in Figure 6-9 below.

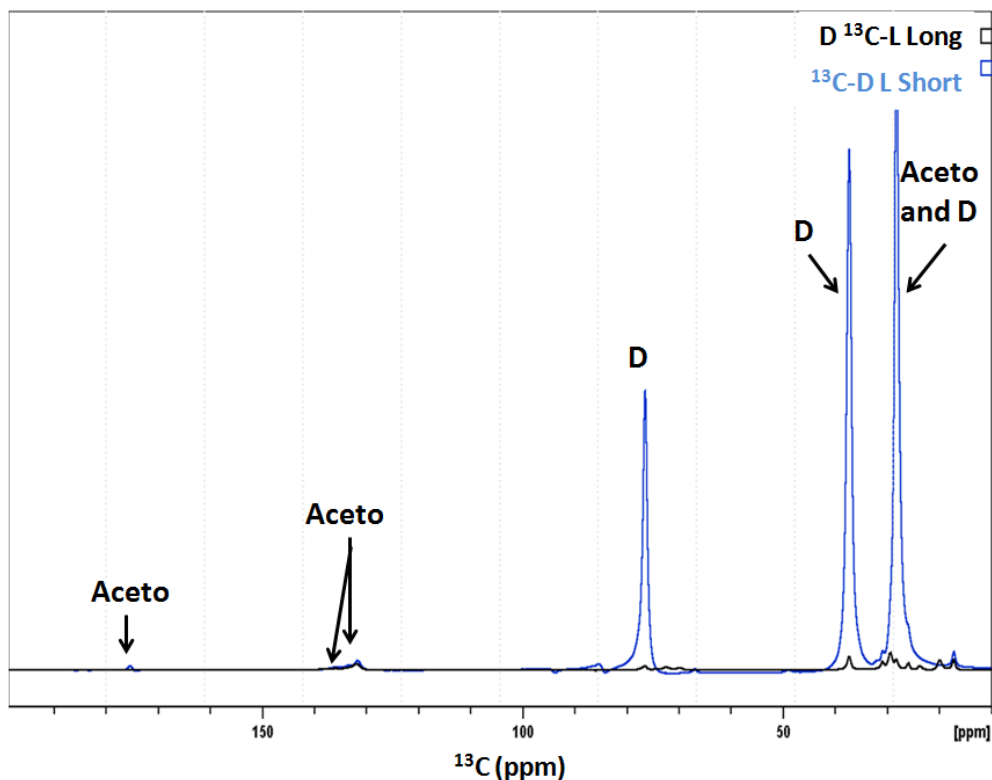


**Figure 6-9** One-dimensional-INEPT spectra for  $^{13}\text{C}$ -DL short MW (blue) and  $\text{D}^{13}\text{C}$ -L Long MW (black) with acetophenone 4 w/w%.

Examination of Figure 6-9 shows that when acetophenone was combined with either short or long DL diblocks the acetophenone peaks were visible. The diblock labeled on the D block is much more intense as this was the mobile component of the DL diblock. Next, the impact of increasing the MW of the blocks was evaluated for both the D and L blocks. Acetophenone was combined with DL diblocks enriched on the D block in both short and long MW and are overlaid in Figure 6-10 below.

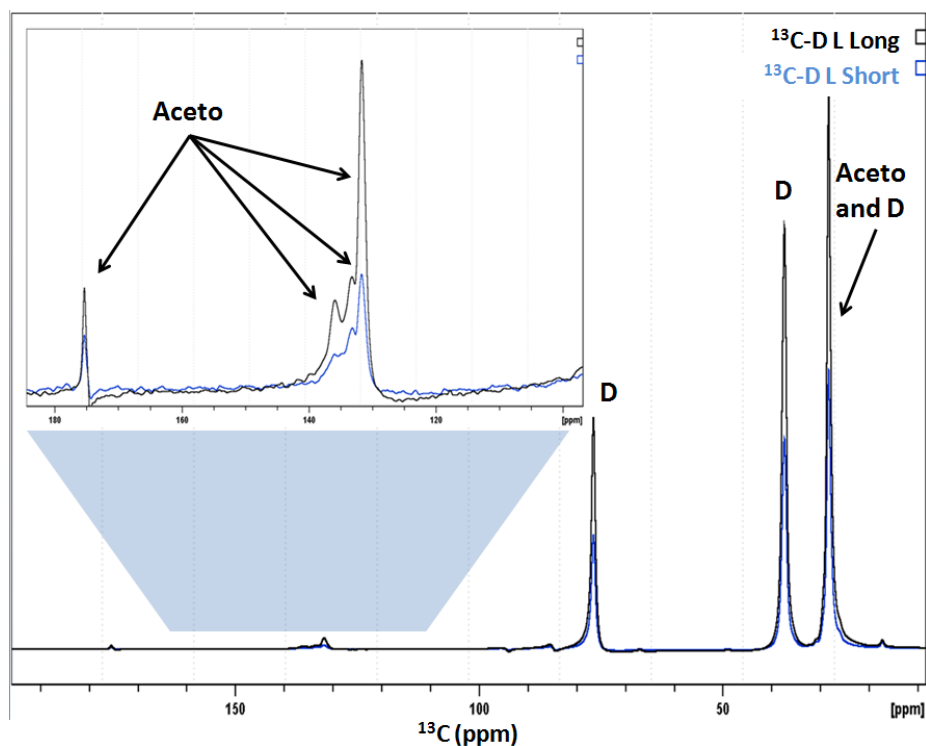


**Figure 6-10 One-dimensional-INEPT spectra for  $^{13}\text{C}$ -DL short MW (blue) and  $^{13}\text{C}$ -DL Long MW (black) with acetophenone 4 w/w%.**

Figure 6-10 shows resonances attributed to both D and acetophenone which vary in intensity. The difference in intensity of the D resonances was due to changes in free volume of the diblock as the MW increases. However, the acetophenone concentration in both samples was held consistent and any changes in intensity of the acetophenone resonances was due to changes in the molecular movement of the acetophenone and not volume changes in the sample. A section of the INEPT spectra containing acetophenone resonances has been enlarged in Figure 6-10 above. This enlarged section clearly shows the acetophenone resonances at around 130 ppm were more intense when combined with the long MW diblock. This suggests that the acetophenone molecules were more mobile in long DL diblocks, less favorable to

form strong intermolecular interaction with the DL diblock and therefore more likely to be released. The INEPT spectra for acetophenone in combination with short and long MW DL diblocks enriched on the L block are overlaid in Figure 6-11 below.

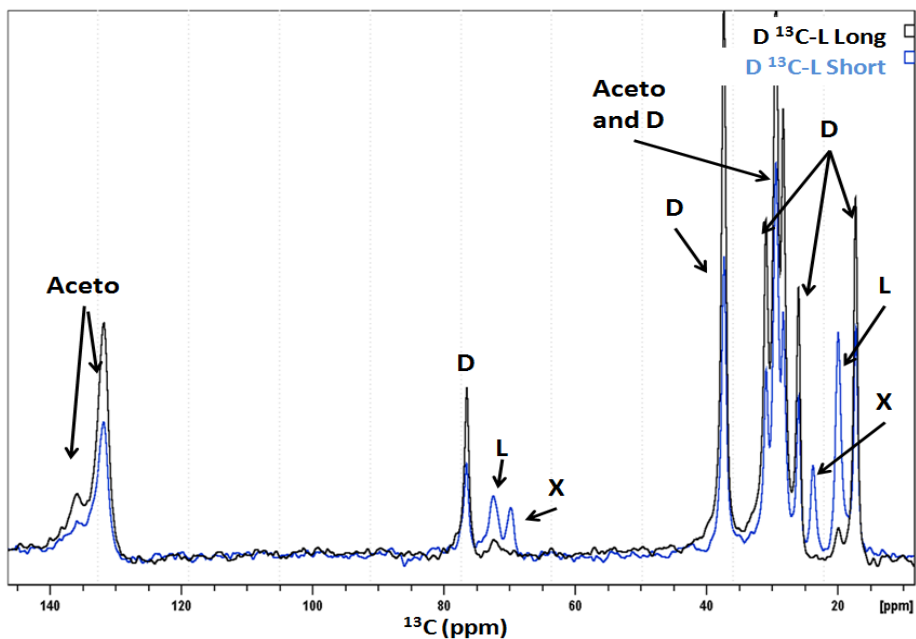


**Figure 6-11** One-dimensional-INEPT spectra for D-<sup>13</sup>C L short MW (blue) and D-<sup>13</sup>C L Long MW (black) with acetophenone 4 w/w%.

Resonances attributed to D, L and acetophenone are visible in Figure 6-11 above.

The overall intensity of the signal from the long MW diblock was again more intense due to volume changes in the sample. However, in this case the short MW DL diblock had increased visibility of resonances attributed to the L block. Normally, the L block had low visibility due to its rigidity however, due to selective carbon-13 labeling of the L block in the short MW D-<sup>13</sup>C L it was now visible. The short MW D-<sup>13</sup>C L was more mobile and therefore had a higher signal intensity for L resonances (20 and 76ppm). Examination of the acetophenone resonances at around 130ppm again showed a greater intensity and therefore mobility for acetophenone when

combined with the longer MW DL diblock. While the one dimensional INEPT spectra can provide confirmation of physical state and molecular dynamics of acetophenone in a DL diblock matrix two dimensional work is necessary to gain more specific observations.

### **Two-dimensional-Solid State Nuclear Magnetic Resonance (ssNMR) Analysis.**

Combinations of acetophenone with short MW D and L homopolymers as well as with short and long MW differentially labeled diblocks were analyzed using two dimensional INEPT and NOESY-INEPT techniques. The two-dimensional INEPT experiments will provide site specific information regarding and the D block how acetophenone is affected by changes to the model matrix. Further, the NOESY-INEPT experiments can provide direct evidence of where on the acetophenone molecule intermolecular interactions are occurring. While it is possible with this technique to gain information about intramolecular interactions between the polymers themselves in the model matrix system; the focus of this study was the interaction of acetophenone with the model matrix materials. Acetophenone and model matrix mixtures were analyzed using two-dimensional INEPT and the two-dimensional spectra can serve as 'fingerprints' for the mobile species in these mixtures. The labeled molecular structures are displayed in Figure 6-12 and will be referred to when discussing the two-dimensional ssNMR data.

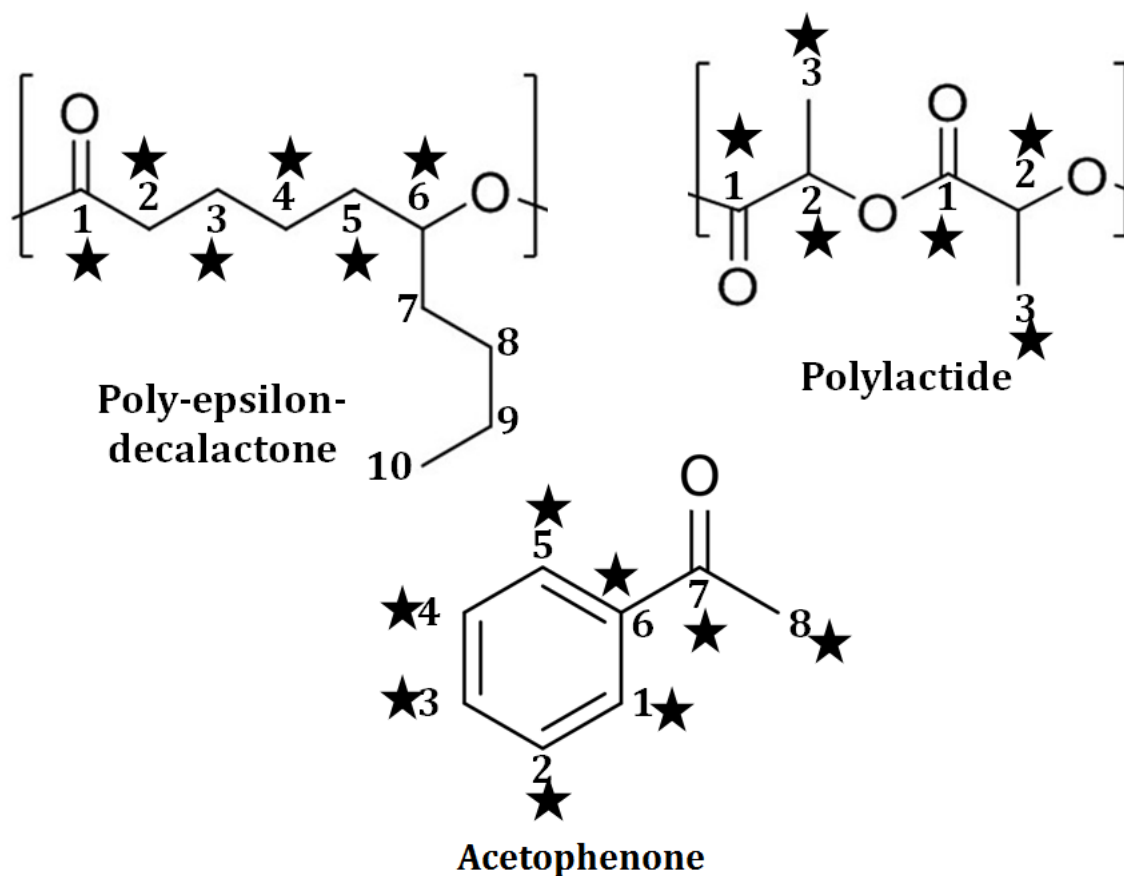


Figure 6-12 Labeled structures for model matrix materials and acetophenone, ★ = position of carbon-13 enrichment.

Resonance assignments for the two-dimensional INEPT cross peaks for the model matrix materials and acetophenone are displayed in Table 6-4 below. Both the model flavor molecule, acetophenone and the model matrix materials were carbon-13 labeled. This labeling increased the sensitivity of the instrument to the sample providing high resolution spectra and decreasing analysis time needed.

**Table 6-4 Carbon and proton resonances for model matrix components and acetophenone.**

	<b>Position</b>	<b><sup>13</sup>C resonance (ppm)</b>	<b><sup>1</sup>H resonance (ppm)</b>
<b>Poly-epsilon decalactone</b>	1	175.3	5.3
	2	37.4	5.3
	3	28.3	4.4
	4	28.3	4.4
	5	37.3	4.6
	6	76.4	8
	7	40.8	4.5
	8	30.9	4.4
	9	25.9	4.4
	10	17.3	4
<b>Poly lactide</b>	2	72.4	8.2
	3	20.0	4.6
<b>Acetophenone</b>	1	131.5	10.5
	2	131.5	10.0
	3	136.0	10.1
	4	131.5	10.0
	5	131.5	10.5
	7	200.0	5.1
	8	29.0	5.0

As indicated in chapter 3, carbons without adjacent protons and rigid species in sample mixtures do not produce cross peaks in two-dimensional INEPT analysis.

The two dimensional traces for acetophenone in combination with model matrix

materials are overlaid in Figure 6-13.

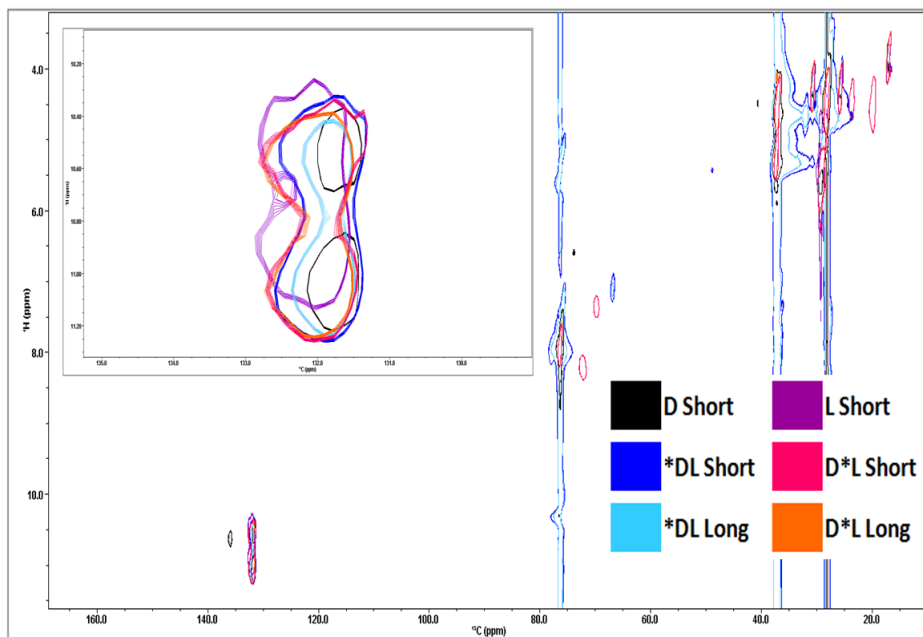


**Figure 6-13** Two-dimensional INEPT spectra for acetophenone combined with model DL matrix materials, 4 w/w%.

Examination of the two dimensional cross peaks showed differences in intensity of the acetophenone peaks when experiencing changes to the surrounding matrix. The intensities of the cross peaks were plotted against the carbon position of the acetophenone molecule, see Figure 6-14.

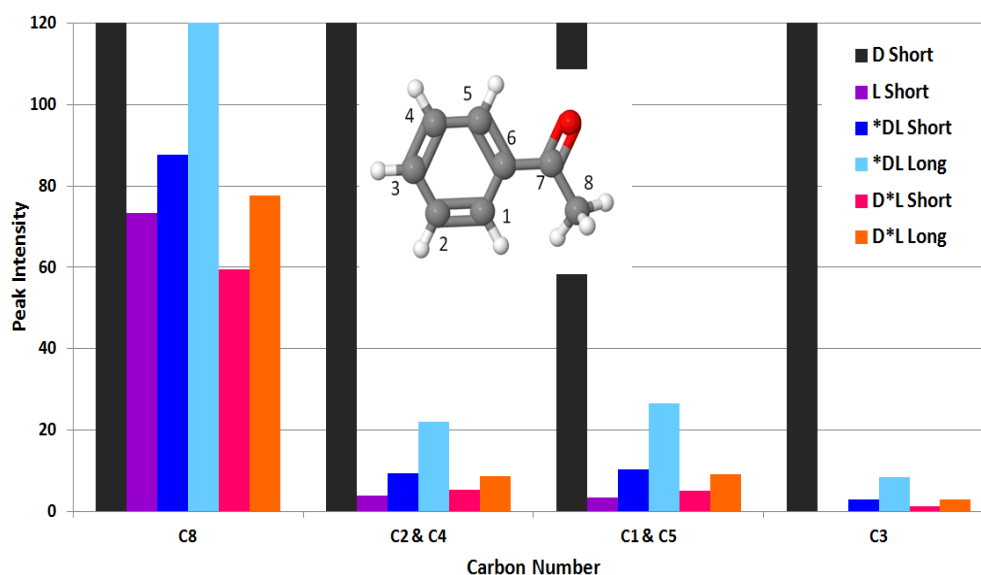


**Figure 6-14 Acetophenone cross peak intensities in various model matrices plotted against carbon position.**

The intensities of the cross peaks for acetophenone vary dependant on the position in the acetophenone molecule and the model matrix. The two-dimensional INEPT intensity is positively correlated with molecular mobility of the atom being observed. The most mobile carbon in the acetophenone molecule was the methyl carbon, C8, followed by the cyclic aromatic carbons, C1-C5. The impact of the sample matrix on the mobility of most carbons in acetophenone was next examined. Across all positions in acetophenone the carbons showed the greatest degree of mobility when combined with the short MW D homopolymer. This was followed by the long MW DL diblock labeled on the D block then the other labeled short and long diblocks. In this case, the pattern of intensities was very similar for each position in acetophenone. However, the overall intensities did vary indicating which carbons in the acetophenone molecule were most mobile as the matrix changed. As shown in

Figure 6-14 the methyl carbon was the most mobile followed by the aromatic carbons. Overall, the two-dimensional INEPT analysis showed that acetophenone experienced changes in molecular spin dynamics as the model matrix changed and that these changes can be mapped based on the region of the molecular structure of acetophenone. Acetophenone was most mobile in combination with D homopolymers and longer MW diblocks suggesting that these factors might influence release of acetophenone from the model polymer matrix.

**Two-dimensional NOESY INEPT.** Two dimensional NOESY-INEPT spectroscopy is a hybrid NMR technique from both solution (NOESY) and solid state (INEPT) NMR applications. This techniques allows for observation of proton to proton interactions between the flavor and matrix. The technique provides the ability to observe the transfer in multiple directions; from the matrix to the flavor and from the flavor to the matrix. Matrix to flavor interactions would be observed by proton transfer from the matrix through space to a proton on the flavor using NOESY and then transferrring from the flavor proton to the flavor carbon. This would result in a NOESY-INEPT crosspeak with a proton shift (y-axis) corresponding to a matrix proton resonance and a carbon shift (x-axis) corresponding to a flavor carbon resonance. The opposite is true for flavor to matrix NOESY-INEPT cross peaks which would have a proton shift (y-axis) corresponding to a flavor resonance and a carbon shift (x-axis) correspoding to a matrix resonance. The NOESY-INEPT spectra for acetophenone in model matrix materials are overlaid in Figure 6-15 below.

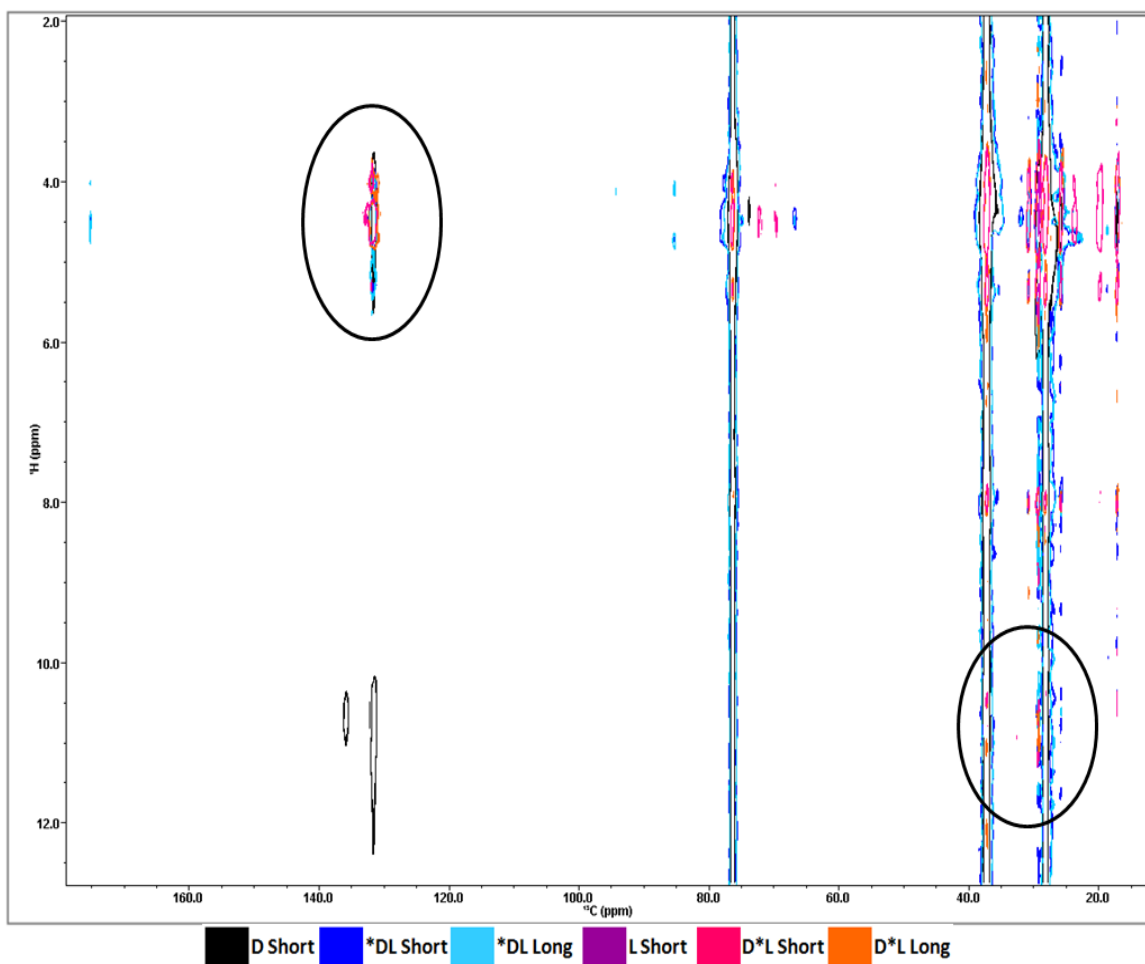
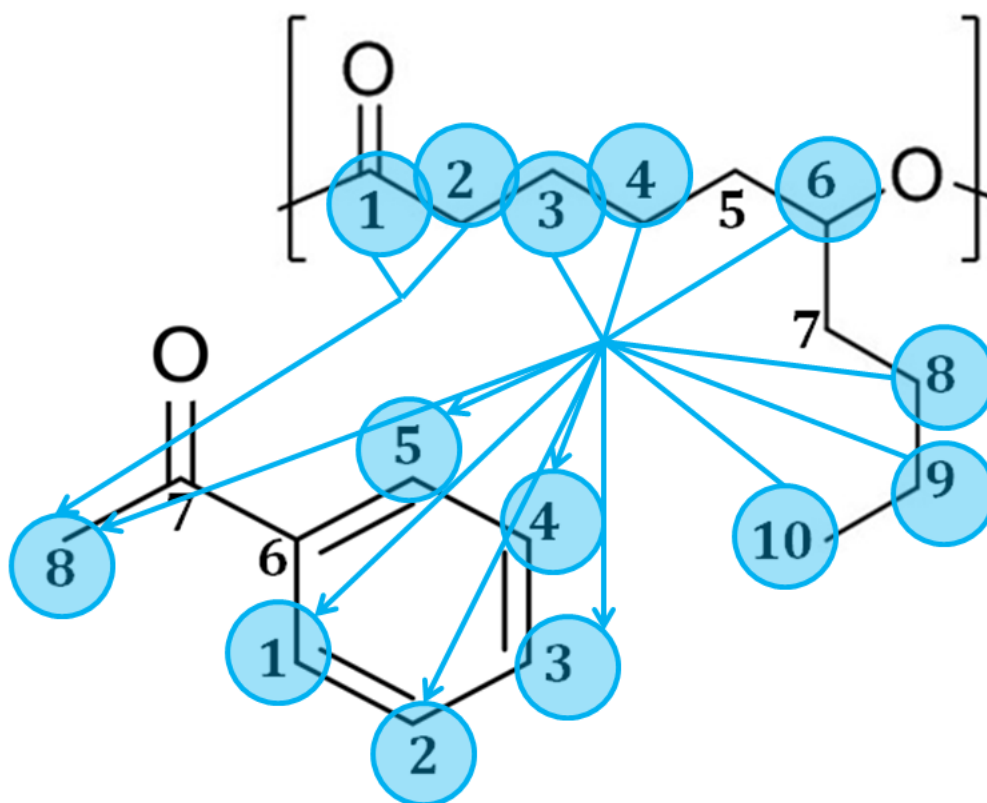
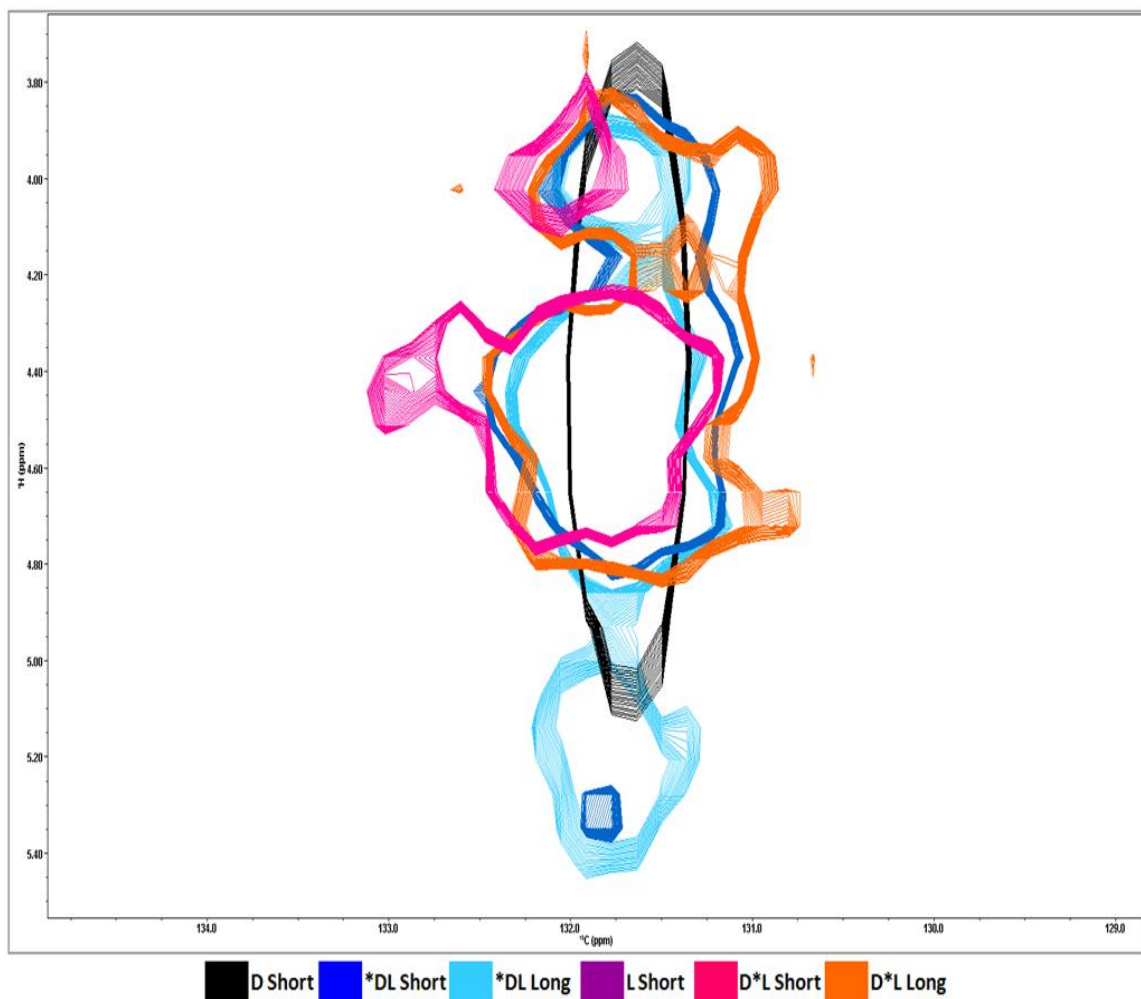


Figure 6-15 Two-dimensional NOESY-INEPT spectra for acetophenone in model DL matrix materials. Examination of the spectra revealed the presence of matrix to acetophenone NOESY-INEPT cross peaks. These cross peaks are circled at the top left in Figure 6-15 and have proton resonances corresponding to the D components of the model matrix and carbon resonances corresponding to the acetophenone. This means that D was very closely associated with acetophenone, between 5 and 9Å. Matrix to acetophenone NOESY-INEPT cross peaks were observed for the atoms highlighted in Figure 6-16 below.



**Figure 6-16** Matrix to acetophenone interactions identified by the presence of NOESY-INEPT cross peaks.

Closer examination of these cross peaks shows differences in intensities dependant on the matrix, which are shown in Figure 6-17.



**Figure 6-17** Matrix material to acetophenone NOESY-INEPT cross peaks for acetophenone in model matrices.

The two-dimensional NMR signals are displayed much like a topographical map and cross peaks which appear to have a larger area have larger peak intensities. The intensities of these cross peaks can be measured and compared. The intensities and carbons involved in NOESY-INEPT D block to acetophenone cross peaks are listed in Table 6-5 below.

Table 6-5 Poly-epsilon-decalactone (D) to acetophenone (Aceto) NOESY-INEPT cross peak intensities.

		Sample ID				
		*D Short	*DL Short	*DL Long	D*L Short	D*L Long
		Peak Intensity				
Resonances <sup>13</sup> C/ <sup>1</sup> H	29.3/4.0		5.48	5.30	3.8	3.2
Participants Aceto/D	C8/C10					
Resonances <sup>13</sup> C/ <sup>1</sup> H	29.3/4.4	21.5	10.09	9.62	7.1	5.5
Participants Aceto/D	C8/C3,4,8,9					
Resonances <sup>13</sup> C/ <sup>1</sup> H	29.3/5.3		2.72	4.61	2.3	2.0
Participants Aceto/D	C8/C1,2					
Resonances <sup>13</sup> C/ <sup>1</sup> H	29.3/8.0	5.8	1.71	1.81	1.3	1.2
Participants Aceto/D	C8/C6					
Resonances <sup>13</sup> C/ <sup>1</sup> H	132/4.0		1.4	1.6	0.9	1.2
Participants Aceto/D	C1,2,4,5/C10					
Resonances <sup>13</sup> C/ <sup>1</sup> H	132/4.4	25.6	2.2	2.7	1.6	1.7
Participants Aceto/D	C1,2,4,5/C3,4,8,9					
Resonances <sup>13</sup> C/ <sup>1</sup> H	132/8.0	3.9		0.9		
Participants Aceto/D	C1,2,4,5/C6					
Resonances <sup>13</sup> C/ <sup>1</sup> H	136/4.4	5.4				
Participants Aceto/D	C3/C3,4,8,9					

In general, the interpretation of NOESY-INEPT signals is not yet well defined and is a combination of the distance between the protons participating in the exchange and the dynamics of the small molecule and matrix. The composition of the sample should be taken into account when interpreting these NOESY-INEPT cross peaks. For D to acetophenone interactions listed in Table 6-5 the enrichment level for D changed as the composition of the model matrices changed. There are fewer enriched (\*D) protons in the \*DL diblock than in the short \*D homopolymer because the diblock is also composed of an unlabeled L block which dilutes the carbon-13 enrichment effect of the \*D block. Further, there were less enriched \*D protons from which to start the NOESY transfer in the DL\* diblocks than the \*DL diblocks. As such, the intensity of the NOESY-INEPT cross peaks from the D polymer to acetophenone follow the pattern of enrichment rather than indicating a change in the interactions between acetophenone and these matrices.

However, the concentration of acetophenone was held constant, confirmed by DP-MAS spectra, in all of the mixtures of matrix and acetophenone and the acetophenone itself is fully carbon-13 enriched. Therefore, the differences in acetophenone to D NOESY-INEPT cross peaks between short and long MW diblocks can be compared.

NOESY-INEPT cross peaks from the flavor to the polymer are not abundantly clear in overlaid spectra for two reasons. One, the majority of the sample mixture was comprised of model matrix material (96 w/w%) and therefore the most abundant protons belong to the matrix materials and provide the largest source of

initial NOESY proton transfer. Two, if flavor to matrix NOESY-INEPT crosspeaks were present they would be located in a region (encircled in the lower right in Figure 6-15 above) very close to the INEPT cross peaks for the matrix. The INEPT peaks for the matrix are so abundant that the region would have to be carefully examined for the presence of flavor to matrix NOESY-INEPT cross peaks. Careful examination of the two-dimensional NOESY-INEPT spectra was performed and NOESY-INEPT cross peaks from acetophenone to decalactone were detected indicating intermolecular interactions between the atoms show in Figure 6-18 below.

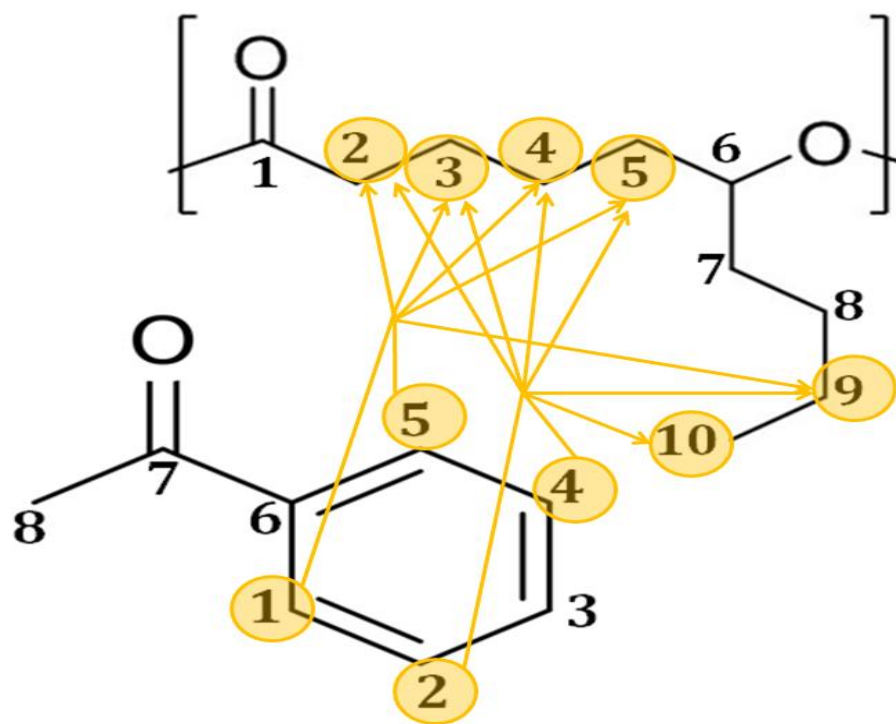


**Figure 6-18 Acetophenone to matrix interactions identified by the presence of NOESY-INEPT cross peaks.**

The intensities for the acetophenone to D interactions were obtained and are listed in Table 6-6 below.

Table 6-6 Acetophenone (Aceto) to poly-epsilon-decalactone (D) NOESY-INEPT cross peak intensities.

		Sample ID				
		D Short	*DL Short	*DL Long	D*L Short	D*L Long
		Peak Intensity				
Resonances <sup>13</sup> C/ <sup>1</sup> H	17/10.5	1.0	0.7	0.9	0.8	0.6
Participants D/Aceto	C10/C2,4					
Resonances <sup>13</sup> C/ <sup>1</sup> H	17/11	0.7		0.7		0.6
Participants D/Aceto	C10/C1,5					
Resonances <sup>13</sup> C/ <sup>1</sup> H	26/10.5	1.0	0.7	1.1		
Participants D/Aceto	C9/C2,4					
Resonances <sup>13</sup> C/ <sup>1</sup> H	26/11	0.7	0.7	0.9		
Participants D/Aceto	C9/C1,5					
Resonances <sup>13</sup> C/ <sup>1</sup> H	28.3/10.5	45.6	18.9	33.2	0.7	0.6
Participants D/Aceto	C3,4/C2,4					
Resonances <sup>13</sup> C/ <sup>1</sup> H	28.3/11		17.7	32.4		
Participants D/Aceto	C3,4/C1,5					
Resonances <sup>13</sup> C/ <sup>1</sup> H	37.3/10.5	31.0	12.1	21.3	0.8	0.7
Participants D/Aceto	C2,5/C2,4					
Resonances <sup>13</sup> C/ <sup>1</sup> H	37.3/11		11.4	21.1		0.9
Participants D/Aceto	C2,5/C1,5					
Resonances <sup>13</sup> C/ <sup>1</sup> H	76.4/10.5	19.2	7.2			
Participants D/Aceto	C6/C2,4					
Resonances <sup>13</sup> C/ <sup>1</sup> H	76.4/11		6.5			
Participants D/Aceto	C6/C1,5					

Examination of the two-dimensional NOESY-INEPT spectra for cross peaks showed correlations primarily from the aromatic carbons of acetophenone to the D component of the matrix and none from the methyl carbon (C8) of acetophenone. The correlations from acetophenone to model matrix materials again showed higher intensity for cross peaks when the acetophenone was combined with the short MW D homopolymer. When the short and long MW diblocks were compared the intensity of the NOESY-INEPT cross peaks increased as the MW increased. This suggests that acetophenone participates in closer and potentially stronger intermolecular interactions with longer MW model matrix materials. Further studies in which the mixing time of the NOESY-INEPT experiment would be varied would need to be performed to definitively confirm the changes to intermolecular distances between the flavor and matrix. These NOESY-INEPT cross peaks suggest that flavor release would be improved with the use of longer diblock copolymers as opposed to shorter diblock copolymers.

To summarize, two-dimensional INEPT peaks located the methyl carbon (C8) as the functional group most affected by changes to the matrix composition with most atoms in acetophenone having greater mobility in longer MW diblocks. NOESY-INEPT analysis showed intermolecular interactions between the aromatic carbons of acetophenone (C1, 2, 4, and 5) and particularly the hydrocarbon backbone (C2, 3, 4 and 5) and side chain (C9 and 10) of D. These interactions are likely dipole-dipole interactions. The strength of interactions are thought to be

enhanced by higher MW polymers. This suggests that this flavor compound, acetophenone, would have greater release from short DL copolymers.

In conclusion, given a model flavor and matrix system several types of information were gained using ssNMR techniques. Use of one-dimensional techniques were able to confirm the peak identities in mixtures of flavor and model matrices. The mobile and rigid parts of the mixtures were identified. CP-MAS of the mixtures suggested that the rigid component of the matrix interacts very closely with flavor. Modification of the analysis temperature during CP-MAS was able to enhance signal from the mobile polymer component and confirm that this component does not appear to interact closely with flavor. One-dimensional INEPT analysis confirmed the identities of the mobile components of the mixtures and identify differences in the mobility of the flavor as the polymer matrix changed.

Further, two-dimensional INEPT analysis produced cross peaks allowing the resonances of both matrix components and the flavor to be mapped. Changes in the intensities of these cross peaks was plotted and identifies which atoms in the flavor molecule are most impacted by changes to the surrounding sample matrix. Lastly, two-dimensional NOESY-INEPT confirmed the presence of intermolecular interactions between the flavor molecules and their surrounding matrix. This technique was able to identify which atoms are involved in these interactions and how they might be impacted by basic physical property changes such as increased molecular weight.

These techniques show enormous potential for the study of complex flavor and food matrix interactions. While a model matrix was employed here for the purposes of a controlled test of the technology it is not necessary to gain insight from these techniques. The flexibility and specificity of these techniques is an excellent complement to the study of flavor and food interactions. The most powerful attribute of these techniques is their ability to study samples of many physical states while gaining information regarding the structure of the sample and the dynamics at play.

## Chapter 7 References

1. De Roos, K.B., *Physiochemical models of flavor release from foods* in *Flavor Release*, D. Roberts, et al., Editor. 2000, American Chemical Society: Washington DC.
2. Seuvre, A.-M., Philippe, E., Rochard, S., Voilley, A.; Kinetic study of the release of aroma compounds in different model food systems. *Food Res. Int.* 2007, 40, p. 480-492.
3. Laws, D.D., Bitter H-M. L., Jerschow, A.; Solid-state NMR spectroscopic methods in chemistry. *Angew. Chem. Int. Ed.* 2002, 41, p. 3096-3129.
4. Tyapkova, O., et al.; Flavor release from sugar-containing and sugar-free confectionary egg albumen foams. *LWT-Food Sci. and Tech.* 2016, 69, p. 538-545.
5. Nishinari, K. and Y. Fang; Sucrose release from polysaccharide gels. *R. Soc. Chem. Food Func.* 2015.
6. Arvisenet, G., et al.; Effect of apple particle state on the release of volatile compounds in a new artificial mouth device. *J. Agric. Food Chem.* 2008, 56, p. 3245–3253.
7. Mestres, J., *Modern chewing gum*, in *Formulation and Production of Chewing and Bubble Gum*, D. Fritz, Editor. 2006, Kennedy's Books Ltd.: Loughton, Essex, UK. p. 47-73.
8. Fritz, D., *Gum Formulation*, in *Formulation and Production of Chewing and Bubble Gum*, D. Fritz, Editor. 2006: Loughton, Essex, UK. p. 239-250.
9. Ponakala, S.V., et al., *High-intensity sweeteners in sugar-free chewing gum*, in *Formulation and production of chewing and bubble gum*, C.G.a.D. Fritz, Editor. 2008, Kennedy's Books, Ltd.: Loughton, Essex, United Kingdom. p. 157-204.
10. Roos, K.B.d., *Flavourings for Chewing Gum*, in *Formulation and Production of Chewing and Bubble gum*, D. Fritz, Editor. 2006, Kennedy's Books: Loughton, Essex, UK. p. 205-231.
11. Harrison, M., *Mathematical models of release and transport of flavors from foods in the mouth to the olfactory epithelium*, in *Flavor Release*, D. Roberts, et al., Editor. 2000, American Chemical Society: Washington, D.C. p. 179-191.
12. De Roos, K.B., *Flavor release from chewing gums*, in *Flavour Science and Technology*, Y. Bessiere and A.F. Thomas, Editors. 1990, John Wiley and Sons Ltd. p. 355-358.
13. De Roos, K.B. and C. Wolswinkel, *Non-equilibrium partition model for predicting flavour release in the mouth*, in *Trends in Flavour Research*, H. Maarse and D.G. van der Heij, Editors. 1994, Elsevier Science B.V.: Amsterdam. p. 15-32.

14. Niederer, B., A. Le, and E. Cantergiani; Thermodynamic study of two different chewing-gum bases by inverse gas chromatography. *J. Chromatogr. A*. 2003, 996, p. 189–194.
15. Potinen, R.V. and D.G. Peterson; Mechanisms of flavor release in chewing gum:cinnamaldehyde. *J. Agric. Food Chem.* 2008, 56, p. 3260–3267.
16. Mielle, P., et al.; From human to artificial mouth, from basics to results. *Sensors and Actuators B*. 2010, 146, p. 440–445.
17. Krause, A.J., L.S. Henson, and G.A. Reineccius; Use of a chewing device to perform a mass balance on chewing gum components. *Flav. Frag. J.* 2010, 26, p. 47–54.
18. Baek, I., et al.; Sensory perception is related to the rate of change of volatile concentration In-nose during eating of model gels. *Chem. Senses*. 1999, 24, p. 155-160.
19. Ovejero -Lopez, A., et al.; Flavor release measurement from gum model system. *J. Agric. Food Chem.* 2004, 52, p. 8119 – 8126.
20. Krause, A.J., *Real-time release of volatile and non-volatile components from chewing gum using a mechanical chewing device*, in *Food Science and Nutrition*. 2010, University of Minnesota: Saint Paul. p. 164.
21. Duizer, L.M., K. Bloom, and C.J. Findlay; Dual-attribute time-intensity measurement of sweetness and peppermint perception of chewing gum. *J. Food Sci.* 1996, 61, p. 636-638.
22. Potinen, R.V. and D.G. Peterson; Influence of flavor solvent on flavor release and perception in sugar-free chewing gum. *J. Agric. Food Chem.* 2008, 56, p. 3254–3259.
23. Davidson, J., et al.; Effect of sucrose on the perceived flavor intensity of chewing gum. *J. Agric. Food Chem.* 1999, 47, p. 4336–4340.
24. Kreutzmann, S. and K.D. Nielsen, *Effect of gum base ingredients on release of specific compounds from strawberry flavour chewing gum.*, in *Proceedings of the 12th Weurman Flavour Research Symposium. July 2008. Interlaken, Switzerland*. 2008.
25. Haahr, A.-M., et al.; Release of peppermint flavour compounds from chewing gum:effect of oral functions. *Physio. Behav.* 2004, 82, p. 531–540.
26. Sostmann, K., R. van Lochem, and K. de Roos; The influence of gum base composition on flavour release from chewing gum. *Flavor Research at the Dawn of the Twenty-first Century*. 2003, p. 252-255.
27. Wright, K.M. and B.P. Hills; Modelling flavour release from a chewed bolus in the mouth: Part II. The release kinetics. *Int. J. Food Sci. Tech.* 2003, 38, p. 361–368.
28. De Roos, K.; Effect of texture and microstructure on flavour retention and release. *Int. Dairy J.* 2003, 13, p. 593–605.
29. Bult, J.H.F., R.A. de Wijk, and T. Hummel; Investigations on multimodal sensory integration: Texture, taste, and ortho- and retronasal olfactory stimuli in concert. *Neuro. Letters*. 2007, 411, p. 6–10.

30. Jeckelmann, N. and O.P. Haefliger; Release kinetics of actives from chewing gums into saliva monitored by direct analysis in real time mass spectrometry. *Rapid Commun. Mass Spectrom.* 2010, 24, p. 1165–1171.
31. Ogawa, K., *Method for increasing flavour retention of chewing gum stuffed with flavour liquid as center ingredient*, L.C. LTD., Editor. 1980.
32. Romer Rassing, M.; Chewing gum as a drug delivery system. *Ad. Drug Deliv. Rev.* 1994, 13, p. 89-121.
33. Barkalow, D.B., et al., *Release of lipophilic active ingredients from chewing gum*, W.W.J. Co., Editor. 2001.
34. Kumazawa, K., et al.; A new approach to estimate the in-mouth release characteristics of odorants in chewing gum. *Food Sci. Technol. Res.* 2008, 14, p. 269–276.
35. Blee, B., et al.; Variation in aroma release between panellists consuming different types of confectionary. *Flav. Frag. J.* 2010, 26, p. 186–191.
36. Wessel, S.W., et al.; Quantification and qualification of bacteria trapped in chewed gum. *PLOS One.* 2015, p. 1-12.
37. Nageswara Rao, B.D.; Nuclear magnetic resonance an early history. *Resonance.* 2015, November, p. 969-985.
38. Claridge, T.D.W., *Introducing high-resolution NMR*, in *High resolution NMR techniques in organic chemistry*, T.D.W. Claridge, Editor. 2009, Elsevier: Oxford, United Kingdom. p. 11-34.
39. Brown, S.P., Spiess, H. W.; Advanced solid-state NMR methods for the elucidation of structures and dynamics of molecular, macromolecular and supramolecular systems. *Chem. Rev.* 2001, 101, p. 4125-4155.
40. Baldus, M.; Molecular interactions investigated by multi-dimensional solid-state NMR. *Current Op Struc Biol.* 2006, 16, p. 618-623.
41. Schantz, S., P. Hoppu, and A.M. Juppo; A solid-state NMR study of phase structure, molecular interactions, and mobility in blends of citric acid and paracetamol. *J. Pharm. Sci.* 2008, 98, p. 1862-1870.
42. Xu, J., et al.; Solid-state NMR spectroscopy provides atomic-level insights Into the dehydration of cartilage. *J. Phys. Chem.* 2011, 115, p. 9948-9954`.
43. Nozirov, F., et al.; Molecular dynamics of poly( L -lactide) biopolymer studied by wide-line solid-state 1 H and 2 H NMR spectroscopy. *Solid State Nuclear Magnetic Resonance.* 2006, 29, p. 258-266.
44. Sroka-Bartnicka, A., et al.; Solid-state NMR spectroscopy as a tool supporting optimization of MALDI-TOF MS analysis of polylactides. *J. Am. Soc. Mass Spectrom.* 2009, 20, p. 67-72.
45. Rondeau-Mouro, C., P. Le Bail, and A. Buleon; Structural investigation of amylose complexes with small ligands: inter- or intra-helical associations? *Int. J. Biol. Macro.* 2004, 34, p. 251-257.
46. Thakur, A.A.M., Kean, R. T., Zupfer, J. M., Buehler, N. U.; Solid State 13C CP-AS NMR Studies of the crystallinity and morphology of poly(L-lactide). *Macromolecules.* 1996, 29, p. 8844-8854.

47. Li, S., Zheng, A., Su, Y., Fang, H., Shen, W., Yu, Z., Chen, L. Deng, F.; Extra-framework aluminum species in hydrated faujasite zeolite as investigated by two-dimensional solid-state NMR spectroscopy and theoretical calculations. *Phys Chem Chem Phys*. 2010, 12, p. 3895-3903.
48. Ader, C., Schneider, R., Seidel, K., Etzkorn, M., Baldus, M.; Magic-angle spinning NMR spectroscopy applied to small molecules and peptides in lipid bilayers. *Biochem. Soc. Trans.* 2007, Signaling, p. 991-995.
49. Elena, B., Lesage, A., Steuernagel, S. Bockmann, A., Emsley, L.; Proton to Carbon-13 INEPT in solid-state NMR spectroscopy. *J. Am. Chem. Soc.* 2005, 127, p. 17296-17302.
50. Wickramasinghe, N.P., Shaibat, M. A., Jones, C. R., Casabianca, L. B., de Dios, A. C., Harwood, J. S., Ishii, Y.; Progress in C 13 and H1 solid-state nuclear magnetic resonance for paramagnetic systems under very fast magic angle spinning. *J Chem. Phys.* 2008, 128, p. 052210-052215.
51. Gopinath, T., *Interpretation of 2D INEPT cross peaks*, M.L. Jilek, Editor. 2014: Minneapolis, MN, USA.
52. Miller, M.C., *Calculation of chemical shift perturbances and chemical shift mapping*, M.L. Jilek, Editor. 2014: Minneapolis, MN, USA.
53. Watts, A.; Solid-state NMR in drug design and discovery for membrane-embedded targets. *Nat. Rev. Drug Disc.* 2005, 4, p. 555-568.
54. Gopinath, T., *Interpretation of NOESY-INEPT cross peaks*. 2016: Minneapolis, MN, USA.
55. Claridge, T.D.W., *Measuring transient NOEs : NEOSY*, in *High-Resolution NMR Techniques in Organic Chemistry*, T.D.W. Claridge, Editor. 2009, Elsevier: Linacre House, Jordan Hill, Oxford, UK. p. 276-292.
56. Keeler, J., *The NOE*, in *Understanding NMR Spectroscopy*, J. Keeler, Editor. 2010, John Wiley & Sons Ltd.: The Strium, Southern Gate, Chichester, West Sussex, United Kingdom. p. 274-285.
57. Krause, A.J., *Real-time release of volatile and non-volatile components from chewing gum using a mechanical chewing device*, in *Food Science and Nutrition*. 2010, University of Minnesota: St. Paul, MN, USA. p. 180.
58. Patching, S.G., et al.; Relative substrate affinities of wild-type and mutant forms of the Escherichia coli sugar transporter GalP determined by solid-state NMR. *Molec. Memb. Biol.* 2008, 25, p. 474-484.
59. Le Bail, P., Rondeau, C., Buleon, A.; Structural investigation of amylose complexes with small ligands: helical conformation, crystalline structure and thermostability. *Int. J. Biol. Macro.* 2005, 35, p. 1-7.
60. Markland, C., Williams, G. R., O'Hare, D.; The intercalation of flavouring compounds into layered double hydroxides. *J. Mater. Chem.* 2011, 21, p. 17896-17903.
61. Savary, G., et al.; Mixture of aroma compounds: Determination of partition coefficients in complex semi-solid matrices. *Food Res. Int.* 2006, 39, p. 372-379.

62. ACD/Labs, *ACD/LogP predict octanol-water partitioning coefficients from structure*, in *Software Modules to Predict Physicochemical, ADME, and Toxicity Properties from Structure*. 2016, Advanced Chemistry Development, Inc.: Toronto, Canada.
63. Estruch, R.A., *Gum base*, in *Formulation and Production of Chewing and Bubble Gum*, D. Fritz, Editor. 2006, Kennedy's Books: Loughton, Essex, UK. p. 93-118.
64. Raithore, S., *Effect of polyols on flavor release during mastication of sugar-free chewing gum*, in *Food Science and Nutrition*. 2012, University of Minnesota: St. Paul, MN, USA. p. 168.
65. Edwards, S.F., Vilgis, Th.; The effect of entanglements in rubber elasticity. *Polymer*. 1985, 27, p. 483-492.
66. Fredrickson, G.H., Bates, F. S.; Dynamics of block copolymers: theory and experiment. *Annu. Rev. Mater. Sci.* 1996, 26, p. 501-550.
67. Morgret, L.D., et al., *Improved gum bases and chewing gums employing block polymers and processes for preparing them*, in *Patentscope*, W.I.P. Organization, Editor. 2013: United States of America.
68. Olsen, P.B., T. Odelius, K. Albertsson, A-C.; e-Declactone: A thermoresilient and toughening comonomer to poly(L-lactide). *Biomacromol.* 2013, 14, p. 2883-2890.
69. Fredrickson, G.H., Bates, F. S.; Block copolymers-designer soft materials. *Physics Today*. 1999, p. 32-38.
70. Schneiderman, D.K., et al.; Sustainable polymers in the organic chemistry laboratory: synthesis and characterization of a renewable polymer from  $\delta$  decalactone and L lactide. *J. Chem. Educ.* 2014, 91, p. 131-135.
71. Hamad, E.Z., Ijaz, W., Ali, S. A., Hastaoglu, M. A.; Influence of polymer structure on protein partitioning in two-phase aqueous systems. *Biotechnol. Prog.* 1996, 12, p. 173-177.
72. Taylor, A.J.; Release and transport of flavors in vivo: physicochemical, physiological, and perceptual considerations. *Comp. Rev. Food Sci. Food Safety*. 2002, 1, p. 45-57.
73. Frank, D., et al.; Effects of agar gel strength on oral breakdown, volatile release, and sensory perception using in vivo and in vitro systems. *J. Agric. Food Chem.* 2015, 63, p. 9093-9102.

## Appendices

### Appendix A: Design and fabrication of an artificial chewing device

#### Rationale

Chewing devices have been developed and produced for the study of food and flavor release from food for decades. The motivation behind these devices comes primarily from two factors; the need to analyze unpalatable samples and reduce variation inherent to using human subjects. Most important to the study of flavor release is the need to reduce variation between sample runs. Human subjects produce varying amounts of saliva, variable chewing force and frequencies and it is unreasonable to attempt to normalize these variables. The development and use of chewing devices have mitigated these concerns. Devices are able to process samples without regard to palatability and with more consistent results.

#### Objectives

- Design an artificial chewing device for evaluation of flavor release from food products.
- Focus of chewing simulation will be to simulated surface renewal of the sample matrix.
- Device will be optimized for a sample size between 0.2 and 2.0g of sample materials
- Device will be fitted for connection to gas and liquid flow in and out of the sample chamber
- Device will be heated, maintain temperature and have programmable temperature control
- Device will have adjustable chewing frequency and be able to maintain approximately 60rpm chewing action for at least 30 minutes of continuous use

#### System Design

The system design was in collaboration between Geoff Harms (Manager, St. Paul. Machine Shop, College of Biological Sciences, University of Minnesota, St. Paul, MN) and Maggie Jilek (Graduate Research Assistant, Flavor Research and Education Center, Department of Food Science and Nutrition, University of Minnesota, St. Paul, MN) to fulfill the objectives outlined in a time and budget conscious manner.

The system is composed of a motor driven piston which fits into central cylindrical sample chamber affixed to a base. The bottom of the piston and sample chamber is fitted with stainless steel 'teeth' which nearly meet and form the chewing action of the device. The tooth plate at the bottom of the sample chamber is removable for

cleaning. The motor rotates the piston and the up and down motion is caused by a sinusoidal roller guide plate above the piston. This plate rolls against two guide pins attached to the base of the chewing device causing the top assembly of the device to move up and down. A schematic drawing of the chewing device is shown in Figure A-7-1 below.

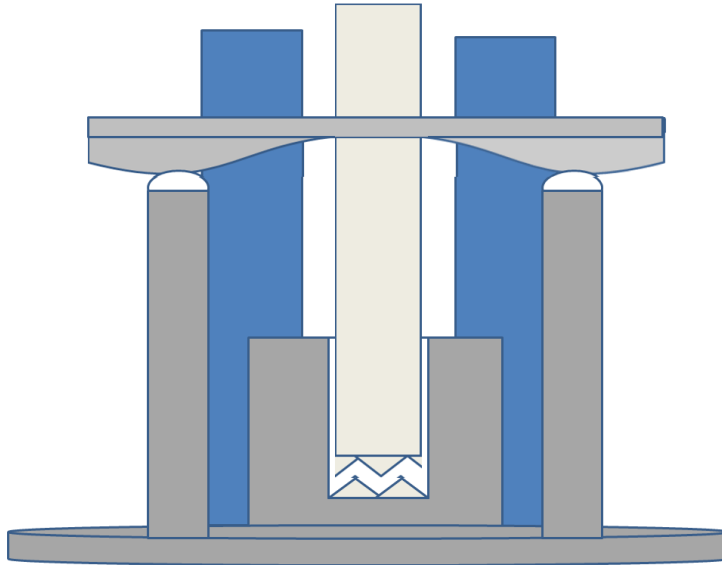


Figure A-7-1. Schematic drawing of the design for an artificial chewing device.

The device was fabricated in stainless steel with a motor control unit containing the on/off switch for the rotation and actuation and a speed control dial for the rotation/actuation speed. The separate temperature controller interfaces with the chewing device by inserting the heating element and thermocouple probe into the sample chamber. The fabricated device is shown in Figure A-7-2 below.

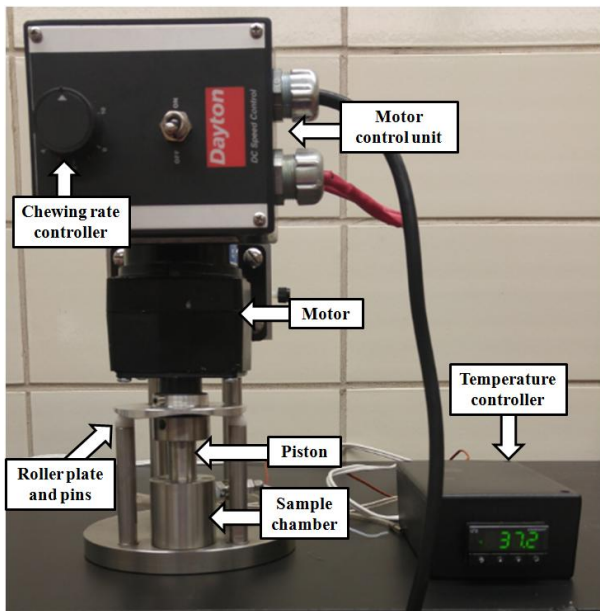


Figure A-7-2 Fabricated artificial chewing device with temperature controller.

The lower assembly or base of the artificial chewing device contains the sample chamber. The interior of the sample chamber is a smooth cylinder with the interior base of the cylinder containing a removal plate containing 'teeth'. The cylinder is modified for connection to gas and liquid flow in and out and also for a heating element and temperature control probe. The base of the chewing machine is also fitted with two poles which guide the top motor assembly. Another set of poles set the depth to which the piston descends into the sample chamber and support the sinusoidal roller guide plate attached to the motor assembly. The lower assembly is visible in Figure A-7-3 below.

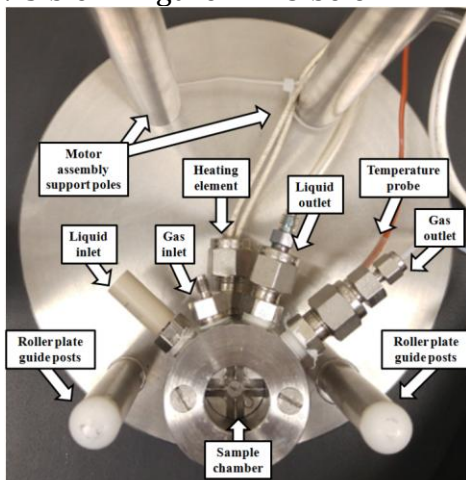


Figure A-7-3 Lower assembly for artificial chewing device.

An image of the interior of the sample chamber is visible in Figure A-7-4 below along with a schematic showing the position of the liquid and gas inlet and outlets with respect to the tooth plate affixed to the bottom of the sample chamber. The tooth plate is affixed to the bottom of the sample chamber with a screw and is easily removable for cleaning.

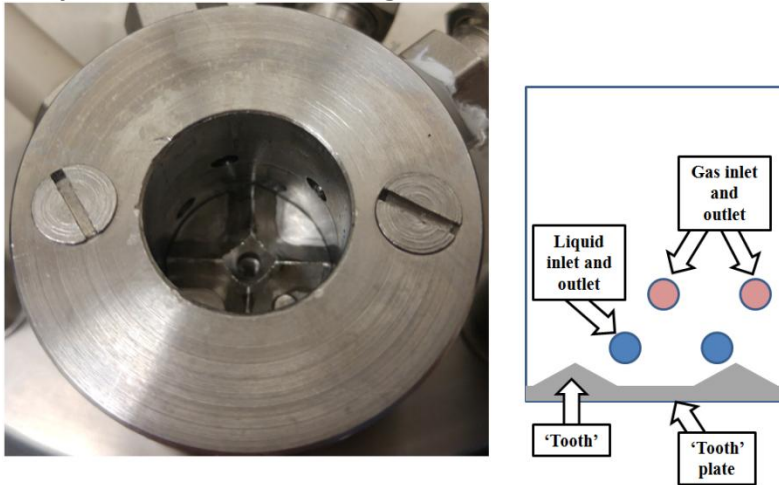


Figure A-7-4 Interior of the sample chamber of the chewing device.

The upper or motor assembly is composed of a motor attached to a sinusoidal roller guide plate and piston. The end of the piston, not attached to the motor, is finished with teeth. Above the teeth the piston is notched in two places and fitted with BUNA O-rings. The motor assembly slides onto two poles attached to the lower assembly and the piston is guided into the sample chamber. When the piston is lowered into the sample chamber the sinusoidal roller guide plate at the top of the piston rests on top of the two support poles attached to the base of the device. Washers placed between the poles and the base of the device can be used to adjust the depth of the piston into the sample chamber. The upper assembly of the device is shown in Figure A-7-5 below.

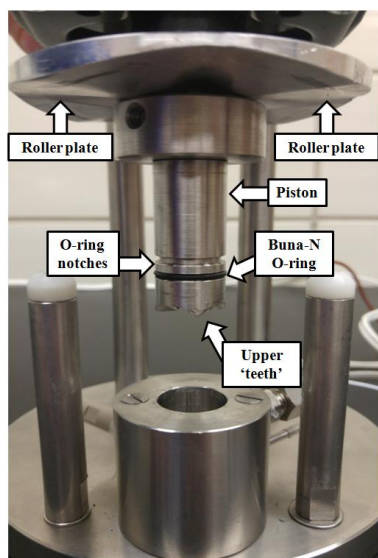


Figure A-7-5 Upper assembly of the artificial chewing device.

### System Components

Manufactured components combined with fabricated parts from the St. Paul Machine Shop are listed below:

Motor: Permanent Magnet D.C. Gearmotor 90 Volt, 0.8 Amps (Leeson® Electric Motors Gearmotors and Drives, Grafton, WI) model:6470K71 Catalog #:CM30D18NZ1C M1125134.00

Temperature Controller: CN132/DP132 i-Series 1/32 DIN Temperature, Process and Strain PID Controller, ¼ inch cartridge heater CIR-1021/120V, Thermocouple Wire K Type Duplex insulated K thermocouple (Omega® Engineering Inc. Stamford, CT)

Chewing device are often interfaced with other analytical techniques in order to generate flavor release profiles and collect liquid or gas samples from the chewing device. The artificial chewing device was connected to an atmospheric pressure chemical ionization mass spectrometer (APCI/MS); water was supplied to the device using a binary pump from a high performance liquid chromatograph

APCI/MS: Waters micromass Quattro Micro™

HPLC pump: High Performance Liquid Chromatograph Binary Pump LC-10AD VP Shimadzu (Columbia, MD)

Peristaltic pump: Masterflex L/S Reversible Drive Peristaltic Pump (Cole Palmer Instrument Co., Vernon Hills, IL)

Flow Meter: J & W Humonics Precision Flow Measurement Veriflow 500 (Sigma Aldrich, St. Louis, MO)

Flow Controller: Hewlett Packard Flow Controller Model 5080-6710 (Hewlett Packard, Palo Alto, CA)

### System Dimensions

The dimensions for the chewing device are displayed in Figure A-7-6 and Figure A-7-7 below.

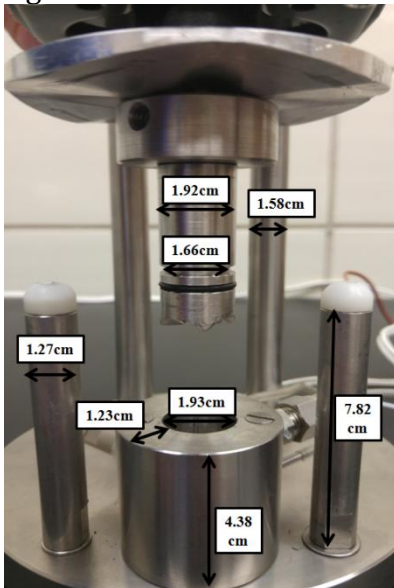


Figure A-7-6 Dimensions for the chewing device in centimeters (cm).

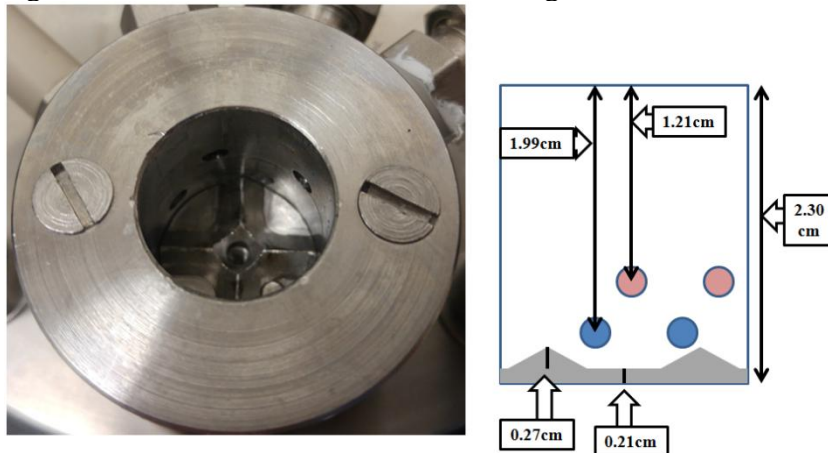


Figure A-7-7 Dimensions in centimeters for the interior of the sample chamber.

The weight of the top assembly is 5.574 kg. The total height of the device is 31.5cm, width 15.5cm and depth 33.5 cm.